Analysis of the Function of DNA Polymerase κ and M17 in the Immune System

Inaugural-Dissertation

zur

Erlangung des Doktorgrades

der Mathematisch-Naturwissenschaftlichen Fakultät

der Universität zu Köln

vorgelegt von

Dominik Schenten

aus Trier

Boston 2003

2

Berichterstatter: Prof. Dr. Klaus Rajewsky

                                     Prof. Dr. Jens Brüning

Tag der mündlichen Prüfung: 10. Februar 2004

TABLE OF CONTENTS

A   INTRODUCTION

The immune system employs complex strategies in the fight against invading pathogens. While the innate immune response is an evolutionary ancient arm of the immune system, vertebrates have also acquired the ability to respond to pathogens in an adaptive fashion. Adaptive immune responses are provided by T and B cells. The central molecules in B cell-mediated immunity are the immunoglobulin (Ig) chains. They form the antigen-recognizing unit of the B cell receptor (BCR) and contribute effector function as secreted antibodies. The generation of a broad repertoire of BCR specificities is essential for the effective humoral immune response. In both human and mouse, this is achieved by two mechanisms: V(D)J recombination and somatic hypermutation (SHM). The hallmark of B cell development is the rearrangement of functional Ig genes from a pool of germline variable (V), diversity (D), and joining (J) gene segments. In T cell-dependent immune responses, B cells further diversify their BCR repertoire through the introduction of somatic mutations into the variable region of the Ig genes, a process called somatic hypermutation (SHM)

A1   V(D)J Recombination

The BCR consists of pairs of identical covalently-linked immunoglobulin heavy (IgH) and light (IgL) chains that form a complex with the signaling component of the BCR, the Ig-α/β heterodimer. Both heavy and light chains comprise a variable (V) region that confers antigen specificity and a constant region that mediates effector function in the case of the IgH chain.

The IgH chain is encoded by one gene locus, while there are two loci, kappa and lambda, that encode the IgL (Honjo and Alt, 1995). Through the process of V(D)J recombination, the V region of IgH chains is assembled by joining a variable (V_H), diversity (D_H), and joining (J_H) gene segment (for the organization of the IgH locus, see Figure 1). The V region of IgL chains is rearranged similarly. However, IgL loci lack D elements and recombination occurs only between V and J gene segments (Bassing et al., 2002; Schlissel, 2003).
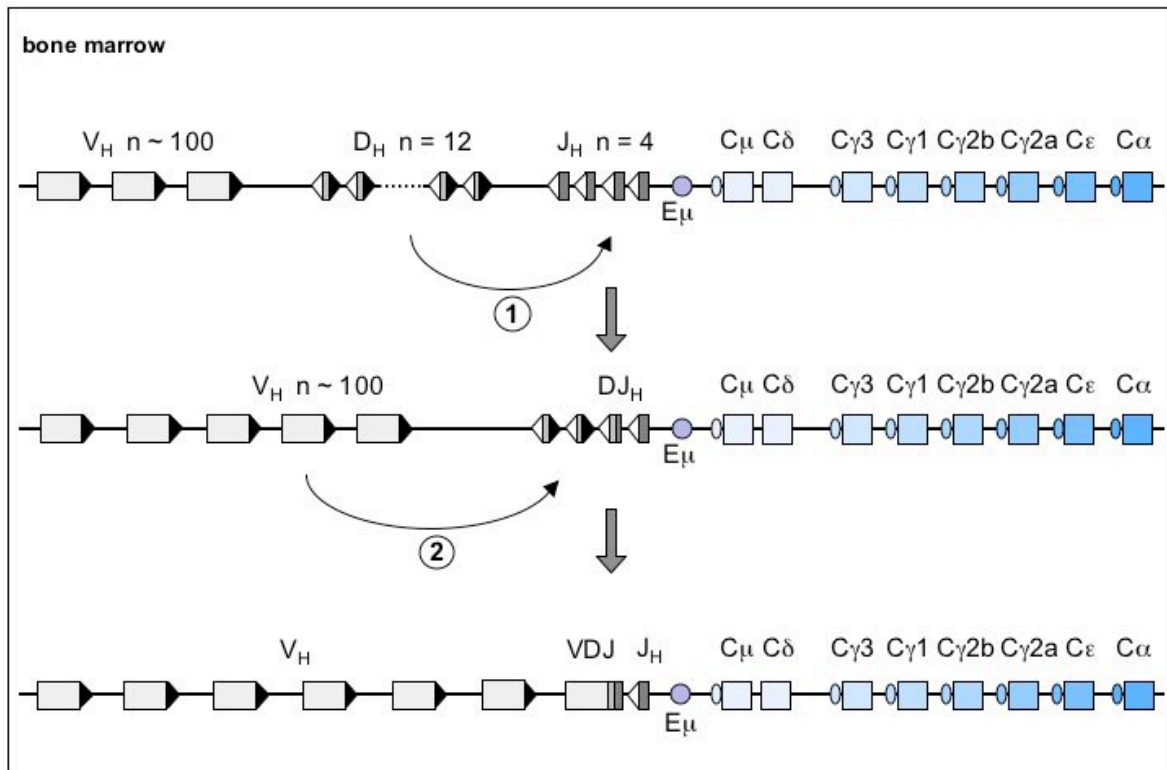
Figure 1. Organization and V(D)J recombination of the murine IgH locus.
Variable (V_H), diversity (D_H) and joining (J_H) gene segments are located in the 5'
part of the locus. The exons of the constant region comprise the 3' part of the
locus. B cells undergo first D_H to J_H rearrangements (1), followed by V_H to $D_H J_H$
rearrangements (2). D_H to J_H rearrangements occur on both alleles, whereas a
productive V_H to $D_H J_H$ rearrangement prevents further rearrangements on the
other allele (allelic exclusion). The reaction is initiated by the enzymes lymphoid-
specific genes RAG-1 and RAG-2 that cleave the DNA within recognition signal
sequences (RSS). Subsequently, ubiquitously expressed non-homologous end-
joining (NHEJ) enzymes resolve the DNA lesions and juxtapose the gene
segments. Rectangles represent gene segments and triangles represent RSSs.
The intronic enhancer ($E\mu$) is shown as a circle and switch (S) regions in front of
the constant regions are depicted as ovals. N indicates the number of particular
gene segments in the locus.

V(D)J recombination is initiated by the lymphoid-specific enzymes recombination-activating genes 1 and 2 (RAG-1 and RAG-2) (Oettinger et al., 1990; Schatz et al., 1989). The RAG proteins recognize recognition signal sequences (RSS) flanking the V, D, and J elements, where they introduce double-strand breaks into the DNA (McBlane et al., 1995; Oettinger et al., 1990; Schatz et al., 1989; van Gent et al., 1995). Resolution of the double strand breaks is then mediated by ubiquitously expressed non-homologous end joining (NHEJ) enzymes and leads to the juxtaposition of a V, D, and J gene segments (Barnes et al., 1998; Blunt et al., 1995; Critchlow et al., 1997; Frank et al., 1998; Grawunder et al., 1997; Kirchgessner et al., 1995; Nussenzweig et al., 1996; Zhu et al., 1996). V(D)J recombination is not precise. In adult mice, the DNA joints are trimmed and the lymphoid-specific terminal desoxynucleotidyl transferase (TdT) (Alt and Baltimore, 1982; Gilfillan et al., 1993; Komori et al., 1993) inserts randomly non-templated nucleotides (N-nucleotides). Recently, the related DNA polymerase μ (Bertocci et al., 2003) has also been implicated in the processing of the DNA joints. Thus, these processes contribute additional antibody diversification.

V(D)J recombination is an ordered process, whose regulation is thought to involve chromatin modifications in the Ig loci, which render the loci accessible for the RAG proteins (Mostoslavsky et al., 2003; Schlissel, 2003). In the majority of B cells, rearrangement of the IgH locus precedes the rearrangement of the IgL loci. Expression of a productive (functional) IgH chain terminates further recombination of the IgH loci, a process termed "allelic exclusion", which induces the onset of IgL rearrangements. Allelic exclusion and light chain isotype exclusion of the IgH and IgL loci confines B cells to the expression of a single BCR specificity.

A2   B Cell Development

Murine B cell development occurs in the fetal liver during embryogenesis and continues in the bone marrow after birth (Owen et al., 1977). Based on the expression of surface antigens, B cell development can be separated into several distinct stages (Figure 2) (Hardy et al., 1991; Rolink et al., 1994; Rolink and Melchers, 1996) that correlate with the progression of V(D)J recombination (Rajewsky, 1996).
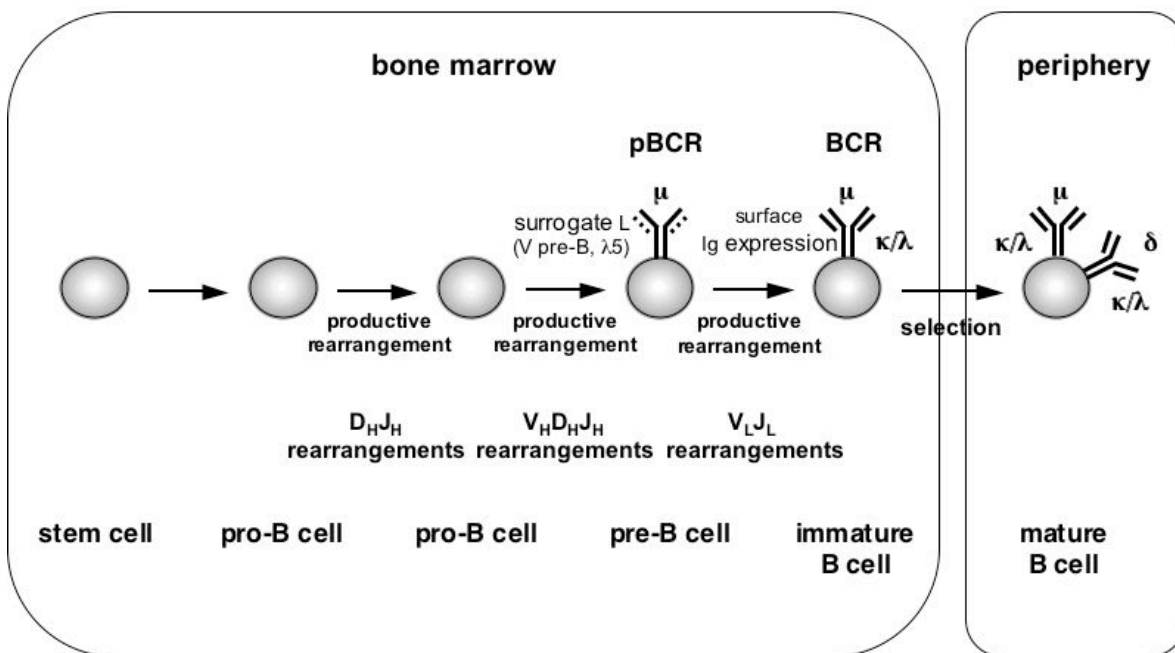
Figure 2. B cell development. Pro-B cells are the earliest B cell progenitors. In most cases, V(D)J recombination commences at the IgH loci. D_H and J_H gene segments are rearranged first, followed by V_H to D_HJ_H rearrangements. Cells carrying a productive (functional) V(D)J rearrangement progress to become pre-B cells. The IgH chain pairs with the surrogate light chain to form the pre-B cell receptor (pre-BCR). Signaling through the pre-BCR terminates further rearrangements at the IgH loci and allows pre-B cells to continue with IgL chain rearrangements. Productive V_L to J_L rearrangements result in the expression of a functional BCR. Signaling through the BCR terminates V(D)J recombination and allows pre-B cells to differentiate into immature B cells, which mature in the secondary lymphoid organs. Figure is adapted from Rajewsky, 1996 (Rajewsky, 1996).

B cell progenitors develop into pro-B cells (B220$^+$CD43$^+$IgM$^-$IgD$^-$), with D_H to J_H rearrangements occurring first, followed by V_H to D_HJ_H rearrangements (Alt et al., 1984). Cells carrying a productive IgH rearrangement become pre-B cells (B220$^+$CD43$^-$IgM$^-$IgD$^-$). In pre-B cells, IgH chains pair with a surrogate light chain, consisting of the VpreB and λ5 molecules, to form the pre-BCR (Karasuyama et al., 1990; Tsubata and Reth, 1990). Signaling through the pre-BCR is thought to

terminate further IgH rearrangements and enables the cell to progress to IgL chain rearrangement (Kitamura et al., 1992; Löffert et al., 1996). Successful completion of the IgL rearrangement allows the expression of a functional BCR, which terminates further IgL chain rearrangements (Grawunder et al., 1995; Li et al., 1993). B cells that recognize auto-antigens through their BCR either alter their BCR specificity by receptor editing of the IgL or are negatively selected (Gay et al., 1993; Nemazee and Burki, 1989; Retter and Nemazee, 1998; Tiegs et al., 1993). Only those cells with "innocent" (non-autoreactive) receptors differentiate into immature B cells (B220$^+$CD43$^-$IgM$^+$IgD$^-$). Further maturation occurs then in the secondary lymphoid organs (Allman et al., 1993).

Mature B cells fall into three subsets that can be distinguished by the differential expression of surface antigen markers and their distinct homing and functional properties. B-1 cells (IgM^{bright}IgD^{low}B220^{low}CD23^{low}CD43$^+$) are self-renewing cells derived from fetal precursors. They are found mainly in the peritoneal and pleural cavities and provide most of the "natural" IgM antibodies, thus contributing to innate immune responses (Hardy and Hayakawa, 2001; Hayakawa et al., 1983; Herzenberg et al., 1986; Kocks and Rajewsky, 1989; Su and Tarakhovsky, 2000). Marginal zone (MZ) B cells (IgM^{high}IgD^{low}CD21^{high}CD23^{low}) are self-renewing cells that appear in the spleen shortly after birth. They are non-circulating and are recruited into humoral responses raised against blood-borne antigens (Martin and Kearney, 2002). Most B cells in adult mice differentiate into follicular B cell (also called B-2 cells). Follicular B cells are IgM^{high}IgD^{low}CD21^{low}CD23^{high}. They are re-circulating cells that home to B cell follicles in the secondary lymphoid organs and are the major B cell subset recruited into antibody responses against T cell-dependent antigens (Rajewsky, 1996). The molecular mechanism that governs the differentiation into the distinct subsets of mature B cells is not fully understood. However, current understanding suggests that the strength of the BCR-mediated signal is the critical determinant for the differentiation into the mature B cell subsets (Cariappa and Pillai, 2002).

A3   The Germinal Center Reaction

In T cell-dependent (TD) antibody responses, follicular B cells are activated in the T cell zone of the secondary lymphoid organs by BCR-mediated antigen recognition and T cell help. Upon activation, most B cells differentiate into short-lived antibody-secreting plasma cells (Ho et al., 1986). The latter cells retain their unmutated Ig genes and provide an initial wave of low-affinity antibodies. A fraction of the activated B cells migrate to the B cell follicles, where they undergo a phase of rapid proliferation and form distinct histological structures in secondary lymphoid organs, the germinal centers (GCs) (MacLennan, 1994; Tarlinton, 1998).

Germinal centers are the sites of secondary antibody diversification. Somatic hypermutation (SHM) introduces mutations into the pre-rearranged Ig genes, thus generating novel mutated BCRs. A second process, called class switch recombination (CSR), modifies the IgH constant region by replacing the constant region of IgM with that of another isotype to modify effector function. Murine GC B cells can be distinguished from follicular B cells by their ability to bind to the plant lectin peanut agglutinin (PNA), the increased surface expression of GL-7 and the Fas receptor, and the reduced surface levels of IgD. Germinal centers at the peak of the GC reaction have a polarized appearance (Figure 3). The dark zone adjacent to the T cell zone contains proliferating B cells (called centroblasts), whereas the light zone comprises non-dividing B cells (called centrocytes) interacting with a network of follicular dendritic cells (FDCs) (Schriever and Nadler, 1992). Centroblasts divide every 7 hours, and undergo SHM (MacLennan, 1994). After the proliferative burst, centroblasts exit the cell cycle and become centrocytes. Centrocytes compete with each other for access to antigens held in the form of immune complexes on the FDCs (Mandel et al., 1980). During affinity maturation, centrocytes with high-affinity BCRs are positively selected and differentiate into long-lived plasma cells or memory B cells, while those cells with a non-functional or low-affinity BCR fail to get selected and die by apoptosis.

Terminal differentiation of plasma cells alters the gene expression required for BCR signaling and GC function (Shaffer et al., 2002). Guided by chemokines, long-lived plasma cells migrate preferentially to the bone marrow, where they
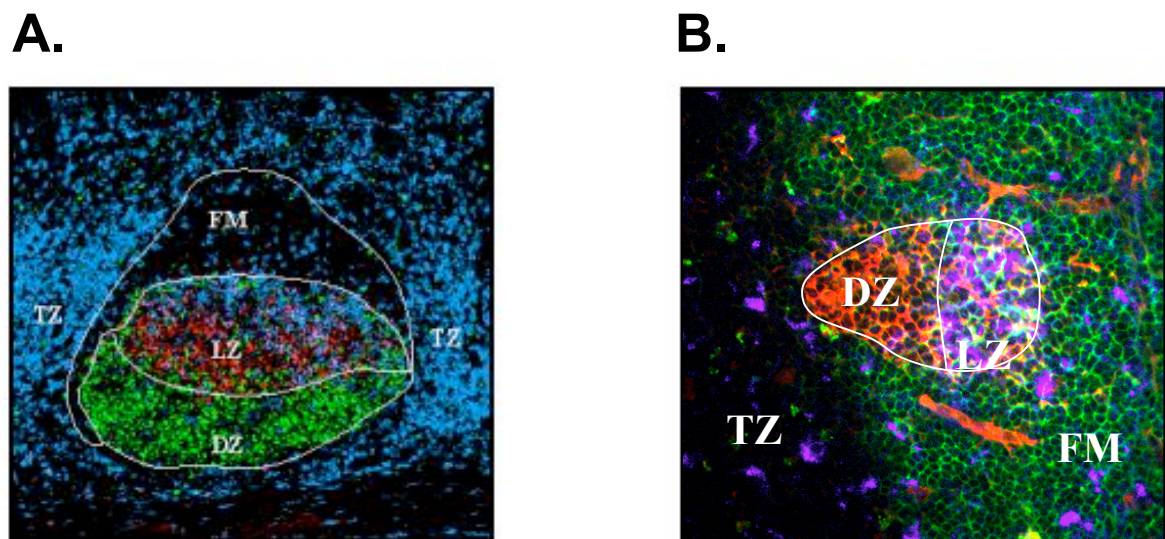
Figure 3. Structure of germinal centers in humans (A) and mice (B). GC B cells can be divided into centroblasts and centrocytes. Centroblast proliferate in the dark zone (DZ) adjacent to the T cell zone and undergo SHM. Centroblasts give rise to centrocytes. The latter cells interact in the light zone (LZ) with follicular dendritic cells (FDCs). **A.** Germinal center in a human tonsil. Centroblasts are stained for the proliferation marker Ki-67 in green, T cells are stained in blue, and FDCs are stained in red. **B.** Germinal center in the spleen of an immunized mouse. PNA-binding GC B cells are stained in red, FDCs in purple, and CD19-positive B cells in green. FM indicates the follicular mantle zone, which consists of resting B cells. Figure 3A is adapted from the homepage of the MacLennan laboratory (http://www.bham.ac.uk/mrcbcir/research.htm#reg%20imm%20responses).

secrete large amounts of antigen-specific antibodies (Benner et al., 1981; Cyster, 2003; Manz et al., 1997; McMillan et al., 1972). Memory B cells persist in secondary lymphoid organs after the termination of the TD immune response in the absence of further contact with antigen (Maruyama et al., 2000) and represent the first B cell subset recruited into secondary antibody responses.

A4 Class Switch Recombination (CSR)

The nature of the IgH constant region defines the antibody isotype. The activation with cognate antigen, the presence of cytokines, and to some degree T-

cell help, induce IgM and IgD-expressing follicular B cells to undergo CSR in order to express other isotypes (Manis et al., 2002; Stavnezer, 1996).

The IgH constant region gene segments (C_H) cluster at the 3' end of the locus, starting in the mouse with the V_H-proximal $C\mu$ encoding IgM followed by $C\delta$, $C\gamma3$. $C\gamma1$, $C\gamma2b$, $C\gamma2a$, $C\epsilon$ and $C\alpha$ (Figure 4). Upon CSR, B cells express a different isotype by replacing $C\mu$ with a downstream C_H and concurrent excision of the intervening DNA (Iwasato et al., 1990; Matsuoka et al., 1990). Each C_H gene segment represents a discrete transcriptional unit that comprises its own promoter, a GC-rich repetitive sequence (switch (S) region) and the exons of the constant region. CSR occurs between the S regions located up-stream of each constant region and is dependent on C_H promoter-driven germline transcription through the S regions (Bottaro et al., 1994; Harriman et al., 1996; Jung et al., 1993; Zhang et al., 1993). Transcription leads to the formation of stable RNA-DNA structures (termed R-loops) that displace the non-coding DNA strand (Reaban and Griffin, 1990; Reaban et al., 1994; Yu et al., 2003; Yu and Lieber, 2003). The R-loops are thought to assist in the targeting of the recombination machinery. The DNA breaks occur within the S regions and the resulting DNA ends are joined by the NHEJ pathway (Casellas et al., 1998; Manis et al., 1998; Rolink et al., 1996). As a result of CSR, the intervening DNA fragment is excised as a circle and the 3' and 5' ends of the IgH locus are juxtaposed.

A5   Somatic Hypermutation (SHM)

During SHM, the pre-rearranged Ig genes acquire point mutations at a very high rate (around 10^{-3}/bp/generation) (Kocks and Rajewsky, 1988; McKean et al., 1984). Transcription of the Ig genes is essential for SHM and the transcription rate correlates with the mutation frequency (Fukita et al., 1998; Storb et al., 1998b). Mutations accumulate in a 2 kb window downstream of the promoter (Neuberger et al., 1998; Rada and Milstein, 2001; Storb et al., 1998a), thus covering the V gene region but not the constant regions. The presence of Ig enhancers is required for SHM and the targeting of the SHM machinery to the Ig genes is thought to involve changes in the chromatin structure of the Ig V region (Jolly and Neuberger, 2001; Woo et al., 2003). The mutations do not occur entirely randomly (Jolly et al., 1996).

Transitions (purine to purine or pyrimidine to pyrimidine mutations) dominate over transversions (purine to pyrimidine or pyrimidine to purine mutations) and guanine mutations often accumulate in the context of the RGYW motif (R = A or G, G, Y = C or T, W = A or T) (Betz et al., 1993; Rogozin and Kolchanov, 1992). These sites are therefore also called hot spots of mutations. Within the V genes, adenine mutations are favored over thymidine mutations, indicating a strand bias for A-T but not G-C mutations. Finally, the occurrence of small deletions and duplications within the Ig genes has led to the suggestion that SHM involves the generation of DNA strand breaks (Goossens et al., 1998; Sale and Neuberger, 1998).

While many *cis*-acting elements required for SHM have been identified (Neuberger et al., 1998; Storb et al., 1998a), less is known about the molecular components necessary for this process. Many models of the mechanism for SHM postulated the introduction of single-strand or double-strand breaks into the DNA with subsequent error-prone short-patch synthesis by one or more DNA polymerases (Bertocci et al., 1998; Brenner and Milstein, 1966; Diaz et al., 1999). The presence of DNA double strand breaks within the RGYW motif in rearranged Ig genes of cells undergoing SHM has indeed been demonstrated (Bross et al., 2000; Papavasiliou and Schatz, 2000). They may occur preferentially during S/G2 phase, suggesting a resolution of the lesion via template-directed homologous recombination. However, the molecular origin of the double-strand breaks and their significance for the SHM process remain unclear (Bross et al., 2002; Papavasiliou and Schatz, 2002).

A6   The Deamination Model

Although SHM and CSR differ in many aspects, they both depend on the function of the GC B cell-specific activation-induced cytidine deaminase (AID) (Muramatsu et al., 2000; Revy et al., 2000). This indicates shared features between the two mechanisms, which is further illustrated by the observation of somatic mutations within the S regions (Nagaoka et al., 2002; Reina-San-Martin et al., 2003). Humans and mice that lack AID are unable to undergo CSR or SHM. Since AID appears to be the only B cell-specific factor required for both CSR and SHM (Okazaki et al., 2002; Yoshikawa et al., 2002), a common initiation event
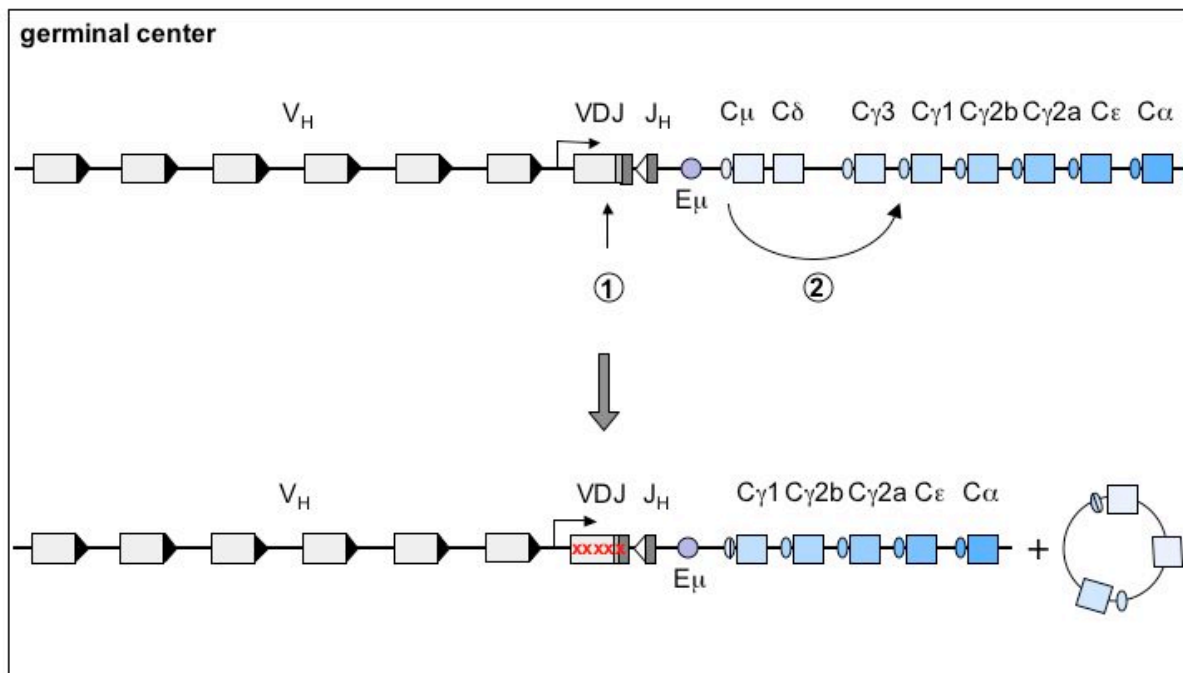
Figure 4. Somatic hypermutation (SHM) and class switch recombination (CSR). SHM (1) introduces mainly point mutations into the rearranged V region of the Ig genes to generate novel mutant BCRs for the immunizing antigen. CSR (2) alters the IgH constant region to modulate the type of antibody response. CSR occurs between two switch (S) regions, thus replacing the Cμ region with the constant region of another isotype. Mutations are depicted as red 'X', exons are represented as rectangles, and S regions are shown as ovals.

likely exists for both reactions, which are then resolved in different ways.

AID shares homologies with the RNA-editing enzyme Apobec-1, a cytidine deaminase that converts a cytidine residue into a uracil residue in the mRNA of apolipoprotein B. Consequently, AID could act on an unknown mRNA to modify one or several factors required for CSR or SHM. Further supporting this assumption, CSR does indeed require the *de novo* protein synthesis. (Doi et al., 2003). Most evidence suggests, however, that AID acts directly on DNA. Over-expression of AID in E.coli results in DNA deamination and increased cytidine mutatagenesis (Petersen-Mahrt et al., 2002). Furthermore, AID has a low affinity for RNA but a high affinity for single-stranded DNA and during transcription also for double-stranded DNA (Bransteitter et al., 2003; Chaudhuri et al., 2003; Dickerson

et al., 2003; Ramiro et al., 2003).

Accordingly, the DNA deamination model of SHM (Neuberger et al., 2003; Petersen-Mahrt et al., 2002) proposes that the localized deamination of cytidine residues by AID at the Ig V loci leads to U-G mismatches, which can be resolved in three ways (Figure 5). First, replication across the uracil templates results in G-C to A-T transitions. Second, excision of the uracil residues by uracil-DNA-glycosylases creates an abasic site, and subsequent error-prone replication of the damaged DNA strand introduces a spectrum of mutations. Alternatively, the abasic site is nicked and further processed by a combination of nucleases and error-prone DNA polymerases. Third, the mismatch-repair enzymes MSH2 and MSH6 recognize the U-G mismatch and the lesion is resolved by nucleases and error-prone short-patch DNA replication. Similar to SHM, AID may initiate the events leading to CSR after association with the non-transcribed DNA strand and subsequent deamination of cytidines. The resulting uracil lesions are then further processed, leading ultimately to the generation of DNA breaks. It is important to note, however, that the C-terminus of AID is required for CSR, but not for SHM (Barreto et al., 2003), suggesting a role for AID in the recruitment of NHEJ or other proteins that are dispensable for SHM. Several aspects of the DNA deamination model are supported by experimental evidence. E. coli over-expressing AID display an increased number of transitions when the uracil glycosylase UNG is inhibited (Di Noia and Neuberger, 2002) and UNG-deficient mice display a significant increase in the number of transition mutations in GC B cells (Rada et al., 2002). Such mice are also impaired in CSR, demonstrating the importance of uracil deglycosylation in the CSR mechanism (Rada et al., 2002). Moreover, AID targets hotspots on single stranded DNA *in vitro* (Pham et al., 2003). Finally, mice that lack enzymes involved in MSH2-mediated DNA repair display a shift towards G-C mutations in their mutational pattern (Ehrenstein et al., 2001; Jacobs et al., 1998; Phung et al., 1998; Rada et al., 1998).
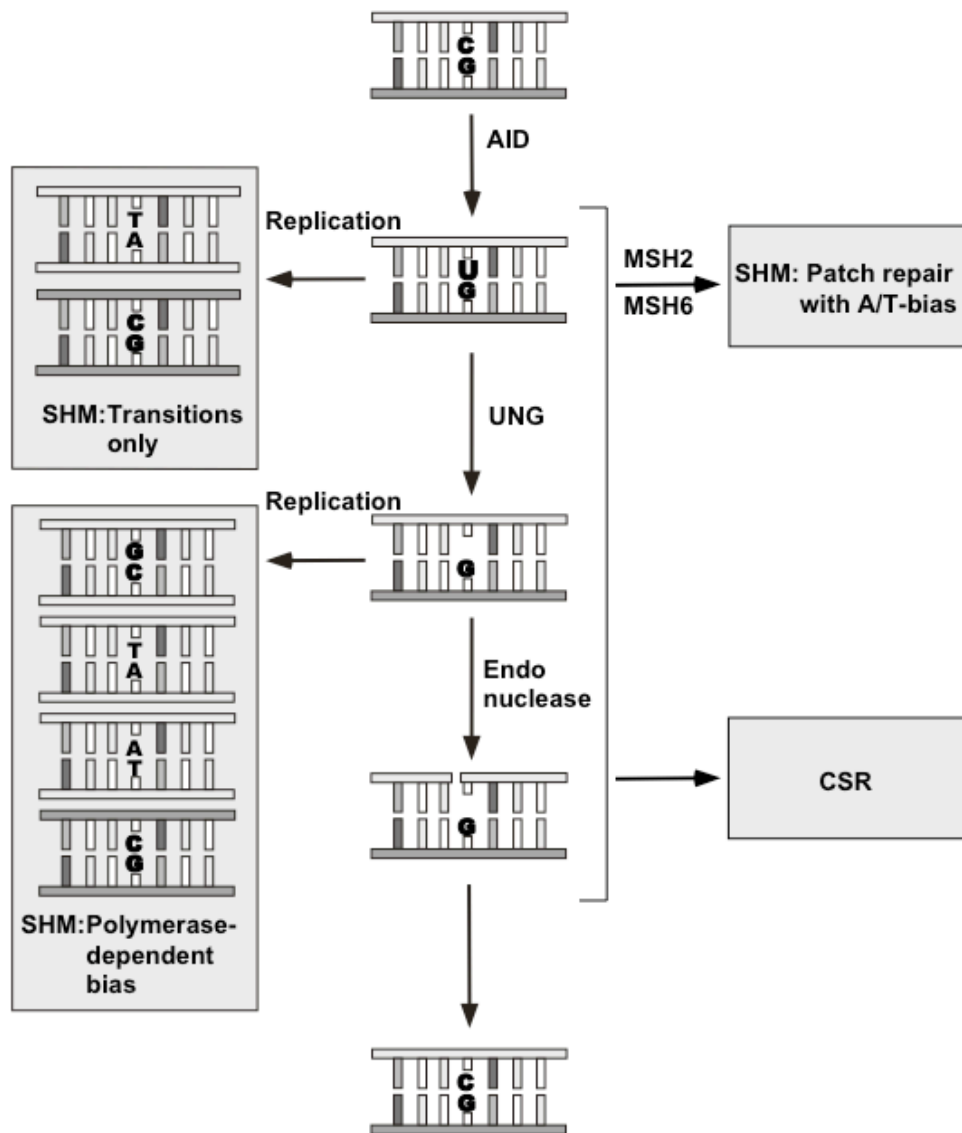
Figure 5. The deamination model. AID deaminates cytidines within the Ig genes. The resulting U-G mismatches are then resolved in three ways. 1) Replication across uracil templates results in G-C to A-T transitions. 2) Excision of the uracil residues by UNG creates an abasic site. Subsequent error-prone replication across the abasic site introduces mutations. 3) MSH2 and MSH6 recognize the U-G mismatch and the lesion is resolved by nucleases and error-prone short-patch DNA synthesis. Cytidine deamination, followed by the removal of the uracil residues and introduction of DNA-strand breaks may also initiate CSR. Adapted from Petersen-Mahrt et al., 2002.

A7   The Role of error-prone DNA Polymerases in SHM

While cytidine deamination by AID may explain the presence of G-C to A-T transitions, SHM encompasses the whole spectrum of both transitions and transversions, suggesting that the mutations are at least in part caused by error-prone DNA polymerases. Besides the proof-reading error-free DNA polymerases required for genome replication, humans and mice express many non-replicative error-prone DNA polymerases that are able to bypass DNA adducts and extend from mismatched termini (Friedberg et al., 2002; Goodman, 2002; Jansen and de Wind, 2003). The specialized function of trans-lesion synthesis marked error-prone DNA polymerases as potential contributors to SHM (Reynaud et al., 2003).

The error spectrum of Polη *in vitro* correlates with hotspot mutations at the RGYW motif in SHM (Pavlov et al., 2002; Rogozin et al., 2001). Polη is defective in patients with the variant form of xeroderma pigmentosum (XP-V), a disease that predisposes to skin cancer due to a increased sensitivity to UV radiation (Masutani et al., 1999). SHM occurs at normal frequencies in XP-V patients but displays a bias towards G-C mutations and a decrease in mutations at A-T base pairs, demonstrating a contribution of Polη to SHM (Zeng et al., 2001).

Polymerase ι is characterized by its very low fidelity and mRNA expression of Polι has been demonstrated in a cell line undergoing SHM (Johnson et al., 2000b; Poltoratsky et al., 2001; Tissier et al., 2000). The inactivation of Polι in the hypermutating cell line resulted in a substantial decrease in the mutation frequency (Faili, 2002). Surprisingly, Polι-deficient mice mutate their Ig genes in GC B cells efficiently and without changes in their mutational pattern (McDonald et al., 2003).

Polymerase ζ is responsible for most of the UV-radiation-induced and spontaneous mutagenesis. It is very efficient in extending DNA from mismatched termini (Lawrence and Hinkle, 1996). Polymerase ζ may introduce mutations *in vivo* by extending from mismatches formed by Polι, a mechanism that has been shown to occur *in vitro* using recombinant yeast rev3 (the catalytic subunit of Polζ) and recombinant human Polι (Johnson et al., 2000b). Expression of Polζ mRNA is upregulated in GC B cells. Lack of Polζ causes embryonic lethality in mice (Bemark et al., 2000; Esposito et al., 2000a; Wittschieben et al., 2000). However,

RNA antisense inhibition of Rev3 (the catalytic subunit of mammalian Polζ) in a hypermutating cell line reduced the frequency of SHM (Zan et al., 2001) and transgenic mice expressing Rev3l antisense RNA exhibited a decreased level of Ig mutations (Diaz et al., 2001). In both experiments, the pattern of the mutations was still normal.

Polymerase μ is the only error-prone DNA polymerase that displays a lymphoid-specific expression pattern (Dominguez et al., 2000; Reynaud et al., 2001). It shares homologies with TdT, acts in a template-dependent but sequence-independent manner (Dominguez et al., 2000; Reynaud et al., 2001), and is involved in the processing of the junctions of IgL genes (Bertocci et al., 2003). Because of its expression in peripheral B cells, it was also considered to play a role in SHM. However, Polμ-deficient mice show normal SHM (Bertocci et al., 2002). Likewise, the analysis of mouse strains deficient of Polβ (Esposito et al., 2000b), Polδ (Longacre et al., 2003), or Polλ (Bertocci et al., 2002) also failed to detect a contribution of these DNA polymerases to SHM. However, the example of Polι-deficient mice (required for SHM in a hypermutating human B cell line but dispensable in mice) raises the possibility of overlapping functions of error-prone DNA polymerases in SHM.

A8   DNA Polymerase Kappa

Polymerase κ (*DinB1*) is expressed in high levels in mouse testis, but also at lower levels in a wide variety of other tissues, including the spleen (Gerlach et al., 1999; Johnson et al., 2000a). Like Polη and Polι, it is a member of the Y family of DNA polymerases (Ohmori et al., 2001) and shares extensive amino-acid homology with the SOS-induced error-prone DNA polymerase PolIV, the product of the E. coli *dinB* gene (Gerlach et al., 1999). Polymerase κ lacks detectable 3'-5' proofreading exonuclease activity and replicates undamaged DNA *in vitro* at a single-base substitution error rate of $\approx 6x10^{-3}$ (Gerlach et al., 2001; Ohashi et al., 2000; Zhang et al., 2000b). Polymerase κ can act as mismatch extender during translesion synthesis (Haracska et al., 2002; Washington et al., 2002) and abasic sites similar to those created by UNG can serve substrates for Polκ (Zhang et al., 2000a). Over-expression of murine Polκ in a mouse cell line results in about a 10-
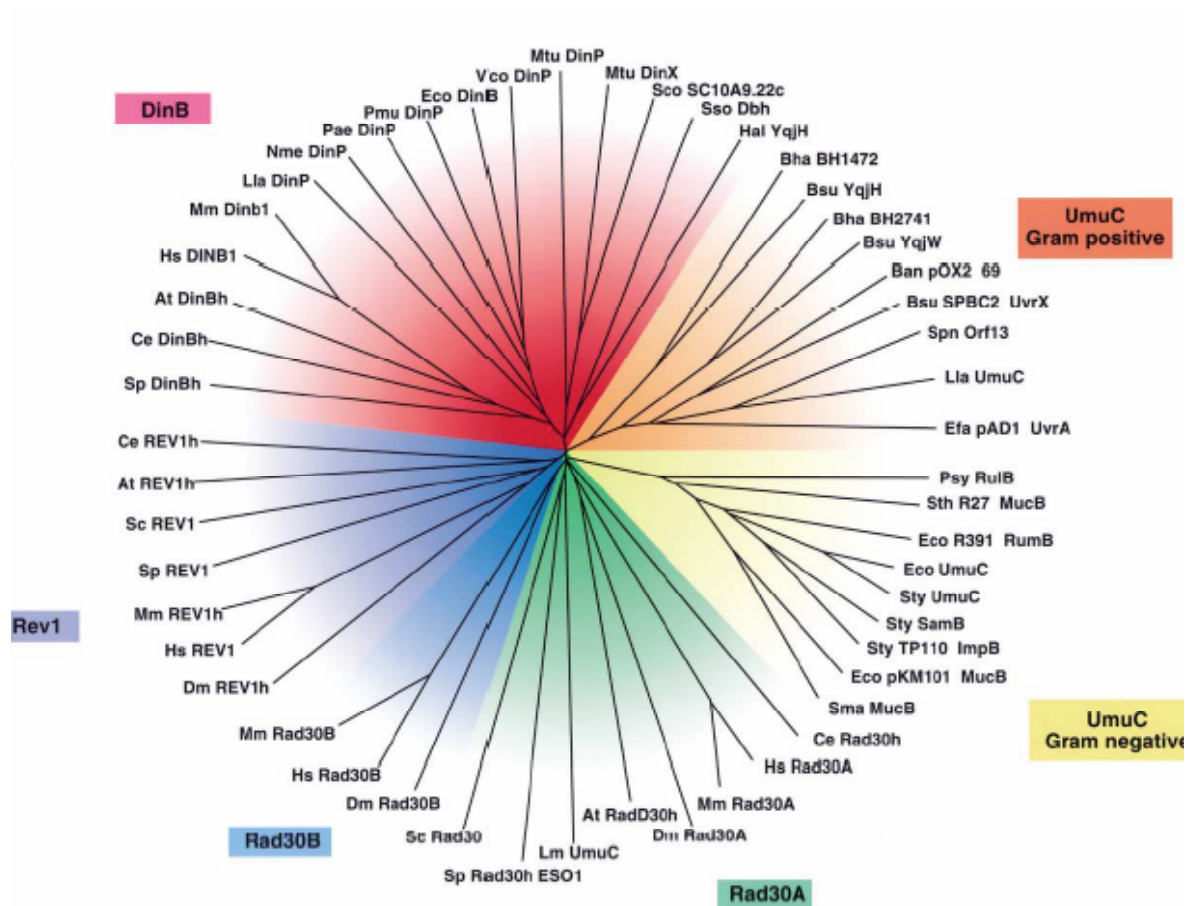
Figure 6. Phylogenetic tree of Y-family error-prone DNA polymerases. Pol κ (DinB1), Polη (Rad30A) and Polι (Rad30B) are members of the the Y-family of DNA polymerases, while TdT, Polμ, and Polλ belong to the X-family of DNA polymerases. Polβ and Polζ (Rev3/Rev7) are members of the B-family of DNA polymerases. Adapted from Ohmori et al., 2001.

fold increase of spontaneous mutagenesis (Ogi et al., 1999). Moreover, a comparison between the mutational patterns of SHM and Polκ *in vitro* suggested a possible contribution of Polκ to SHM (Rogozin et al., 2001). These features mark Polκ as a potential candidate for a specialized DNA polymerase required for SHM.

A9   M17

GCs are the origin of several B cell malignancies due to aberrant SHM or CSR (Klein, 1999; Kuppers et al., 1999; Pasqualucci et al., 2001). Diffuse large B cell lymphomas (DLBCL) represent a heterogeneous group of GC-derived tumors, which often harbor mutations characteristic of SHM in proto-oncogenes like *BCL6* and *MYC* (Pasqualucci et al., 2001). Human germinal center-associated lymphoma (*HGAL*) is a cytosolic protein that is expressed at high levels in GCs and at moderate levels in the thymus (Lossos et al., 2003; Pan et al., 2003). Expression of *HGAL* mRNA is also found in a subset of DLBCL, where it can serve as a marker for the clinical prognosis of patients with DLBCL (Lossos et al., 2003; Rosenwald et al., 2002). High expression of the *HGAL* gene correlates with a better prognosis and longer survival.

In an attempt to identify genes that govern the GC reaction, the cDNA encoding the murine counterpart of HGAL, M17, was previously isolated in our laboratory by cDNA subtraction between GC B cells and LPS-stimulated splenocytes. M17 is a putative cytosolic 25 kD protein, which is predominantly expressed in GC B cells (Christoph et al., 1994) Within the GCs, *M17* mRNA expression appears stronger in centroblasts than in centrocytes (Christoph, 1993). The *M17* and *HGAL* genes share a similar exon-intron structure. At the protein level, they contain several potential phosphorylation sites that also include a non-canonical immune tyrosine activation motive (ITAM), indicating a role in cell signaling (Christoph et al., 1994). The function of M17 is unknown. However, its site of expression is suggestive of a role of M17 in the GC reaction, where it may contribute to CSR, SHM or to the proper selection and differentiation of GC B cells to the memory B cell or plasma cell compartments.

A10   Objectives of This Study

When I started my thesis, a plethora of novel error-prone DNA polymerase had just been discovered, some of which had been implicated to play a role in SHM mechanism. Polymerase κ showed features *in vitro* that were compatible with such a role. Consequently, I sought to study its contribution to the SHM mechanism *in vivo*. I first inactivated the Polκ gene by conditional gene targeting

and subsequently probed Polκ-deficient mice for SHM. I then extended the initial study and asked whether Polκ acts in concert with other DNA polymerases in SHM. In addition to its role in SHM, Polκ may also affect DNA repair, survival, or reproduction. I briefly addressed these aspects in the context of this thesis.

In a quest to identify gene that are specifically expressed in GCs, our laboratory had previously identified the novel M17 gene and also generated a mouse strain, in which M17 had been inactivated. Because of my interest in mechanisms regulating the GC reaction, I started to characterize the function of M17 *in vivo* and the findings of this investigation are presented here.

B   MATERIAL AND METHODS

B1   Molecular Biology Experiments

All molecular biology techniques were based on standard protocols (Sambrook et al., 1989). Enzymes were obtained from Roche, GIBCO-BRL, New England Biolabs, Stratagene, Takara, Invitrogen, Promega, Eppendorf, and USB.

B1.1   Competent Cells and Isolation of Plasmid DNA

Escherichia coli XL-1 Blue cells were made chemically competent according to the protocol of Inoue et al. (Inoue et al., 1990). Plasmid DNA was isolated from transformed *Escherichia coli* XL-1 Blue bacteria by alkaline lysis (Birnboim, 1983). For higher quality plasmid DNA purification, QIAGEN spin columns (QIAGEN) were used according to manufacturer's instructions.

B1.2   Isolation of Genomic DNA from Mammalian Cells

Cells were lysed in lysis buffer (10 mM Tris-HCl, pH 8; 10 mM EDTA; 150 mM NaCl; 0.2% SDS; 400 mg/ml Proteinase K) over night at 56°C. DNA was precipitated from the solution by the addition of an equal volume of isopropanol and pelleted by centrifugation. The pallet was washed in 70% ethanol and resuspended in TE-buffer (10 mM Tris-HCl, pH 8; 1 mM EDTA). For ES cell clones that were grown in 96-well tissue culture dishes, a modified protocol was used (Pasparakis and Kollias, 1995).

Mouse tissues were incubated in lysis buffer (0.1 M Tris-HCl, pH 8.5; 5 mM EDTA; 0.2% SDS; 0.2 M NaCl; 600 mg/ml Proteinase K) over night at 56°C. The solution was freed of undissolved debris by centrifugation and the supernatant was mixed with an equal volume of isopropanol to precipitate the DNA. The DNA was washed in 70% ethanol, dried, and resuspended in TE buffer.

B1.3   Agarose Gel Electrophoresis and DNA Gel Extraction

Separation of DNA fragments by size was achieved by electrophoresis in agarose gels (0.7% - 2.5%; TAE buffer (Sambrook et al., 1989); 0.5 mg/ml ethidiumbromide). DNA fragments were recovered from agarose gel slices with either the QIAEX II or the QIAquick Gel Extraction Kits (QIAGEN) according to the supplied protocols.

B1.4 DNA Sequencing

DNA fragments were sequenced using the Taq DyeDeoxyTerminator Cycle Sequencing Kit (Applied Biosystems) The fluorescently labeled DNA pieces were separated and analyzed on ABI373A and ABI377 systems (Applied Biosystems) with the help of S. Wilms. Alternatively, the sequencing was performed by the Harvard Cancer Center High Throughput Facility, Boston, USA. The *Polκ* locus was sequenced by the Friedberg laboratory at the Southwestern Medical Center, Dallas, USA.

B1.5 Polymerase Chain Reaction (PCR)

PCR (Mullis and Faloona, 1987; Saiki et al., 1985) was employed for the amplification of DNA fragments used for cloning, the generation of Southern probes, and the screening of mice for the presence of targeted alleles. Reactions were performed with either Taq polymerase (Eppendorf) or the High Fidelity Expand kit (Roche) following manufacturer's instructions. The primers are listed in Tables 1a-c.

Table 1a: Primers used for cloning and generation of Southern probes

NAME	SEQUENCE (5'-3')	LOCATION	T_{Ann} [C]
SABamFor	CGGGATCCCGTGGGGGAGGGGCAGCGG	Polκ	57
SANotBack	ATTTGCGGCCGCTTTAACAGTGTGAGTCTTAG	Polκ	57
LANotFor	AACATGCTCGAGTACTCTAGAGTAGTTGCAGAGC	Polκ	57
LANotBack	CCGCTCGAGCGGAGTGTTTTTGCTGTTTGTC	Polκ	57
ExSalForII	ACGCGTGACGTCGACGTTTCGTGTGATAACGC	Polκ	57
ExSalBack	ACGCGTCGACGTGGCACAGCAAGGTCTATGGTG	Polκ	57
DinProbeA-F2	CAATGGCTACTCTTGCCTTGTG	Polκ	57
DinProbeA-Re	CTTGAAAGATCCACCAATCACCTG	Polκ	57
M26	CTACTTATTCTGCTTGGATGC	M17	58
M57	CCACCAGGCACTGCAAATGGC	M17	58

Table 1b: Primers used for the typing of mice

NAME	SEQUENCE (5'-3')	LOCATION	T_{Ann} [°C]
DinB1Seq6	CTGATGTGACCGCTGTTAAATGTT	Polκ	57
DinB1Seq8	CTGTGGAGATGCCTTAGCGG	Polκ	57
DinB1Seq10	GATCCTGCAATCAATAGCTCACGG	Polκ	57
PT26	GTGCTGATCACAGAAATGGAAGGACCTGGA	Polλ	65
PT29	GGTCAAGGACACTAAGCTACATGGCTGTTC	Polλ	65
Seq9new	CTGGTCTCTGGGAACCAAAGGAC	Polλ	65
ScNeoR1	GGGGCCACCAAAGAACGGAGC	neo	65
MuexIInew	ACCAATGGAGAGGTGCTCTCCC	Polμ	65
T2.14OAs	GGCAGGGCAGGGACTTGAGCA	Polμ	65
mRad30X2F	CAGTTTGCAGTCAAGGGCC	Polι	57
mRad30X2R	TCGACCTGGGCATAAAAGC	Polι	57
M17-FLS#87	CTACTTATTCTGCTTGGATGC	M17	58
M17-FLA#88	AGGCTAGACAGAGAACATACG	M17	58
M17-SAS#74	TGTGGAGAGAAAGGCAAAGTG	M17	58
MP 57	CCACCAGGCACTGCAAATGGC	M17	58
MP 26	CTACTTATTCTGCTTGGATGC	M17	58
5'Del	CGCATAACCAGTGAAACAGCAT	Del-Cre	58
Mx-CreR	GAAAGTCGAGTAGGCGTGTACG	Del-Cre	58

Table 1c: Primer combinations and expected sizes of PCR products for the typing of mice

PRIMERS	MOUSE STRAIN	ALLELE	PRODUCT [bp]
DinB1Seq6, DinB1Seq10	Polκ	WT	685
DinB1Seq6, DinB1Seq10	Polκ	FL	731
DinB1Seq6, DinB1Seq8	Polκ	WT	1655
DinB1Seq6, DinB1Seq8	Polκ	DEL	413

PT29, Seq9new	Polλ	WT	500
PT26, ScNeoRI	Polλ	DEL	600
MuexIInew, T2.14OAs	Polμ	WT	780
MuexIInew, ScNeoRI	Polμ	DEL	600
mRad30X2F, mRad30X2R *	Polι	WT	87
mRad30X2F, mRad30X2R *	Polι	DEL	47, 40
M17-FLS#87, M17-FLA#88	M17	WT	256
M17-FLS#87, M17-FLA#88	M17	FL	300
M17-FLS#87, M17-SAS#74	M17	DEL	500
5'Del, Mx-CreR	Deleter-Cre	Cre	600

* plus digestion of PCR product with TaqI

B1.6   Southern Blot Analysis

5-15 μg DNA were digested with 50 to 100 U of the appropriate restriction enzyme over night. Subsequently, the DNA fragments were resolved by agarose gel electrophoresis and transferred onto Hybond™-N+ (Amersham) by an alkaline capillary transfer according to the method of Chomczynski and Qasba (Chomczynski and Qasba, 1984). Membranes were baked at 80°C for 2 hours to fix the DNA, equilibrated in 2x SSC (Sambrook et al., 1989) and then prehybridized in hybridization solution (1M NaCl, 1% SDS, 10% dextran sulfate, 50 mM Tris-HCl pH 7.5, 500 μg/ml sonicated salmon sperm DNA) over night at 65 °C.

25 to 60 ng of probe DNA were radioactively labeled with 2.5 mC [$^{\alpha 32}$P]-dATP (Amersham) using the Ladderman™ Labeling Kit (Takara) Unincorporated radiolabeled nucleotides were removed with MicroSpinTM S-200HR columns (Pharmacia). The probe was denatured for 5 min at 95 °C before it was added to the hybridization solution. Washes were performed twice in 1 x SSC/0.1 % SDS and then followed by washes in 0.5 x SSC/0.1 % SDS and 0.25 x SSC/0.1 % SDS, if necessary. All washes were done at 65 °C under gentle agitation for 15 min to 1 hour. After each wash, the filter was monitored with a Geiger-counter. The washes were stopped when specific signals of no more than 100 cps were detectable. The membrane was sealed in a plastic bag and exposed to X-ray film (Kodak XAR-5 or BioMAX MR; Eastman Kodak) at –70 °C.

B1.7   Construction of the *Polκ* Targeting Vector

A phage library containing 129/Sv mouse genomic DNA (a gift from Pila Estess and Mark Siegelman, Department of Pathology, UT Southwestern, USA) cloned into the phage l 2001 vector was screened by plaque hybridization according to published protocols (Sambrook and Russell, 2001). Two different mouse *PolK (DinB1)* probes were used to screen the library: the 550 bp-Xba I/EcoN I fragment from pMDPH5'-0.7 (corresponding to mouse *Polκ* 5' UTR and amino acids 1-138) and the 700 bp-MDPH1C/4NC PCR product (corresponding to mouse Polκ amino acids 110 to 332). DNA
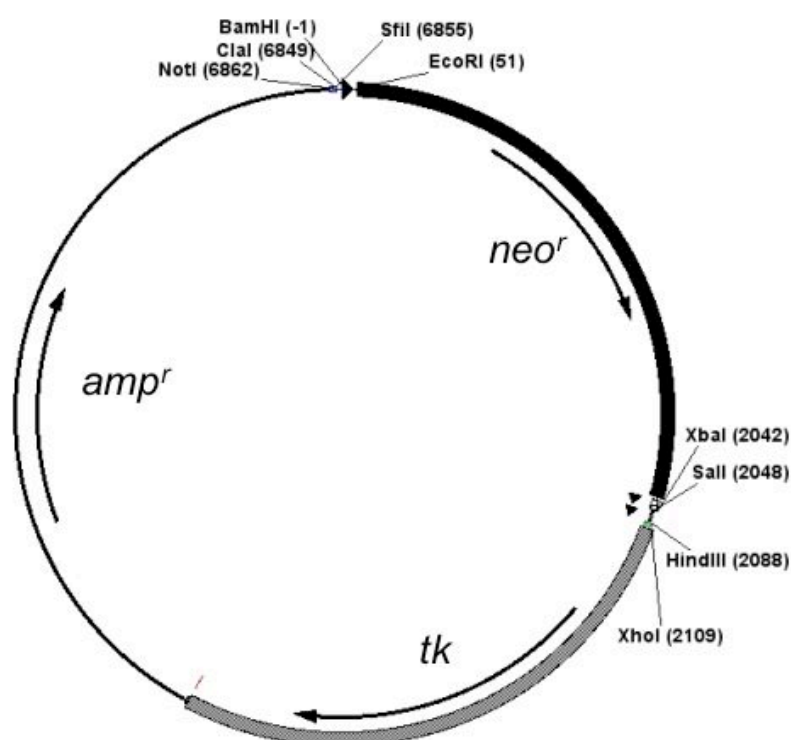
Figure 7. Drawing of the pEasyFLox vector. LoxP sites are represented as black triangles. *neo^r^, neomycin resistance* gene; *tk, thymine kinase* gene; *amp^r^, ampicillin resistance* gene.

from positively hybridizing plaques was isolated, cloned into pBlueScript, and subsequently sequenced. The sequences were assembled into contigs using the assembly software DNASTAR (the genomic clone was cloned in collaboration with Valerie Gerlach and Errol Friedberg, UT Southwestern Medical Center, Dallas, TX, USA).

A genomic subclone, p129Xh9, spanning exons 4-6 was used for the construction of the targeting vector. The targeting vector is based on the pEasyFlox(Pac) vector (Figure 7, M. Alimzhanov, unpublished), which contains a *neomycin resistance* gene under the control of the *phosphoglycerol kinase* promoter flanked by two *loxP* sites. An additional *loxP* site is placed downstream of the *neomycin resistance* cassette. An 800 bp fragment of genomic DNA located downstream of exon 6 was used as short arm of homology (SA). It was generated by PCR amplification with the Expand High Fidelity Kit (Roche), using the primers SABamFor1 and SANotBack, which introduced the restriction sites Not I and BamH I. Similarly, the primers LAXhoFor and LAXhoBack were used to amplify a 4.3 kb fragment including exon 5 for the long arm of homology (LA). A 1.3 kb fragment containing exon 6 was inserted into a Sal I site separating the second and third *loxP* site of pEasyFlox(Pac). The required Sal I sites in the PCR fragment were introduced with the primer pair Ex6SalForII and ExSalBack. All PCR products were first cloned into the T/A cloning vector pGEM-T easy (Promega) (plasmids pGEM-SA, pGEM-LA, and pGEM-Ex6) and then subcloned into the targeting vector. The exons and exon/intron boundaries were sequenced to confirm the absence of PCR-introduced errors.

B1.8   Construction of the M17 Targeting Vector

DNA fragments containing parts of the *M17* locus were obtained by screening a phage library containing C57BL/6 mouse genomic DNA. Two EcoR I-fragments were subcloned into the pBluescript II KS vector (pBS-IIKS). The first vector, designated pDS#9, contained a fragment of 6.9 kb encoding M17 exons 3, 4 and a part of exon 5 and the second vector, termed pDS#10, contained a fragment of 7.8 kb encoding M17 exon 5. A Sca I-EcoR I fragment was cut out of pDS#9 and a EcoR I-EcoR V fragment was cut out of pDS#10 and both fragments were cloned together into pBS-IIKS using the EcoR V restriction site. The new plasmid was termed pBS-M17LA1. Next, a EcoR V-fragment derived from pDS#9 was cloned into the EcoR V restriction site of pBS-IIKS, which contained a destroyed Xba I restriction site, and the new vector was named pBS-M17-EcoRV. To clone the *frt*-flanked SAS-IRIS-EGFP cassette, a 900bp-long Sca I-Sma I fragment containing a SAS internal ribosome entry site (*IRES*) was cut out from vector pCIN4(5257) and ligated into the Sma I restriction site of pGEM.FRTOR1. The correct orientation was confirmed by digestion with Xba I. Next, pGEM.FRTOR1 was digested with BamH I, filled in and relegated to generate plasmid p31HR123-EGFPII. The latter plasmid was digested with EcoR I and Sma I to obtain the first part of the EGFP cassette. The second part of the EGFP gene was cut out with Sma I and Age I from p31HR123-

EGFPII, which contained a second Sma I site downstream of the EcoR I site, and cloned into the Sma I and BamH I sites of the pGEM.FRTOR1 to generate the new plasmid pGEM-FRT-IRIS-EGFP. The second *frt* site was derived from pGEM-FRT. An EcoR I-BamH I fragment was cloned into pBSIIKS to create pBS-FRT. Next, the XhoI-fragment derived from pGEM-FRT-IRIS-EGFP was inserted into pBS-FRT using the EcoR V site. The new plasmid was named pGEM-FRT-IRIS-EGFP-FRT. The FRT-IRIS-EGFP-FRT cassette was cut out with Cla I and cloned into filled-in EcoR I site of pGEMloxP to introduce the 3rd l*oxP* site. Next, the Not I/Aat II-digested pGEM-loxP-FRT-IRIS-EGFP-FRT insert was cloned into pBS-M17-EcoR V using a Xba I restriction site. An EcoR V-Sal I fragment from pDS#10 was ligated into the EcoR V/Sal I-digested vector pBS-M17LA1 to generate pBS-M17LA2. The plasmid pMMneoFlox8 was opened with Not I filled with a Xba I/Sca I insert derived from pDS#9. The new plasmid was called pMMneo-flox-SA-M17. The latter plasmid was cut with Cla I and Xba I and the insert was ligated into the Sma I restriction site of pBS- M17-LA2, thus generating pBS-M17-SA-neo-LA2. Next, the pGEM-loxP-FRT-IRIS-EGFP-FRT was digested with EcoR V and the resulting fragment was ligated into the EcoR V site of pBS-M17-SA-neo-LA2. Finally, a fragment containing a *thymindine kinase* gene under the control of a *phosphoglycerol kinase* promoter was cut out with EcoR I and Hind III from plasmid pNT and was ligated into the BamHI restriction site of pBS-M17-SA-neo-LA2. The final targeting vector was named pBS-M17-TV. Plasmid pBS-M17-TV was linearized with in a Sal I for the transfection of embryonic stem cells. Construction of the M17 targeting vector was done by Angela Egert and Manolis Pasparakis.

B1.9   RNA isolation and RT-PCR

RNA was isolated from homogenized organs or single cell suspensions with Trizol (Invitrogen/Gibco) according to manufacturer's instructions. First strand synthesis was performed with the Thermoscript RT-PCR System (Invitrogen/Gibco) using the primer P2R annealing downstream of exon 6 between nt 1427 and 1453 of the published mouse *Polκ cDNA* sequence for analysis of Polκ. An oligoT primer was used for the first-strand synthesis of mRNA for the analysis of *M17* expression. PCR amplification was performed on 1/20 of the reverse-transcribed products.

Table 2a: Primers used for RT-PCR

NAME	SEQUENCE (5'-3')	LOCATION	T_{Ann} [C]
DinBfor	GCTAAGAGGCTCTGCCCACAAC	Polĸ, exon 5	58
DinB-P2R	CACTGAATGTCCTTTCAACACTCATGC	Polĸ, exon 7	58
M17Seq1	ATGGGGAACTGTTTGCAGAGGACAACCAG	M17, exon 1	57
M17Seq2	GGGAGCTGAAGTCATCCCTTCA	M17, exon 3	57
M17Seq3	CTTTGGAGACTCTTGTCTGGC	M17, exon 4	57
M17Seq4	GCTGTTGAAAGGCATGTGAGG	M17, exon 5	57
m-b-actinB	TCTTCATGGTGCTAGGAGCCA	β-actin	57
m-b-actinT	CCTAAGGCCAACCGTGAAAAG	β-actin	57

Table 2b: Primer combinations and expected sizes of PCR products obtained by RT-PCR

GENE	FIRST STRAND SYNTHESIS	PRIMERS	PRODUCT [bp]
Polĸ	DinB-P2R	DinBfor, DinBP2R	800
M17	oligo·dT	M17Seq1, M17Seq2	156
M17	oligo·dT	M17Seq1, M17Seq3	109
M17	oligo·dT	M17Seq1, M17Seq4	431

B2   Cell Biology Experiments

B2.1   Embryonic Stem Cell Culture and Generation of Mice

Embryonic stem (ES) cells were cultured described by Pasparakis and Kollias or Torres and Kuehn (Pasparakis and Kollias, 1995; Torres and Kuehn, 1997). ES cells were grown in ES cell medium (DMEM supplemented with 15 % FCS, 1 mM sodium pyruvate, 2 mM L-glutamine, non-essential amino acids, 1:1000 diluted LIF containing supernatant, and 0.1 mM 2-β-mercaptoethanol) on a layer of neomycin-resistant embryonic feeder (EF) cells. The FCS had been tested previously for the promotion of ES cell growth and maintenance of pluripotency. LIF was obtained from conditioned medium of the LIF-secreting cell line L929. EF cells were cultured in EF medium (DMEM supplemented with 10% FCS, 1 mM sodium pyruvate, 2 mM L-glutamine, and non-essential amino acids) for

a maximum of three passages. EF cells were mitotically inactivated with mitomycin-C (10 μg/ml for 2 h) 1 day before co-culture of ES and EF cells. ES cells were split before reaching confluence using trypsin (0.05 % trypsin, 0.02 % EDTA; GIBCO-BRL), supplemented the with 1% chicken serum.

For the generation of *Polκ*-targeted ES cell clones, 1×10^7 129-derived IB10 ES cells (Torres and Kühn, 1997) were transfected with 30 μg of Not I-linearized targeting vector by electroporation (500 mF, 230 V) in RPMI1640 without Phenolred (Gibco). 24 h post transfection, cells were subjected to selection with G418 (200μg/ml). Five days post transfection, cells were additionally subjected to selection with Gancyclovir (2 μM). Genomic DNA samples from double-resistant colonies were screened for homologous recombination by BamH I digestion and subsequent Southern blot analysis using an external 3' probe. The probe was obtained by PCR amplification with the primers DinProbeA-F2 and DinProbeA-Re using p129Xh9 as template. Co-integration of the third *loxP* site was confirmed using the internal probe B by digesting the genomic DNA of the targeted clones with Hind III. Probe B was excised from the plasmid pGEM-Ex6 using a Taq I/Sal I double restriction digest. The absence of random integrantion of the targeting vector was confirmed with a *neomycin resistance* gene-specific probe after digestion of genomic DNA with BamH I. Two correctly targeted ES cell clones were injected into blastocysts derived from CB.20 mice and transplanted into the uteri of CB.20 foster mothers.

C57BL/6-derived Bruce 4 ES cells were used for the targeting of the *M17* locus. Cells were transfected with 30 μg of Sal I-linearized targeting vector and subsequently subjected to G418 (170μg/ml) and Gancyclovir selection as described before. Homologous recombinants were identified by Southern hybridization of an EcoRI genomic restriction digest with the 5' probe A. Probe A was derived from plasmid pDS10 by double digestion with the Hinc II and Xba restriction enzymes. Co-integration of the third *loxP* site was confirmed by EcoR I digestion of genomic DNA using probe B. To obtain the 3' probe B, plasmid pDS9 was cut with Sal I, and the new religated plasmid was cut again with HinD III and subsequently Pst I to obtain a 1.3 kb fragment, which was used as probe. Finally, Cre-mediated deletion was confirmed with the internal probe C. The latter probe was generated by PCR with the primer pair MP57 and MP26 using plasmid pDS10 as template. Chimeric mice were derived from two correctly target ES cell clones that had been injected into blastocysts from CB.20 mice and transplanted into the uteri of CB.20 mice. M17 mice were generated by Angela Egert and Manolis Pasparakis.

B2.2   Preparation of Cell Suspensions from Lymphoid Organs

Isolated spleens, lymph nodes, Peyer's patches were kept in RPMI medium containing 3% FCS and squashed between frosted sides of two microscope slides to obtain single cell suspensions. Bones were flushed with medium to extract bone marrow cells and the peritoneal cavity was flushed with 10 ml of medium to recover cells. Erythrocytes were lysed from spleen and bone marrow preparations by incubation in lysis buffer for 3 min on ice (140 mM NH_4Cl, 17 mM Tris-HCl pH7.65). *Ex vivo* isolated cells were resuspended in B cell medium (DMEM, 5% FCS, 2 mM L-glutamine) and kept on ice.

B2.3   Flow Cytometry

10^6 cells per sample were surface stained in 50 µl PBS, 1 % BSA, 0.01 % N_3 with combinations of fluorescein isothiocyanate (FITC), phycoerythrin (PE), Cy-Chrome (Cyc), PERCP, or APC conjugated monoclonal antibodies (mAbs) for 15 min on ice. Stainings involving biotinylated mAbs were followed by a second staining step with streptavidin coupled to one of the fluorescent dyes. Subsequently, cells were washed and resuspended with PBS/BSA/N_3. Samples contained propidium iodide or Topro-3 for the exclusion of dead cells. Flow cytometry was performed on a FACScan or FACSCalibur and data were analyzed using CellQuest software (Becton Dickinson). All mAbs used in this study were either commercially available or prepared in our laboratory by C. Uthoff-Hachenberg, B. Hampel, and S. Willms. MAbs are listed in Table 3. Peanut agglutinin (PNA) coupled to either FITC or biotin was purchased from Vector Laboraties (USA).

Table 3. List of antibodies used for flow cytometry

Specificity	Clone	Reference and Manufacturer
IgM	R33-24.12	(Gruetzman, 1981), lab-made
IgD	1.3-5	(Roes et al., 1995), lab-made
IgMb	MB86	(Nishikawa et al., 1986), lab-made
IgG2ab	G12-47/30	(Seemann, 1981), lab-made
IgG2b	R14-50	(Müller, 1983), lab-made
IgE	95.3	(Baniyash and Eshhar, 1984), lab-made
B220/ CD45R	RA3-6B2	(Coffman, 1982), lab-made/Pharmingen
CD3e	145-211	(Leo et al., 1987), Pharmingen
CD4	GK.1.5/4	(Dialynas et al., 1983), Pharmingen

CD5	53-7.3	(Ledbetter and Herzenberg, 1979), Pharmingen
CD8	53-6.7	(Ledbetter and Herzenberg, 1979), Pharmingen
CD19	1D3	(Krop et al., 1996), Pharmingen
CD21/CD35	7G6	(Kinoshita et al., 1988), Pharmingen
CD23	B3B4	(Rao et al., 1987), Pharmingen
CD24/HSA	M1/69	Springer et al. 1978, Pharmingen
CD43	S7	(Gulley et al., 1988), Pharmingen
CD45Rb	16A	(Bottomly et al., 1989), Pharmingen
CD69	H1.2F3	(Yokoyama et al., 1988), Pharmingen
CD95 (Fas)	Jo2	Pharmingen
MHC class II	M5/114	(Bhattacharya et al., 1981), Pharmingen
HSA	30F1	(Ledbetter and Herzenberg, 1979), lab-made

B2.4   Magnetic Cell Sorting

Specific cell populations were either enriched or depleted from a heterogeneous cell suspension by magnetic cell sorting (MACS; Miltenyi Biotec, Bergisch Gladbach). The cells were incubated with antibody-coupled microbeads (10 μl beads, 90 μl PBS/BSA/N$_3$ per 10^7 cells) at 4 °C for 15 min and washed once in PBS/BSA/N$_3$. Next, the cells were applied to LD columns in a magnetic field (Miltenyi et al., 1990) and the columns were washed 3 times with 3 ml of PBS/BSA/N$_3$. MACS-purified cell populations were stained for specific surface markers to assess the purity of the populations. MACS-purification achieved typically a purity of 85%.

B2.5   Immunohistochemistry.

Immunostaining was performed on a BioTek Solutions TechMate 1000 automated immunostainer (Ventana BioTek Systems, USA). Buffers, blocking solutions, streptavidin/biotin complex reagents and chromogen were used as supplied in the Level 2 USA UltraStreptavidin Detection System purchased from Signet Laboratories (Dedham, MA). Biotinylated secondary antibody was purchased from Vector Laboratories (Burlingame, USA) Heat-induced epitope retrieval (HIER) buffer was obtained from BioPath (Oklahoma City, USA). Paraffin sections were cut at 3 micron a rotary microtome, mounted on positively charged glass slides (POP100 capillary gap slides, Ventana BioTek Systems), and air dried overnight. Sections were deparaffinized and quenched with fresh

3% hydrogen peroxide to inhibit endogenous tissue peroxidase activity. HEIR was then performed using HIER buffer, pH 6.8 followed by incubation in unlabeled blocking serum solution to block non-specific binding of secondary antibody. Sections were incubated for 4 hours either with a primary monoclonal antibody to mouse Polκ protein at a 1:10 dilution in antibody diluent, or with antibody diluent alone as a negative reagent control. Sections were incubated with biotinylated goat antibodies to hamster immunoglobulin, with horseradish peroxidase-conjugated Streptavidin-biotin complex, followed by diaminobenzidine (DAB) and H_2O_2 in substrate buffer. Sections were counterstained with Mayer's hematoxylin and examined by light microscopy. Immunohistochemistry was done in collaboration with the Friedberg laboratory at the Southwestern Medical Center, Dallas, USA.

B2.6   Immunofluoresence

Mice were immunized with 50 µg NP-CG. 14 days post immunization, spleens or Peyer's patches were embedded in OTC and frozen in methyl butane that was cooled in liquid nitrogen. The frozen organs were cut by the Pathology Core Facility of the Brigham's and Women Hospital, Boston, USA. Frozen sections were fixed in cold acetone, air-dried and rehydrated in PBS and subsequently incubated with blocking buffer (PBS containing 1% BSA and 5% goat serum) for 30 min. Next, the sections were incubated with a mixture of either rat anti-mouse CD19 (Pharmingen) and biotinylated PNA (Biosearch) or rat anti-mouse FDCM1 (Pharmingen) and biotinylated PNA for 30 min. Following 3 washes in PBS, the sections were stained with a mixture of goat anti-mouse IgG1-FITC and streptavidin-PE for 30 min. Sections were washed again in PBS, mounted with Fluorotec medium, and examined by fluorescence microscopy.

B2.7   Sensitivity of Mouse Embryonic Fibroblasts to UV Radiation.

Mouse embryonic fibroblasts (MEFs) were isolated from day 13.5 embryos as described in Meira et al. (Meira et al., 2001). Survival following exposure to UV radiation was measured essentially as described by McWhir et al. (McWhir et al., 1993). Briefly, cells at passage 6 were plated at a density of 3×10^5 cells/60-mm dish. The following day the medium was aspirated and cells were irradiated with 0, 1.6, 3.2, 4.8 and 6.4 J/m^2 of UVC radiation at a fluence of 0.8 $J\ m^{/2}\ s^{-1}$. Medium was replaced and the dishes were incubated for 4 days. Cells were washed with PBS, fixed and stained with crystal violet. The extent of cell growth and survival in individual dishes was determined by measuring the incorporation of crystal violet in viable cells. Fixed cells were treated with 70% ethanol

and the percentage of incorporation was determined by measuring optical density at 575 nm. Each dose point was performed in triplicate and results were confirmed in multiple independent experiments. Survival relative to unirradiated controls at each dose was calculated as the ratio of the mean OD_{575} of each dose/mean OD_{575} of unirradiated controls, expressed as a percentage. $Xpc^{-/-}$ homozygous mutant MEFs were used as a control (Cheo et al., 1997). The experiments were done in collaboration with Friedberg laboratory at the Southwestern Medical Center, Dallas, USA.

B2.8   CFSE Labeling

Splenic B cells were enriched by the depletion of $CD43^+$ cells using the MACS system (CD43 magnetic beads, LD columns, Miltenyi). Cells in the flow-trough were spun down, washed 3 times with PBS, and resuspended in 1 ml/10^7 cells of 2.5 µM CFSE (5 mM stock in DMSO, Molecular Probes) in PBS at 37 °C for 10 min (Lyons and Parish, 1994). The labeling reaction was stopped by addition of 10 ml ice-cold DMEM medium containing 10% FCS. The cells were washed once in medium, plated in B cell medium at 2 x 10^6 cells per well in 12-well plates, and stimulated with 10 µg/ml αIgM mAb (Pharmingen), 10 µg/ml αIgM mAb and 25 ng/ml IL-4 (R&D Systems), 20 µg/ml LPS, 20 µg/ml LPS and 25 ng/ml IL-4, 0.5µg/ml anti-CD40 mAb (clone HM40-3, Pharmingen), or 0.5µg/ml anti-CD40 mAb and 25 ng/ml IL-4. The cells were harvested three days after stimulation and analyzed by flow cytometry.

B2.9   ELISA - Serum Analysis

Ig serum concentrations were determined by enzyme-linked immunosorbent assays (ELISA) as described in Roes and Rajewsky (Roes and Rajewsky, 1993). Microtiter plates (Costar) were coated with NP-BSA or antibodies of known isotype (see table 4) in PBS at 4 °C over night, and subsequently blocked at room temperature for 30 min with PBS, 0.5 % BSA, 0.01 % N_3, pH 7.2. Serially diluted sera samples were applied to the wells and incubated at 4 °C over night. Next, the plates were incubated with a secondary biotinylated anti-Ig antibody at 37 °C for 1 hour, followed by the incubation with SA-conjugated alkaline phosphatase (AP, Roche) at room temperature for 30 min. The amount of bound AP was detected by incubation with p-nitrophenylphosphate as substrate (Roche). Following each incubation step, unbound antibodies or SA-conjugated AP were removed by 3 washes with tapwater. The OD_{405} was measured with an ELISA-photometer (Spectramax 340, Molecular Devices) and the relative antibody concentrations were determined by comparison to a standard curve. Affinities of NP-specific IgG1 and Igλ

antibodies were determined by calculating the association constant as described by Cumano and Rajewsky (Cumano and Rajewsky, 1986), following a method developed by Herzenberg et al. (Herzenberg and Black, 1980).

Table 4. Reagents used to determine serum antibody isotypes.

Coating	Biotin-Conjugate	Specificity	Standard
R33-24.12	goat anti-mouse IgM (SBA)	IgM	B1-8μ
goat anti-mouse IgG1 (Sigma)	goat anti-mouse IgG1 (SBA)	IgG1	N1G9
rat anti-mouse IgG2a (Nordic)	goat anti-mouse IgG2a (SBA)	IgG2a[a]	41.2-3
G12-47/30	G12-47/30	IgG2a[b]	S43-10
R14-50 goat anti-mouse	IgG2b (SBA)	IgG2b	D3-13F1
2E.6 goat anti-mouse	IgG3 (SBA)	IgG3	S24/63/63
goat anti-mouse IgA (Sigma)	goat anti-mouse IgA (SBA)	IgA	IgA 233.1.3
95.3	rat anti-mouse IgE (Pharmingen)	IgE	B1-8e
187.1	R33-18-10.1	Igκ	S8
NP-BSA	goat anti-mouse IgM (SBA)	NP-IgM	B1-8μ
NP-BSA	goat anti-mouse IgG1 (SBA)	NP-IgG1	N1G9
NP-BSA	goat anti-mouse λ (SBA) - LS136	NP-Igλ	N1G9
NP-BSA	goat anti-mouse κ (SBA)	NP-Igκ	S8

B2.10 Analysis of Class Switch Recombination

B cells were purified from splenic single cell suspensions by MACS-depletion using anti-CD43 microbeads (Miltenyi Biotech). Subsequently, the cells were cultured at a concentration of 10^6 cells/ml and stimulated with either 20 µg/ml LPS alone, 20µg/ml LPS and 2ng/ml IFN-γ (R&D Systems), 20µg/ml LPS and 2ng/ml TGFγ (R&D Systems), or 0.5µg/ml anti-CD40 mAb (clone HM40-3, Pharmingen) and 25 ng/ml IL-4 (R&D Systems). Cells were cultured for 5 days during which the cell numbers were kept constant by addition of fresh medium. The percentage of class switched cells was determined on day 4 or day 5 by flow cytometry.

B2.11 Somatic Hypermutation Analysis

14 days post immunization with 100 μg NP-CG, splenic GC B cells were enriched by magnetic cell seperation using the MACS system (Miltenyi Biotech). After erythocyte lysis, splenocytes were first incubated with an anti-IgD-biotin mAb (clone 1.3-5, ref.), followed by a combination of streptavidin- and anti-CD43-microbeads (Miltenyi Biotech). The cells were then subjected to an LD separation column (Miltenyi Biotech). GC B cells (B220$^+$PNA^{high}) were purified from the flow through by fluorescence-assisted cell sorting (FACS) using an anti-B220-fluorecein isothiocyanate (FITC) mAb (clone R33-24.12, ref.) and peanut agglutinin (PNA) coupled to phycoerythrin (PE). Likewise, naïve B cells (B220$^+$IgD$^+$) were isolated from the eluate with anti-IgD-FITC (clone 1.3-5) and anti-B220-PE (clone R33.24-12) mAbs. Cells were sorted on a FACS 440 cell sorter (Becton Dieckinson). Alternatively, GC B cells from spleen or Peyer's patches were purified directly after incubation with PNA-FITC, anti-Fas-PE mAb and anti-B220-Cyc mAb on a FACSVantage cell sorter (Becton Dickinson) into a naïve fraction (B200$^+$PNA^{low}Fas^{low}) and a GC fraction (B220$^+$PNA^{high}Fas^{high}).

Sorted cell populations were lysed in 50 µl/10^5 cells of 10 mM Tris•HCl and 0 .5 mg/ml proteinase K (Roche) for 2.5 h at 50∞C, followed by the denaturation of proteinase K at 95∞C for 10 min. For the analysis of somatic mutations, PCR fragments were obtained using primer pair J558Fr3 5'-CAGCCTGACATCTGAGGACTCTGC and JHCHint 5'-CTCCACCAGACCTCTCTAGACAGC. Primer J558Fr3 anneals in the framework 3 region of most J558 V genes and primer JHCHint hybridizes in the intron 3' of exon J$_H$4 (Jolly et al., 1997). PCR amplification was done with a 60/1 mixture of Taq and Pfu DNA polymerase from 20 µl of cell lysate in a total volume of 50 µl (30 s at 95∞C, 30 s at 65∞C and 2 min at 72∞C, 32 cycles). Alternatively, the Expand High Fidelity Kit (Roche) was used. Subsequently, the PCR products were purified with a QiaEx II Kit (Qiagen) and incubated for 15 min at 72°C with Taq polymerase to produce A-overhangs. PCR products were ligated into the A/T-cloning vector pGEM-T easy (Promega). Plasmids were isolated using the GFX Micro Plasmid Prep Kit (Pharmacia) and sequenced by dye-terminated automatic sequencing (Applied Biosystems) using primers JHCHint and JHCHj.2 (5'-ACTATCCCTCCAGCCATAGG). A 500 nt stretch of intron sequence was analyzed with the GeneJockey II software (Biosoft). Mutation frequencies were calculated as the total number of mutations devided by the number of sequenced nucleotides in mutated sequences.

B3   Mouse Experiments

Mouse experimental procedures like vasectomy of males, tail bleeding as well as breeding of foster mothers and the general handling, marking of mice were performed according to Hogan (Hogan et al., 1987) and Silver (Silver, 1995). Blastocyst injection of ES cells was performed by Angela Egert and Anke Leinhaas.

B3.1   Mice

C57BL/6 and 129/Sv mice were obtained from Bomholtgard, Charles River, Harlan Winkelmann, or Jackson Laboratories. CB20 mice were taken from breedings in our animal facility. *Deleter* mice (Schwenk et al., 1995) were intercrossed with chimeras harboring the *loxP*-flanked *Polκ* allele to generate a mouse strain deficient of Polκ. *Polκ$^{-/-}$* mice were kept on a mixed genetic background of 129/Ola and C57BL/6. *Polμ$^{-/-}$*and *Polλ$^{-/-}$* mice were generated in our laboratory by Gloria Esposito in collaboration with Luis Blanco (Universidad Autonoma de Madrid, Madrid, Spain). *Polμ$^{-/-}$* mice were kept on a C57BL/6 genetic background, while *Polλ$^{-/-}$* mice were kept on 129/Ola genetic background. To generate compound mutants of DNA polymerase-deficient mice, *Polκ$^{-/-}$* mice were crossed with either *Polμ$^{-/-}$* or *Polλ$^{-/-}$* mice to generate *Polκ$^{-/-}$Polμ$^{-/-}$* and *Polκ$^{-/-}$Polλ$^{-/-}$Polι$^{-/-}$* strains. The latter two strains were intercrossed to produce compound mutants deficient of Polκ, Polμ, Polλ, and Polι. *M17$^{-/-}$* mice were generated in our laboratory by Angela Egert and Manolis Pasperakis. Mice containing the floxed *M17* allele were intercrossed with *Deleter-Cre* mice. Mice carrying a deleted M17 allele were crossed to homozygosity and kept on a pure C57BL/6 genetic background.

All mice used in this study were derived from single ES cell clones. Mice were at an age of 8 to 14 weeks at the time of analysis. One analysis of SHM in *Polκ$^{-/-}$* mice was performed with 8 month-old mice derived from an independent ES cell clone (referred to as *Polκ$^{-/-}$**).

B3.2   Immunizations

Primary T-dependent antigen responses were induced with alum-precipitated NP-CG (4-hydroxy-3-nitrophenylacetyl coupled to chicken γ-globulin) (Weiss and Rajewsky, 1990). The immunogen was prepared by mixing of NP-CG (1 mg/ml in PBS) and 10 % KAl(SO$_4$)$_2$ in a volume of 1:1. The solution was adjusted to pH 6.5 with 5N NaOH and kept on ice for 30 min. After the incubation, the precipitate was washed three times in PBS and resuspended in PBS. Mice were immunized by intra-peritoneal injections with 10, 50 or

100 µg NP_{16-36}-CG in a volume of 200 µl. For secondary immunizations, mice were injected intra-peritoneally with 10 µg NP-CG without alum in 200 µl PBS.

C.   RESULTS

C1   The Function of DNA Polymerase κ

C1.1   Generation of Polκ-Deficient Mice

To investigate the role Polκ in the mouse, I generated a conditional *Polκ* allele by gene targeting. I flanked exon 6 of the *Polκ* (*DinB1*) gene with *loxP* sites rendering it susceptible to Cre recombinase-mediated deletion. Additionally, I introduced a *loxP*-flanked *neomycin resistance* (*neo^r*) gene as selection marker. Exon 6 was chosen for two reasons. First, it contains two essential catalytic residues: Aspartate 197 and Glutamate 198. Replacement of these two amino acids by alanine residues results in a complete loss of the DNA polymerase function *in vitro* (Ogi et al., 1999; Ohashi et al., 2000). Second, mRNA splicing from exon 5 to exon 7 leads to a frame-shift mutation. The wild-type *Polκ* locus, the modified locus after homologous recombination with the targeting vector and the locus after Cre-mediated recombination are depicted in Figure 8A. Two independent embryonic stem (ES) cell clones containing the *loxP*-flanked exon 6 and the *neo^r* gene were used to generate chimeric mice; both transmitted the targeted allele into the germline. Conventional *Polκ* knock-out mice were generated by crossing the chimeras to a *deleter* mouse (Figure 8B). Mice homozygous for the deletion of exon 6 are viable, present at the expected Mendelian ratio and do not exhibit obvious abnormalities. In contrast to Polζ (Bemark et al., 2000; Esposito et al., 2000a; Wittschieben et al., 2000) and Polβ (Gu et al., 1994b; Sugo et al., 2000), lack of Polκ protein does not interfere with embryonic development. To create a conditional allele for *Polκ*, I deleted the *neo^r* gene in the two targeted ES cell clones *in vitro* by transfection of a Cre-expressing plasmid. Two ES cell clones deficient of the *neo^r* gene but retaining the loxP-flanked (floxed) exon were used to generate chimeras, which both transmitted the floxed *Polκ* (*Polκ^fl*) allele into the germline (not shown).
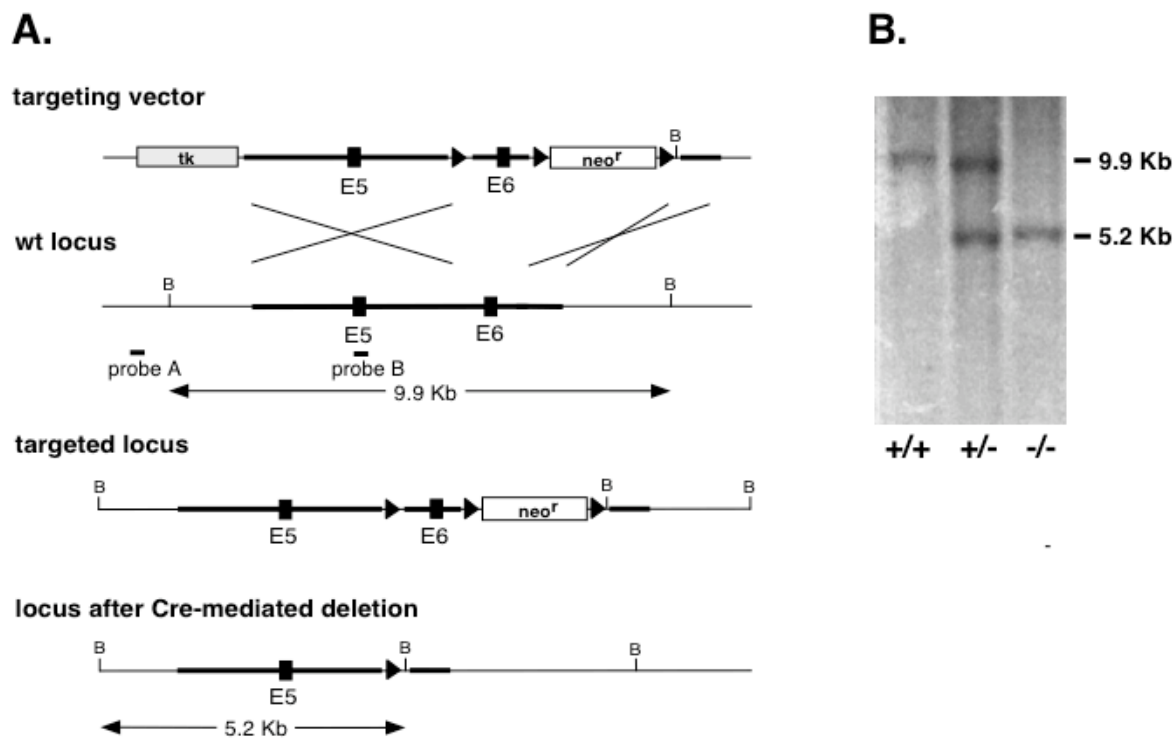
Figure 8. Generation of *Polκ*^{-/-} mice. (A) Schematic representation of the gene targeting in the *Polκ* locus by homologous recombination. 129/Ola-derived ES cells were targeted with a vector containing the *loxP*-flanked exon 6 and a *neomycyin resistance* cassette for positive selection. A *thymidine kinase* gene was used to select against random integration of the vector. ES cells were screened by Southern blot of BamH I-digested DNA with the external probe A located at the 5' end. Rectangles represent coding DNA, filled triangles indicate *loxP* sites, and bold lines show regions of homology. E, exon; B, BamH I site; tk, *thymidine kinase* gene; neo^r, *neomycin resistance* gene. Only exons 5 and 6 of the wild-type locus are shown. **(B)** Cre-mediated deletion of exon 6 and the *neomycin resistance* cassette. A Southern blot of BamH I-digested tail DNA from wild-type, heterozygous and homozygous mice, respectively, is shown. Probe B containing exon 5 of the *Polκ* locus was used. The wild-type fragment migrates at 9.9 kb and the fragment from the targeted locus migrates at 5.2 kb.

To confirm the inactivation of the *Polκ* gene, I amplified *Polκ* transcripts from testis by RT-PCR using primers spanning exon 6. As shown in Figure 9A, cDNA from *Polκ*$^{+/+}$ mice gave rise to two alternative splice-products. In contrast, cDNA from *Polκ*$^{-/-}$ mice gave rise to one PCR product only, which was shorter than the larger wild-type product and consistent with the lack 153 basepairs corresponding to exon 6 in the mRNA (Figure 9A), as confirmed by sequencing (not shown). Additionally, Northern blot analysis using equal amounts of mRNA from wild-type and mutant mice revealed that the intensity of the band from the latter was 5 times less than the band from the wild-type sample (Figure 9B). The presence of a frameshift mutation leading to premature stop codons presumably renders mRNA lacking exon 6 less stable than wild-type mRNA.

In collaboration with Errol Friedberg and Valerie Gerlach (E. C. F. and V. G., Southwestern Medical Center, Dallas, TX, USA), I analyzed histological sections of mouse testis by immunohistochemistry to confirm the absence of Polκ protein in the mutant mice. Frozen sections of testis from either wild-type or *Polκ*-deficient mice were incubated with a monoclonal antibody against human Polκ protein. Polκ protein was mainly localized in the nuclei of spermatocytes and round spermatids of the seminiferous tubules in wild-type animals (Figure 9C). In contrast, no signal could be detected in mice homozygous for the deletion of exon 6 (Figure 9C).

C1.2   Polκ-Deficient Mice are Fertile

As shown in Figure 7C, the overall histological structure of the testis from Polκ-deficient mice is indistinguishable from that of wild-type controls. I also failed to detect abnormalities in the shape and mobility of sperm cells from mice lacking Polκ. Furthermore, both male and female Polκ mutants are fertile and the litter size does not differ from wild-type mice (data not shown). At the present time, the functional significance of the high levels of tissue-specific expression of Polκ in the

A.

B.

C.
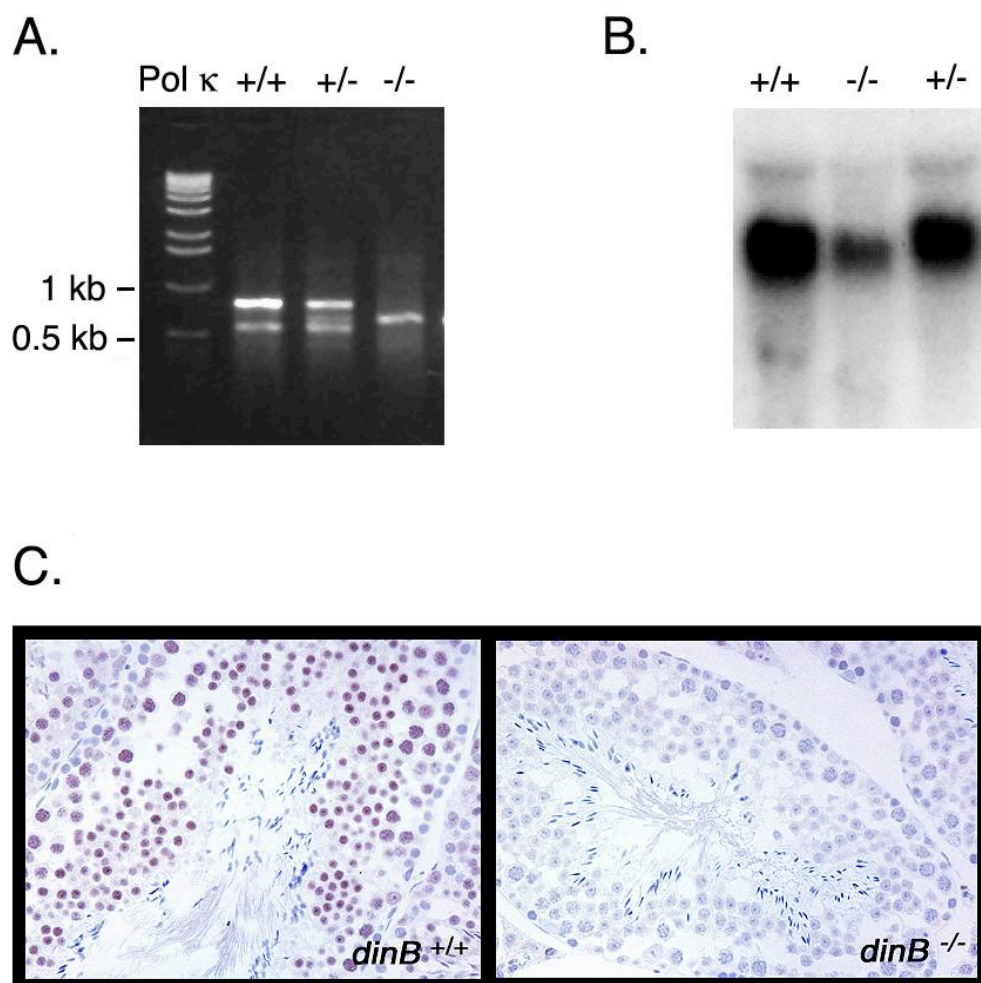
Figure 9. *Polκ^{-/-}* mice are unable to express Polκ. (A) RT-PCR of *Polκ^{+/+}*, *Polκ^{+/-}* and *Polκ^{-/-}* mice with primers annealing in exon 5 and downstream of exon 6, respectively. **(B)** Northern hybridization of equal amounts of RNA from *Polκ^{+/+}* and *Polκ^{-/-}* mice with a *Polκ-specific* probe spanning nucleotide 483 to nucleotide 1493 of the cDNA sequence. **(C)** Immunohistology of sections from testis with a monoclonal antibody against human Polκ. Shown are sections from a wild-type mouse (left panel) and from a Polκ-deficient mouse (right panel). Figure 9B and C was done in collaboration with E. C. F. and V. G.

mouse testis is not clear. Several other error-prone DNA polymerases are also highly expressed in the testis. In particular, Polλ and Polι share a similar expression pattern with Polκ (Garcia-Diaz et al., 2000; McDonald et al., 1999). It was therefore conceivable that Polκ, Polλ and Polι serve overlapping functions in the testis and in *Polκ*⁻/⁻ mice the other two polymerases may compensate for the loss of Polκ activity. However, compound mutants deficient of Polκ, Polλ, and Polι are fertile and produce litters of normal size (data not shown).

C1.3 Polκ-Deficient Embryonic Fibroblasts are Sensitive to Killing by UV Radiation

Base damage can stall or arrest normal DNA replication. Polymerase κ is one of multiple specialized DNA polymerases that may be used in cells to bypass such sites of DNA damage. Purified Polκ is not able to bypass thymine dimers, [6-4] photoproducts (quantitatively major photoproducts produced by UV radiation) or cisplatin lesions *in vitro* (Gerlach et al., 2001). However, the purified enzyme is able to extend from mismatched termini opposite of thymine dimers (Washington et al., 2002) and can bypass thymine glycol lesions *in vitro* (Fischhaber et al., 2002). Thymine glycols are a form of oxidized thymine that can be produced by various treatments of cells, including exposure to UV radiation. Therefore, I compared the sensitivity of embryonic fibroblasts (MEFs) from homozygous mutant and wild-type Polκ mice to UV light (in collaboration with E. C. F. and V. G.). As shown in Figure 10, the Polκ-deficient cells are moderately sensitive to UV radiation as measured by crystal violet staining and are comparable to MEFs from homozygous mutant *Xpc*⁻/⁻ mice defective in genome-wide DNA repair but proficient in transcription-coupled nucleotide excision repair (Cheo et al., 1997). These results indicate that in the absence of Polκ, some form of UV radiation damage (possibly thymine glycol) results in cell death.
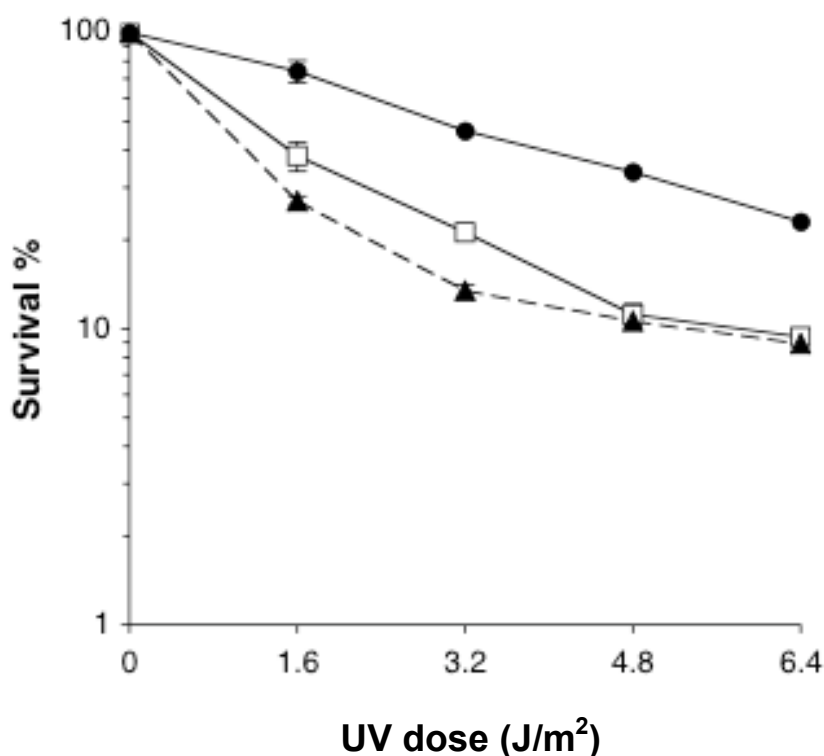
Figure 10. Polκ-deficient cells are abnormally sensitive to killing following exposure to UV radiation. Mouse embryonic fibroblasts were irradiated with UV light. The survival of the cells was scored four days later by crystal violet staining. Closed circles $Pol\kappa^{+/+}$ MEFs; closed triangles, $Pol\kappa^{-/-}$ MEFs; open squares $Xpc^{-/-}$ MEFs.

C1.4 Polκ-Deficient Mice Show Normal B and T Cell Compartments

Cellular proliferation or viability may be impaired by the absence of a DNA polymerase. Hence, I investigated whether Polκ-deficiency affects the size of B and T cell compartments. B and T cell development occurs normally in Polκ-deficient mice (not shown). Likewise, B and T cells subsets are present at normal numbers in the spleen (Figure 11A). T cells subsets are also present in normal numbers in the spleen (data not shown).

GC B cells represent a highly proliferating cell population. They may be particularly affected by the absence of Polκ. Polκ-deficient mice and wild-type controls were immunized with NP-CG and monitored for the presence of GC B
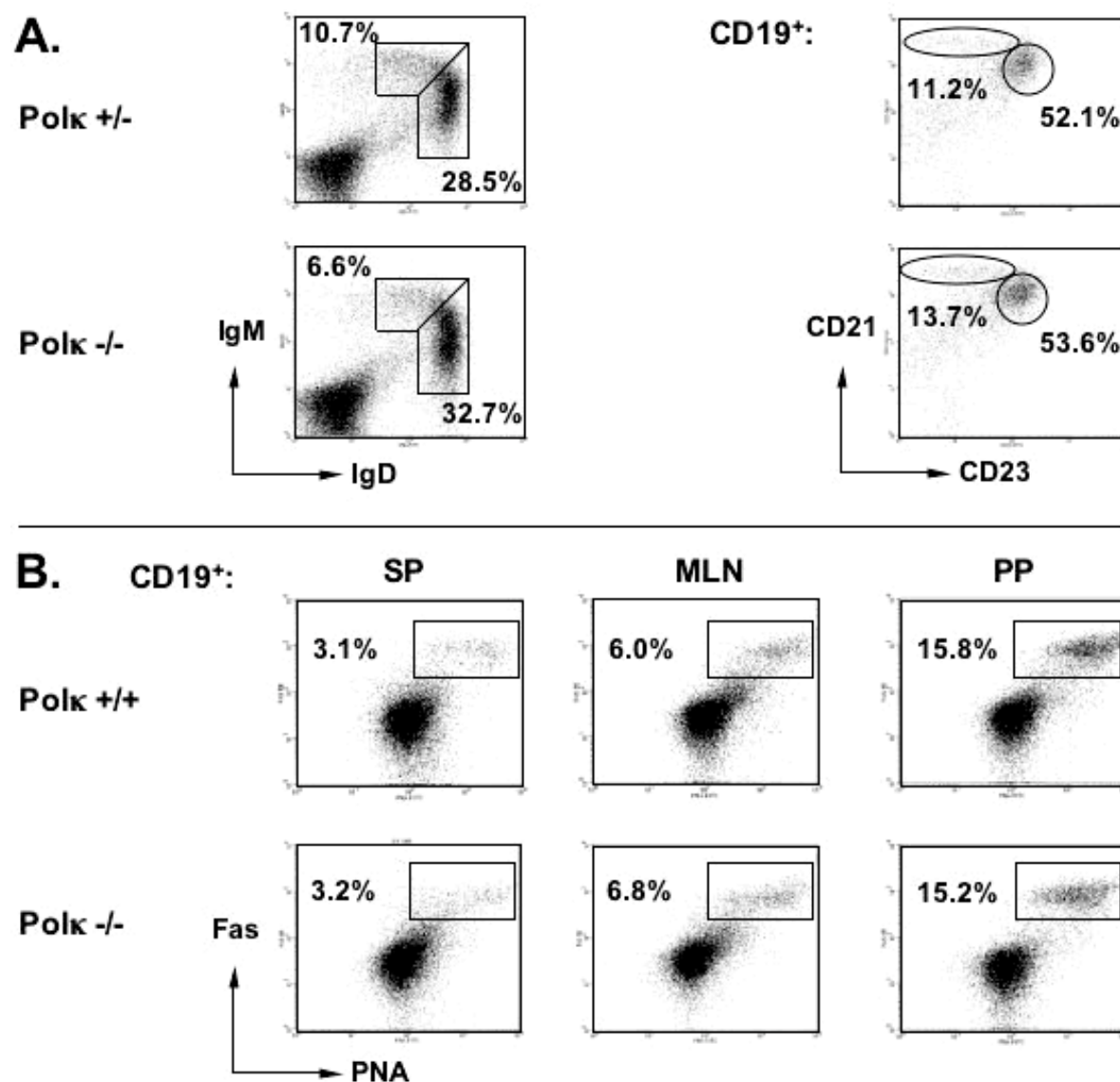
Figure 11. B cell populations in spleen (A) and GC B cells in spleen, mesenteric lymphnodes, and Peyer's patches (B). (A) Splenocytes were stained with α-IgM and α-IgD mAbs to visualize IgM^{high}IgD^{low} immature and mature IgM^{low}IgD^{high} B cell populations. CD21^{high}CD23^{low} MZ and follicular CD21^{low}CD23^{high} B cells are shown by staining with α-CD21 and α-CD23 mAbs. Only CD19^{+} cells are shown. **(B)** Mice were immunized with 50 μg NP-CG and analyzed for the presence of CD19^{+}PNA^{+}Fas^{+} GC B cells 14 days post immunization. Only CD19^{+} cells are shown. SP, spleen; MLN, mesenteric lymph nodes; PP, Peyer's patches.

cells 14 days later. However, I did not observe any significant variations between the two cohorts with respect to CD19$^+$Fas$^+$PNA^{high} GC B cells in spleen, mesenteric lymph nodes, and Peyer's patches (Figure 11B). Thus, Polκ is not required for B and T cell development and is unlikely to influence cell proliferation during an immune response.

C1.5 Polκ-Deficient Mice respond to the T Cell-Dependent Antigen NP-CG and Display Normal Serum Ig Titers

The mechanisms of SHM and CSR share common elements (Ehrenstein and Neuberger, 1999; Muramatsu et al., 2000; Nagaoka et al., 2002; Reina-San-Martin et al., 2003; Revy et al., 2000). Therefore, I measured the serum levels of the different Ig isotypes of Polκ-deficient mice and wild-type controls by ELISA to investigate whether in Polκ-deficient mice can undergo CSR and form antibody-secreting plasma cells. As shown in Figure 12A, Polκ-deficient mice are able to generate antibodies of all isotypes at levels comparable to wild-type controls. Hence, Polκ-deficiency is unlikely to affect CSR and the generation of plasma cells.

Next, I investigated whether *Polκ$^{-/-}$* B cells are able to mount an efficient T cell-dependent immune response and differentiate into plasma cells secreting antigen-specific IgG1. Groups of four age-matched mice were immunized with (4-hydroxy-3-nitrophenyl) acetyl-chicken globulin (NP-CG) and the levels of NP-specific IgG1 were determined 14 days later. The serum levels of NP-specific IgG1 are similar in *Polκ$^{-/-}$, Polκ$^{+/-}$, Polκ$^{+/+}$ and Polκ$^{fl/fl}$* mice (Figure 12A). Thus, Polκ-deficient B cells are able to participate in T-cell dependent immune responses similarly to control B cells and efficiently secrete antigen-specific antibodies.

C1.6 Polκ-Deficient GC B Cells Mutate Their Ig Genes Efficiently

To investigate whether Polκ is involved in SHM of Ig genes, groups of 7-9 week (2 *Polκ$^{-/-}$*, 2 *Polκ$^{+/-}$* and 1 *Polκ$^{fl/fl}$* animals) and 8 month (2 *Polκ$^{-/-}$* mice, designated *Polκ$^{-/-}$**) old mice were immunized with NP-CG. 14 days post immunization, GC B cells were isolated and analyzed for the level and
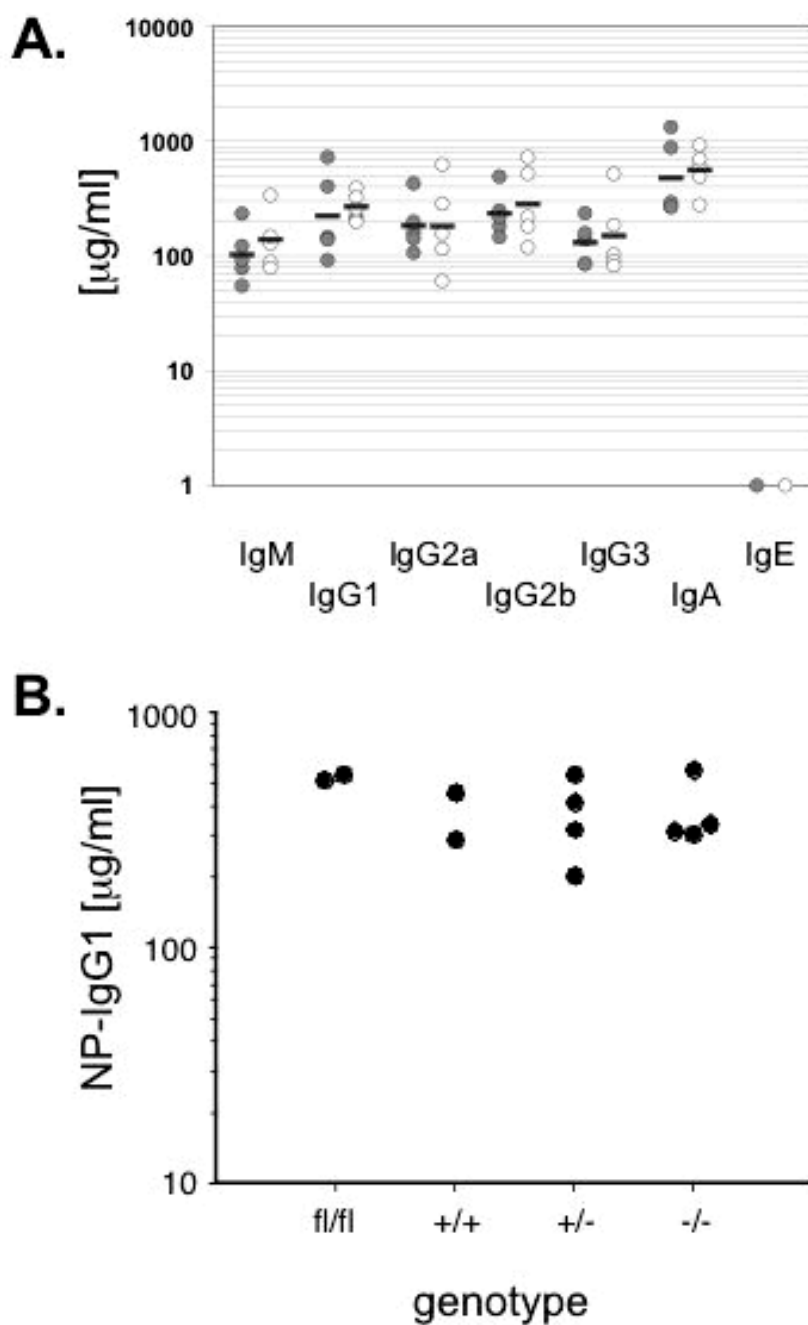
Figure 12. Antibody titers in serum (A) and antibody response to NP-CG (B) of Polκ-deficient mice. (A) Antibody titers in the serum of unimmunized wild-type (closed circle) and Polκ-deficient (open circle) mice as determined by ELISA. Black bars indicate the geometric means. **(B)** Antibody response of Polκ-deficient mice and control mice to NP-GC. Mice were immunized with NP-CG and the serum concentrations of NP-specific IgG1 were measured 14 days post immunization in an ELISA assay. Each dot represents the serum titer of an individual mouse. Polκ genotypes are as indicated.

pattern of somatic mutations. To study the intrinsic features of the hypermutation process, I analyzed the accumulation of mutations in the intronic sequence downstream of the rearranged V gene as previously described (Jolly et al., 1997). GC B cells (B220$^+$PNA$^+$) and naïve B cells (B220$^+$PNA$^-$IgD$^+$) were isolated by FACS-purification from spleens of immunized $Pol\kappa^{-/-}$, $Pol\kappa^{+/-}$, and $Pol\kappa^{fl/fl}$ mice (spleens from age matched mice with identical genotype were pooled). All mice responded to the NP-CG immunization, as demonstrated by the elevated levels of NP-specific IgG1 antibodies in the blood (data not shown).

Genomic DNA from the FACS-purified cells was PCR-amplified from 40,000 cell equivalents using primers annealing in the framework region 3 of most members of the J558 V gene family (Jolly et al., 1997) and in the intron downstream of the J$_H$4 gene segment (see Materials and Methods), thus covering a large fraction of rearranged V genes. PCR products were cloned and sequenced. All sequences analyzed showed unique rearrangements.

In agreement with previous analyses (Esposito et al., 2000b; Gu et al., 1991), the vast majority of the sequences derived from the naïve B cell population

Table 5. Analysis of somatic hypermutation of the JH-CH intron of splenic GC B cells from $Pol\kappa^{-/-}$, $Pol\kappa^{+/-}$ and $Pol\kappa^{fl/fl}$.

genotype	clones	mutated clones	range (mut./clone)	mutations/bp	% mutations
$Pol\kappa$ -/-	28	22	1-15	104/10679	1.0
$Pol\kappa$ -/- *	19	19	1-15	108/9485	1.1
$Pol\kappa$ +/-	21	18	1-17	111/8363	1.3
$Pol\kappa$ fl/fl	20	15	1-14	72/7975	0.9

% mutations in naïve B cells:	$PolK$ -/-	0.04
	$PolK$ -/-*	0.02

$Pol\kappa^{-/-}$* mice: 8 months old

Polκ fl/fl	n = 72	to				Sum	Tr./Tv.
		A	G	C	T		
from	A	—	19.5	7	5.5	32	
	G	14	—	7	4	25	1.1
	C	3	4	—	8.5	15.5	
	T	9.5	7	11	—	27.5	

Polκ +/-	n = 111	to				Sum	Tr./Tv.
		A	G	C	T		
from	A	—	19	11.5	10	40.5	
	G	13.5	—	3.5	5.5	22.5	1.0
	C	2	7	—	7	16	
	T	8	2	10	—	20	

Polκ -/-	n = 109	to				Sum	Tr./Tv.
		A	G	C	T		
from	A	—	22	9.5	14.5	46	
	G	14.5	—	5	6.5	26	1.2
	C	1	4	—	7.5	12.5	
	T	4	2	9.5	—	15.5	

Polκ -/-*	n = 108	to				Sum	Tr./Tv.
		A	G	C	T		
from	A	—	17.5	11	5.5	34	
	G	14	—	9	6.5	29.5	1.0
	C	6.5	4	—	9	19.5	
	T	4.5	2	10	—	16.5	

Figure 13. SHM patterns in Polκ-deficient mice. Patterns of nucleotide exchanges in a 500 bp-long region in the intron downstream of the rearranged $V_H D_H J_H 4$ joints of GC B cells derived from *Polκ*$^{fl/fl}$, *Polκ*$^{+/-}$, and *Polκ*$^{-/-}$ mice, respectively. GC B cells were isolated 14 days post immunization with NP-CG. Following cell lysis, a 600 bp fragment was PCR-amplified from 40.000 cell equivalents using a primer pair that anneals in the framework 3 region of most J558 V genes and in the intron downstream of $J_H 4$ gene segment. All values are shown in %. n, the number of mutations; Ts., transitions; Tv., transversions; Ts./Tv., the transions over transversions ratio. *Polκ*$^{-/-}$* mice: 8 months old.

were unmutated (Table 4). Somatic mutations were present in most sequences derived from the *Polκ*$^{-/-}$, *Polκ*$^{+/-}$, and *Polκ*$^{fl/fl}$ GC B cell populations. Sequences bearing one or more mutations were included in the analysis of mutational patterns. Both the number of mutations per sequence and the average mutation frequency (≈ 1%) of the mutated clones were similar (Table 5). The mutational patterns of the J_H-C_H introns derived from the *Polκ*$^{-/-}$ mice did not reveal significant

differences from the patterns derived from the control mice (Figure. 13). Excluding respectively the Gs in the second position of the intrinsic hot spot motifs RGYW (Rogozin and Kolchanov, 1992) or all mutations present at hotspots (I defined all RGYW motifs in which at least 15% of the sequences presented 1 or more mutations, as hot spots), the mutational patterns did not change significantly (data not shown). Adenine was still the most frequently mutated base and the ratio of transitions over transversions remained essentially the same. Likewise, I did not observe any differences with respect to the frequency of frameshift or tandem mutations (data not shown). I therefore conclude that the $Pol\kappa^{-/-}$ mice mutate their Ig genes normally.

C1.7 SHM in DNA Polymerase $Pol\kappa^{-/-}Pol\lambda^{-/-}Pol\iota^{-/-}$ Compound Mutants

SHM in mouse mutants deficient of $Pol\lambda$ or $Pol\iota$ is normal (Bertocci et al., 2002; McDonald et al., 2003). To investigate whether error-prone DNA polymerases can substitute for each other's function, I intercrossed $Pol\kappa^{-/-}$ mice with $Pol\lambda^{-/-}$ and $Pol\iota^{-/-}$ to generate $Pol\kappa^{-/-}Pol\lambda^{-/-}Pol\iota^{-/-}$ compound mutants. $Pol\kappa^{-/-}Pol\lambda^{-/-}Pol\iota^{-/-}$ mice are viable and show no obvious abnormalities. Moreover, both male and female mice are fertile.

Table 6. Analysis of somatic hypermutation of the JH-CH intron of GC B cells from Peyer's Patches of $Pol\kappa^{+/+}Pol\lambda^{+/+}Pol\iota^{+/+}$ and $Pol\kappa^{-/-}Pol\lambda^{-/-}Pol\iota^{-/-}$ mice

genotype	clones	mutated clones	range (mut./clone)	mutations/bp	% mutations
$Pol\kappa^{+/+}$ $Pol\lambda^{+/+}$ $Pol\iota^{+/+}$	41	27	1-14	124/13494	0.9
$Pol\kappa^{-/-}$ $Pol\lambda^{-/-}$ $Pol\iota^{-/-}$	25	20	1-13	107/9600	1.1
% mutations in naïve B cells: $Pol\kappa^{+/+}Pol\lambda^{+/+}Pol\iota^{+/+}$				0.02%	

Naïve and GC B cell populations were isolated by FACS-purification from the Peyer's patches of pairs of unimmunized wild-type and *Polκ⁻/⁻Polλ⁻/⁻Polι⁻/⁻* mice. As expected, naïve B cells harbored very few mutations (0.02%) and reflected the frequency of mutations introduced by PCR. In contrast, somatic mutations were present in the majority of sequences derived from GC B cell populations of *Polκ⁻/⁻Polλ⁻/⁻Polι⁻/⁻* mice and wild-type controls. Sequences bearing one or more mutations were included in the analysis of mutational patterns. Both the number of mutations per sequence and the average mutation frequency (1.1 and 0.9%, respectively) of the mutated clones were similar (Table 6). The mutational patterns of the J_H-C_H introns derived from the *Polκ⁻/⁻Polλ⁻/⁻Polι⁻/⁻* mice did not reveal significant differences from the patterns derived from the control mice (Figure. 14). In

Polκ⁺/⁺Polλ⁺/⁺Polι⁺/⁺

n = 124	to					
from	A	G	C	T	Sum	Tr./Tv.
A	–	29	6	12	47	
G	15	–	7	3	25	1.4
C	3	2	–	6	11	
T	6	3	8	–	17	

Polκ⁻/⁻Polλ⁻/⁻Polι⁻/⁻

n = 117	to					
from	A	G	C	T	Sum	Tr./Tv.
A	–	20	7	18	45	
G	13	–	7	4	24	1.0
C	1	5	–	9	15	
T	5	3	8	–	16	

Figure 14. SHM patterns in *Polκ⁻/⁻Polλ⁻/⁻Polι⁻/⁻*-deficient mice. Patterns of nucleotide exchanges in a 500 bp-long region in the intron downstream of the rearranged $V_HD_HJ_H4$ joints of GC B cells derived from *Polκ⁻/⁻Polλ⁻/⁻Polι⁻/⁻* mice, respectively. GC B cells were isolated from Peyer's patches. Following cell lysis, a 600 bp fragment was PCR-amplified from 40.000 cell equivalents using a primer pair that anneals in the framework 3 region of most J558 V genes and in the intron downstream of J_H4 gene segment. All values are shown in %. n, the number of mutations; Ts., transitions; Tv., transversions; Ts./Tv., the transions over transversions ratio.

addition, the ratio of transitions versus transversions in sequences derived from *Polκ⁻/⁻Polλ⁻/⁻Polι⁻/⁻* mice did not change dramatially. Excluding respectively the Gs in the second position of the intrinsic hot spot motifs RGYW, the mutational patterns did not change significantly (data not shown). Adenine was still the most frequently mutated base and the ratio of transitions over transversions remained essentially the same. Likewise, I did not observe any differences with respect to the frequency of frameshift or tandem mutations (data not shown). I therefore conclude that the *Polκ⁻/⁻Polλ⁻/⁻Polι⁻/⁻* mice efficiently mutate their Ig genes.

C2   The Function of M17 in the Immune System

C2.1   Generation of M17-Deficient Mice

To investigate the *in vivo* function of M17, the *M17* locus had been previously inactivated in the mouse by conditional gene targeting (Angela Egert and Manolis Pasparakis, Cologne, Germany). A *neomycin resistance* (*neo^r*) gene flanked by *loxP* sites was introduced 5' of exon 4 and an additional *loxP* site 3' of exon 5, thus enabling the deletion of those exons by Cre-mediated recombination. In addition, a cassette containing a *splice-acceptor site*, an *internal ribosome entry site* (*IRES*) and a *green fluorescence protein* gene was introduced 3' of exon 5 to mark cells having undergone Cre-mediated deletion. Deletion of exon 4 and 5 removes most of the coding sequence of *M17 gene* including the ITAM motif and the putative C-terminal lipid-binding domain plus the 3' UTR. This strategy likely results in a nonfunctional *M17* gene. The wild-type locus, the targeting vector and the modified locus after homologous recombination with the targeting vector and arGeted locus after Cre-mediated recombination are depicted in Figure 15A. Two independently targeted ES cell clones were injected into blastocysts to generate chimeric animals. Chimeric mice that transmitted the targeted allele into the germ line were crossed to the *Cre-deleter* strain to delete exons 4 and *5 in vivo*. Successful deletion was confirmed by Southern blot of Bgl II or EcoR I-digested tail DNA of the offspring (Figure 15B). Mice homozygous for the deletion of M17 are viable, born at a Mendelian ratios and display no obvious abnormalities.

M17 is predominantly expressed in GC B cells. To confirm the inactivation of the *M17* gene on the level of RNA transcripts, I immunized *M17$^{-/-}$* mice and wild-type controls with NP-CG and isolated CD19$^+$Fas$^+$PNA^{high} GC B cells 14 days later by flow cytometry. I purified RNA from these cells for analysis by RT-PCR using a primer pair that anneals in exon 1 and 4 of the *M17* mRNA, respectively. In contrast to *M17$^{+/+}$* mice, amplification from equal amounts of GC B cell-derived cDNA from *M17$^{-/-}$* mice did not yield a PCR product (Figure 15C).

Figure 15. Generation of *M17^{-/-}* mice. (A) Schematic representation of the gene targeting in the M17 locus by homologous recombination. C57BL/6-derived ES cells were targeted with a vector containing the *loxP*-flanked exons 4 and 5, a frt-flanked *IRES-gfp* cassette, and a *neomycin resistance* cassette for positve selection. Negative selection of clones harboring randomly integrated vectors was mediated by a *thymindine kinase* gene. Only exons 3-5 are shown. Rectangles, coding DNA; filled triangles, *loxP* sites; ovals, *frt* sites; RI, EcoR I; BII, Bgl II. Bold lines indicate regions of homology and Southern probes are shown as thin black lines under the wild-type locus. **(B)** Successful homologous recombination was identified by Southern blot of EcoR I-digested genomic ES cell DNA and a probe located at the 5' of *M17* exon 3. The wild-type fragment migrates at 6.9 kb, while the fragment from the targeted locus migrates at 4.6 kb. Cre-mediated deletion of *M17* exon 4 and 5 was confirmed by Southern blot of Bgl II-digested genomic DNA using a probe located 5' of exon 4. The wild-type fragment migrates at 2.1 kb and the fragment of the deleted locus migrates at 1.0 kb. **(C)** Confirmation of the successful inactivation of M17 by RT-PCR. RNA was isolated from sorted CD19$^+$PNA$^-$ Fas$^-$ naïve B cells (N) or CD19$^+$PNA$^+$Fas$^+$ GC B cells from either *M17$^{+/+}$* or *M17$^{-/-}$* mice and reverse transcribed using an oligoT primer. PCR products were amplified with primers annealing either in exons 1 and 4 (primer M17 1/4) or in exons 1 and 3 (M17 1/3). Intron-spanning primers annealing in the β-*actin* gene were used as loading control. **(D)** Sequence comparison of the larger and smaller RT-PCR product amplified with the primer pair annealing in *M17* exons 1 and 4. The smaller PCR product is identical with the published cDNA sequence of *M17*, while the larger product reveals a novel exon located downstream of exon 1. The size and location of the new exon can account for the discrepancy between *HGAL* and *M17* at the 5' end of the cDNA.

A. WT locus

B.

EcoR I
+/+ tgt
— 6.9 kb
— 4.6 kb

Bgl II
+/+ +/- -/-
— 2.1 kb
— 1.0 kb

C.
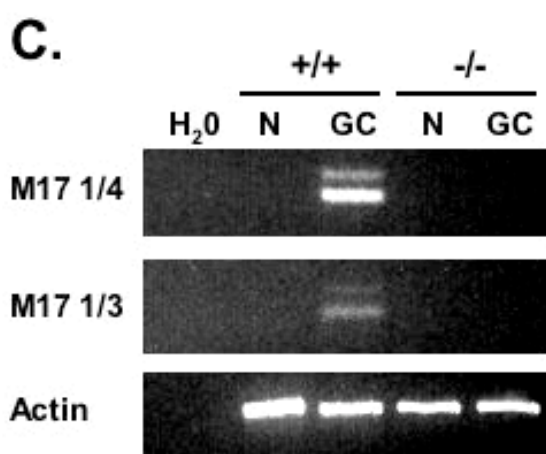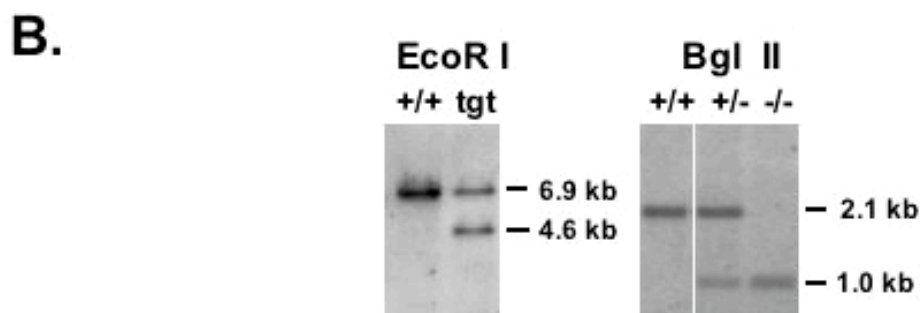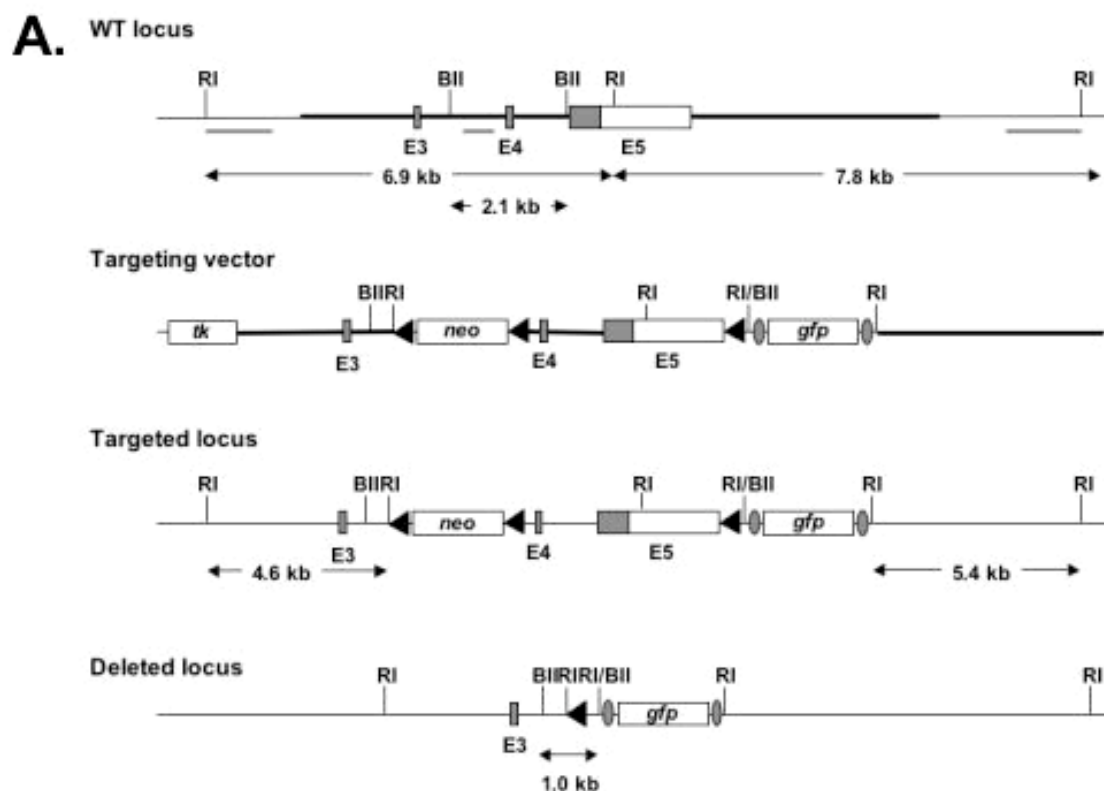
D.

...exon 1
ATGGGGAACTGTTTGCAGAGGACAACCAG-------------
ATGGGGAACTGTTTGCAGAGGACAACCAGATGGCAGCTGGACAT

GCAGGAAACACCTTGGAATCTGAGACTCAGTGCCAAGGGAAGAA

exon 2
--------ATACTTCAGGGGCTGGAGTTGTTGTCACAGCGTTGAA
CATGCAGATACTTCAGGGGCTGGAGTTGTTGTCACAGCGTTGAA

exon 3
GGATGCTCCTGCCTTCCTTGGAAAAACATACGCACATTTAAAGC
GGATGCTCCTGCCTTCCTTGGAAAAACATACGCACATTTAAAGC

exon 4....
CAGACAAGAGTCTCCAAAGCAAAATGAAGGGATGACTTCAGCTC
CAGACAAGAGTCTCCAAAGCAAAATGAAGGGATGACTTCAGCTC

PCR amplification with a reverse primer that hybridizes in exon 3 also failed to yield a PCR product from cDNA of *M17⁻/⁻* mice, suggesting a destabilized mRNA of the inactivated *M17* gene and the *IRES-GFP* cassette (data not shown). Surprisingly, the PCR using cDNA from wild-type mice revealed the presence of two products. The smaller one was consistent with the expected size of 155 bp. Sequencing of the larger product demonstrated the existence of a previously unknown exon of 66 bp that is located between exon 1 and 2 (Figure 15D). M17 and HGAL differ most significantly at the N-terminus, with the cDNA of *HGAL* being longer than the one of M17. The discovery of the new exon helps to account for this discrepancy. A sequence analysis of the new exon on both the DNA and protein level did not reveal any homologies to other known DNA or protein sequences besides *HGAL*.

C2.2   M17 mRNA is Upregulated by IL-4

Interleukin-4 (IL-4) induces the expression of *HGAL* in peripheral blood B lymphocytes. The *M17* gene contains two putative *STAT6* binding sites, suggesting similar regulation and response to IL-4. To determine whether the expression of *M17* is also regulated by IL-4, I stimulated MACS-purified B cells *in vitro* with either lipopolysaccaride (LPS) or a monoclonal antibody (mAb) directed against CD40 in the absence or presence of IL-4. I isolated total RNA from equal numbers of cells 48 hours later, and determined *M17* mRNA expression by RT-PCR using intron-spanning primers specific for the *M17* and β-*Actin* genes. As expected, unstimulated or LPS-stimulated cells did not express *M17*. Stimulation with an αCD40 mAb alone also failed to induce *M17* expression. In contrast, activation of the cells with LPS or αCD40 mAb in the presence of IL-4 upregulated the expression of *M17* mRNA (Figure 16). Thus, IL-4 induces the expression of *M17* mRNA in LPS or αCD40-activated B cells *in vitro*. The *M17* gene appears to be regulated in a fashion similar to the *HGAL* gene and M17 may be involved in IL-4 induced immune responses *in vivo.*
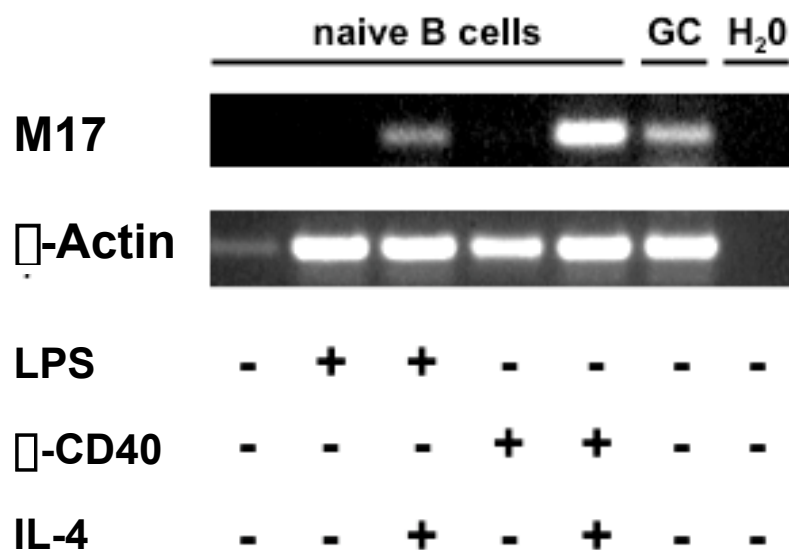
Figure 16. M17 is upregulated by IL-4. Isolated splenocytes were MACS-depleted of CD43$^+$ cells and subsequently activated with the indicated stimuli. Following isolation of total RNA 48 h later, RT-PCR was performed using intron-spanning primers for the *M17* and *β-Actin* genes. A representative experiment is shown.

C2.3   B and T Cell Compartments in M17-Deficient Mice

The predominant sites of *M17* mRNA expression *in vivo* are the GCs. However, expression of M17 mRNA is also found in developing B cells in the bone marrow (Christoph, 1993). The analysis by flow cytometry of the bone marrow-derived cells did not reveal differences in absolute cell numbers or proportions of major subsets of developing B cells, indicating that M17 is dispensable for B cell development (data not shown).

In the peripheral lymphoid organs, the number of total cells in spleen and mesenteric lymph nodes was equivalent in M17-deficient mice and wild-type control mice. In contrast, the number of total cells in Peyer's patches is reduced by 2-3 fold (Figure 17A). The reduction of total cells in the latter organ reflected both a reduced number of Peyer's patches per mouse (5.1 ± 1.3 versus 7.8 ± 1.1 Peyer's patches in *M17$^{-/-}$* and *M17$^{+/+}$* mice, respectively) and a reduced size of some but
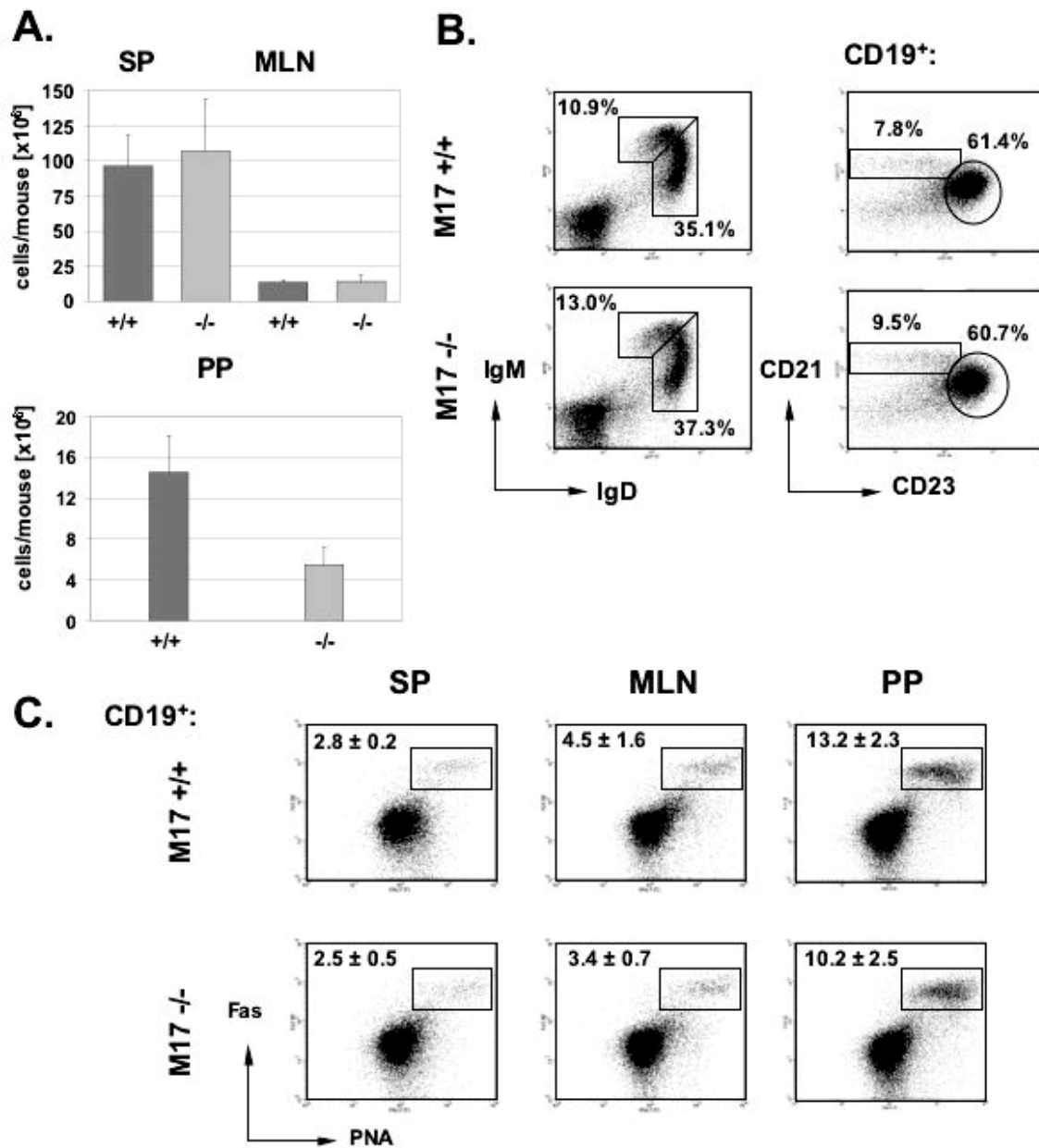
Figure 17. Cell numbers and B cell subsets in peripheral lymphoid organs. (A) The total number of cells in peripheral lymphoid organs. **(B)** Splenocytes were stained with α-IgM and α-IgD mAbs to identify IgM^{high}IgD^{low} immature and mature IgM^{low}IgD^{high} B cell populations. CD21^{high}CD23^{low} MZ and follicular CD21^{low}CD23^{high} B cells are shown by staining with α-CD21 and α-CD23 mAbs. Only CD19^{+} cells are shown. **(C)** Mice were immunized with 50 μg NP-CG and analyzed for the presence of CD19^{+}PNA^{+}Fas^{+} GC B cells 14 days post immunization. Only CD19^{+} cells are shown Numbers, average in % plus standard deviation. SP, spleen; MLN, mesenteric lymph nodes; PP, Peyer's patches.

not all Peyer's patches in $M17^{-/-}$ animals.

The proportions of splenic immature $IgM^{high}IgD^{low}$ and mature $IgM^{low}IgD^{high}$ B cell populations were comparable to wild-type controls and the ratio of $CD21^{high}CD23^{low}$ MZ B cells to $CD21^{low}CD23^{high}$ follicular B cells was unchanged in $M17^{-/-}$ mice (Figure 17B). $CD4^{+}$ and $CD8^{+}$ T cells were also present at wild-type levels. Although the number of total cells was reduced in Peyer's patches, the proportion of total B cells stayed the same. The ratio of B and T cells was unchanged and the proportions of B cell subsets were normal when compared to wild-type mice (not shown).

To analyze the proportions of $CD19^{+}Fas^{+}PNA^{high}$ GC B cells in $M17^{-/-}$ mice and wild-type controls, the mice were immunized with 50 μg NP-CG and the percentage of GC B cells was determined 14 days later. The proportion of $CD19^{+}Fas^{+}PNA^{high}$ GC B cells in the spleen and mesenteric lymph nodes is not significantly changed in M17-deficient mice (Figure 17C). Despite the general reduction of total cells in Peyer's patches, GC B cells are still generated efficiently in this compartment. Hence, M17 is dispensable for the generation and maintenance of the major B and T cell populations in bone marrow, spleen, and mesenteric lymph nodes, but surprisingly affects the number of B and T cells in Peyer's patches. M17 is not essential for the generation of GC B cells.

C2.4   Stimulated M17-Deficient B Cells Proliferate Normally

To analyze the proliferative capacity of M17-deficient B cells, I isolated splenic B cells from $M17^{-/-}$ mice and wild-type controls by MACS-depletion of $CD43^{+}$ cells and labeled the B cells with the protein-binding dye CFSE to study cell division. Following CFSE-labeling, the cells were stimulated with either LPS or an αCD40 mAb in the presence of IL-4. Cell proliferation was measured three days post stimulation by flow cytometry. M17-deficient B cells proliferate at levels comparable to wild-type cells upon LPS or CD40 stimulation in the presence of IL-4 (Figure 18). Stimulation with αIgM in the presence IL-4 results in a similar outcome (data not shown). The measurement of cell proliferation by cell counting gave similar results. Therefore, M17 is dispensable for efficient cell proliferation *in vitro*.
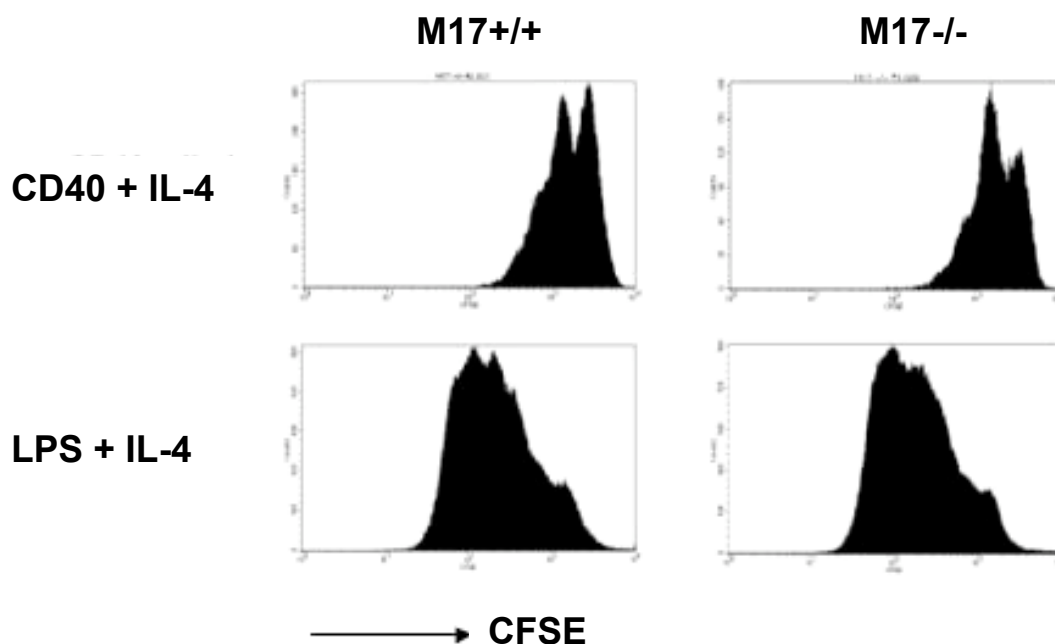
Figure 18. Proliferation of M17$^{-/-}$ B cell *in vitro*. Splenocytes were depleted of CD43+ cells, labeled with CFSE, and stimulated with an αCD40 mAb plus IL-4 or LPS plus IL-4. After three days of culture, cell proliferation was determined by flow cytometry. All histrograms represent CD19$^+$ B cells. A representative experiment is shown.

C2.5   Germinal Center Architecture Is Not Affected in M17-Deficient Mice

Next, I studied cryosections from spleen and Peyer's patches by immunofluorescence to analyze the impact of M17-deficiency on the architecture of the GCs. Spleens were isolated 14 days after the immunization of either wild-type or M17-deficient mice with NP-CG. Frozen splenic sections were incubated with PNA and mAbs against CD19 or FDCM1 coupled to fluorescent conjugates to visualize B cells follicles, GC B cells and the network of follicular dendritic cells (FDCs), respectively. As shown in Figure 19A, M17-deficient are able to develop GCs (PNA$^+$ cells, red) and B cell follicles (CD19$^+$ cells, green) comparable in size and shape to wild-type animals. M17-deficient mice also show a polarized network of FDCs (FDCM1$^+$ cells, green), highlighting the GC light zone containing centrocytes.

Despite the reduced cell numbers in the Peyers patches, the architecture of GCs remained unchanged in these tissues (Figure 19B). *M17*$^{-/-}$ mice are still able to form GCs with an intact network of FDCs (not shown) and resemble GCs from wild-type mice. Hence, M17 is not an essential component required for GC formation.

Next page:

Figure 19. GC architecture in *M17*$^{-/-}$ mice. (A) Mice were immunized with 50 μg NP-CG. Spleens were analyzed for GC formation 14 days later. Frozen splenic were stained by immunofluorescence. Sections were incubated with either αCD19 mAb (green) and PNA (red) to visualize B cell follicles and GCs or PNA (red) and αFDCM1 mAb (green) to visualize the network of FDCs within the GCs. SP, spleen; column 1, 10x magnification; column 2 and 3, 20x magnification. **(B)** Frozen sections of the Peyer's patcheswere stained with αCD19 mAb (green) and PNA (red) to visualize B cells and GCs. Sections were derived from 2 independent experiments with 2 mice per genotype. Representative pictures are shown.
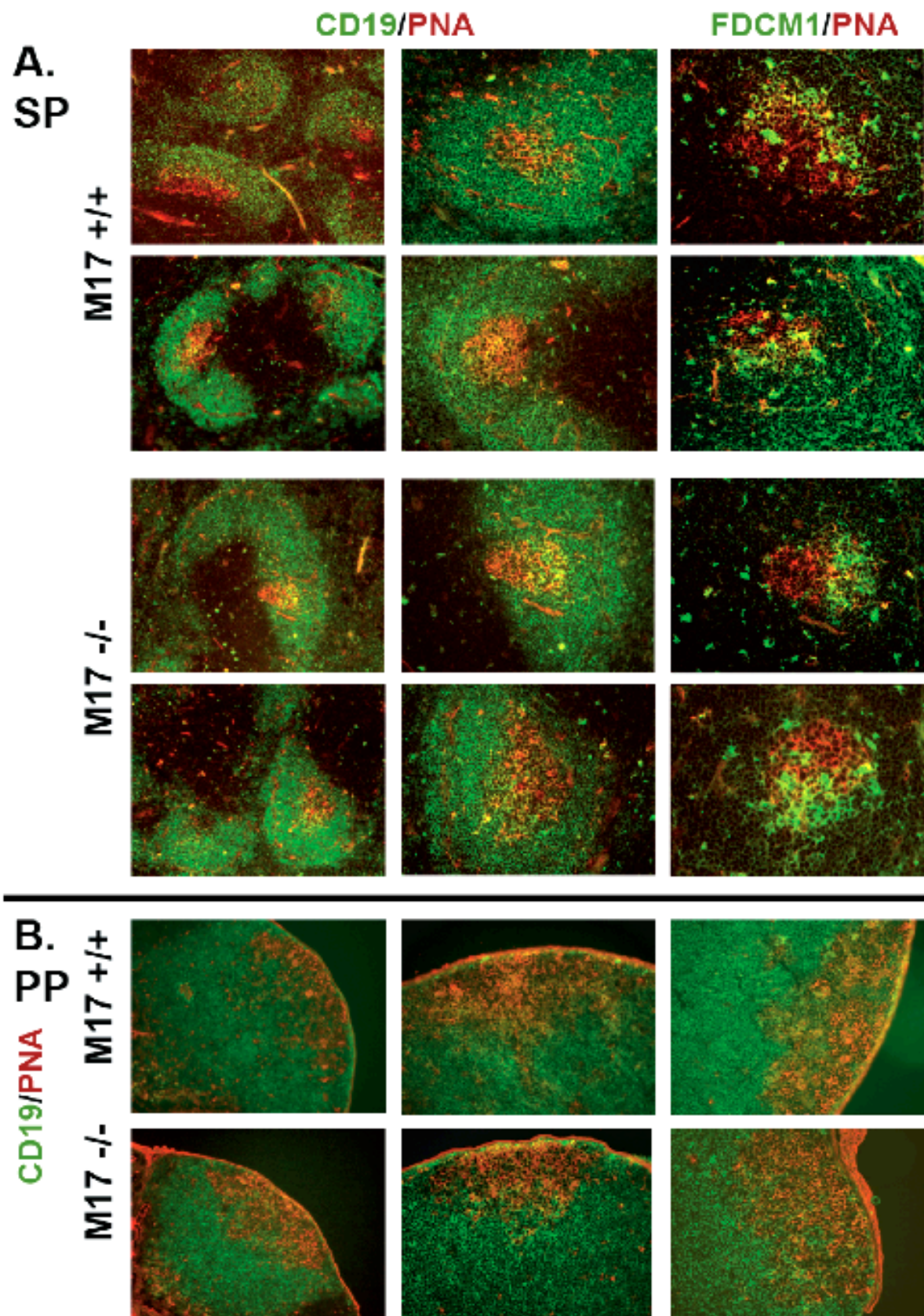
C2.6 Normal Ig Serum Titers and Efficient Class Switching in M17-Deficient Mice

To analyze the ability of *M17*$^{-/-}$ mice to undergo CSR, I first measured Ig antibody titers in the blood serum of unimmunized mice by ELISA. As shown in Figure 20, *M17*$^{-/-}$ mice are able to secrete antibodies of all isotypes and reach antibody levels in their blood serum comparable to wild-type controls. Thus, deficiency of M17 does not appear to have a major impact on CSR.

While *M17*$^{-/-}$ mice produce normal amounts of antibodies, M17 may modulate CSR in more subtle ways. Hence, I determined the ability of *M17*$^{-/-}$ B cells to undergo CSR to particular isotypes *in vitro*. Splenic B cells from *M17*$^{-/-}$ mice and wild-type controls were isolated by MACS depletion of CD43$^+$ cells and induced with various stimuli to undergo CSR *in vitro*. After 4 days of culture, the percentage of class-switched cells was measured by flow cytometry. As expected, LPS is able to induce efficient CSR to IgG2b and IgG3 in M17-deficient mice as this stimulus does not induce the expression of M17 mRNA (Figure 21A). Activation of *M17*$^{-/-}$ B cells with LPS plus TGF-β or LPS plus IFN-β induces CSR to IgA and IgG2a at wild-type levels. Activation of *M17*$^{-/-}$ B cells with αCD40 mAb plus IL-4 induces the expression of M17 mRNA. However, *M17*$^{-/-}$ B cells efficiently switch to IgG1 and IgE isotypes when stimulated with αCD40 mAb plus IL-4.

Finally, I analyzed whether GC B cells in the Peyer's patches also undergo efficient CSR (Figure 21B). Most GC B cells in the gut switch to IgA, which is secreted into the intestinal lumen. Around 40% of GC B cells were IgA$^+$ in M17-deficient mice, which compared to around 35% in wild-type mice. Therefore, M17 is not required for the induction of CSR or its mechanism in general and switching to specific isotypes in particular.
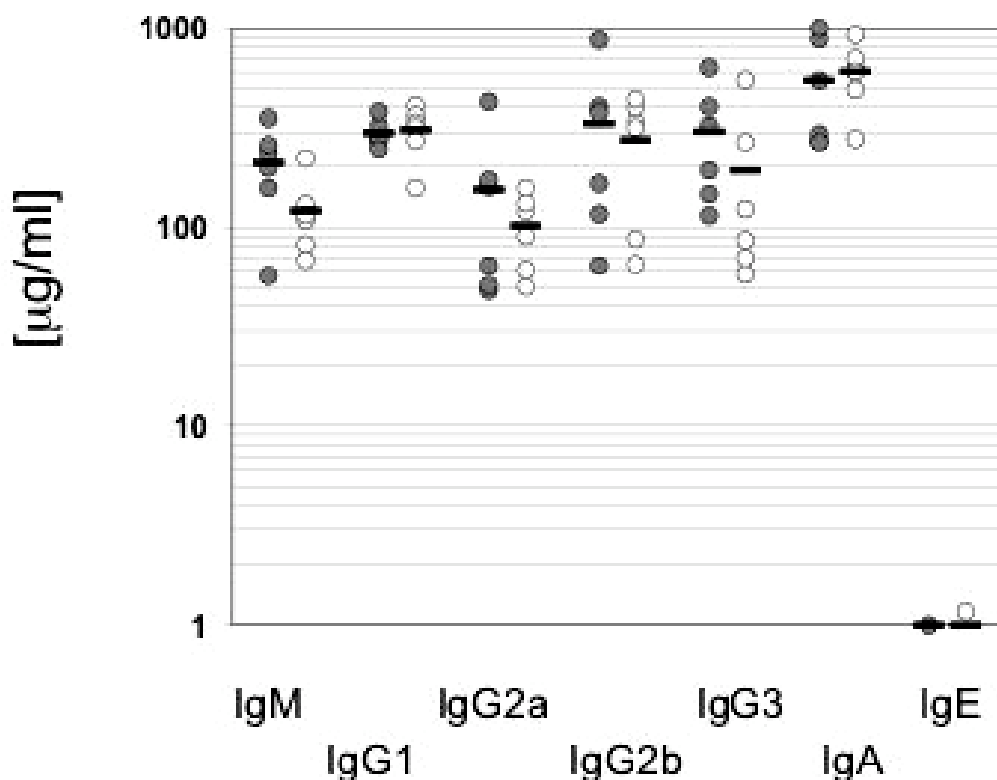
Figure 20. Antibody titers in serum M17-deficient mice. Antibody titers in the serum of unimmunized wild-type and M17-deficient mice were determined in an ELISA assay. Each circle represents one mouse. Black bars indicate the geometric means. Closed circles, wild-type mice; open circles, M17-deficient mice.

Next page:

Figure 21. Class-switch recombination in *M17⁻/⁻* mice. (A) *In vitro* stimulation of isolated B cells of *M17⁻/⁻* mice and wild-type controls. B cells were induced to undergo CSR with the indicated stimuli. The percentage of class-switched cells was determined 4 days later by flow cytometry. Numbers in the graphs represent the percentages of switched cells. The experiment was performed 3 times and a representative experiment is shown. (B). Percentage of IgA⁺ GC B cells in the Peyer's patches of *M17⁺/⁺* (left) or *M17⁻/⁻* mice (right). A representative experiment is shown.

A. M17+/+ M17-/- M17+/+ M17-/-

LPS — CD40 + IL-4
20.1 — 25.9 — 28.0 — 32.0
IgG2b — IgG1

LPS — CD40 + IL-4
7.4 — 5.7 — 5.3 — 7.9
IgG3 — IgE

LPS + TGF-β — LPS + IFN-γ
B220 — 6.0 — 5.6 — 8.5
IgA — IgG2a
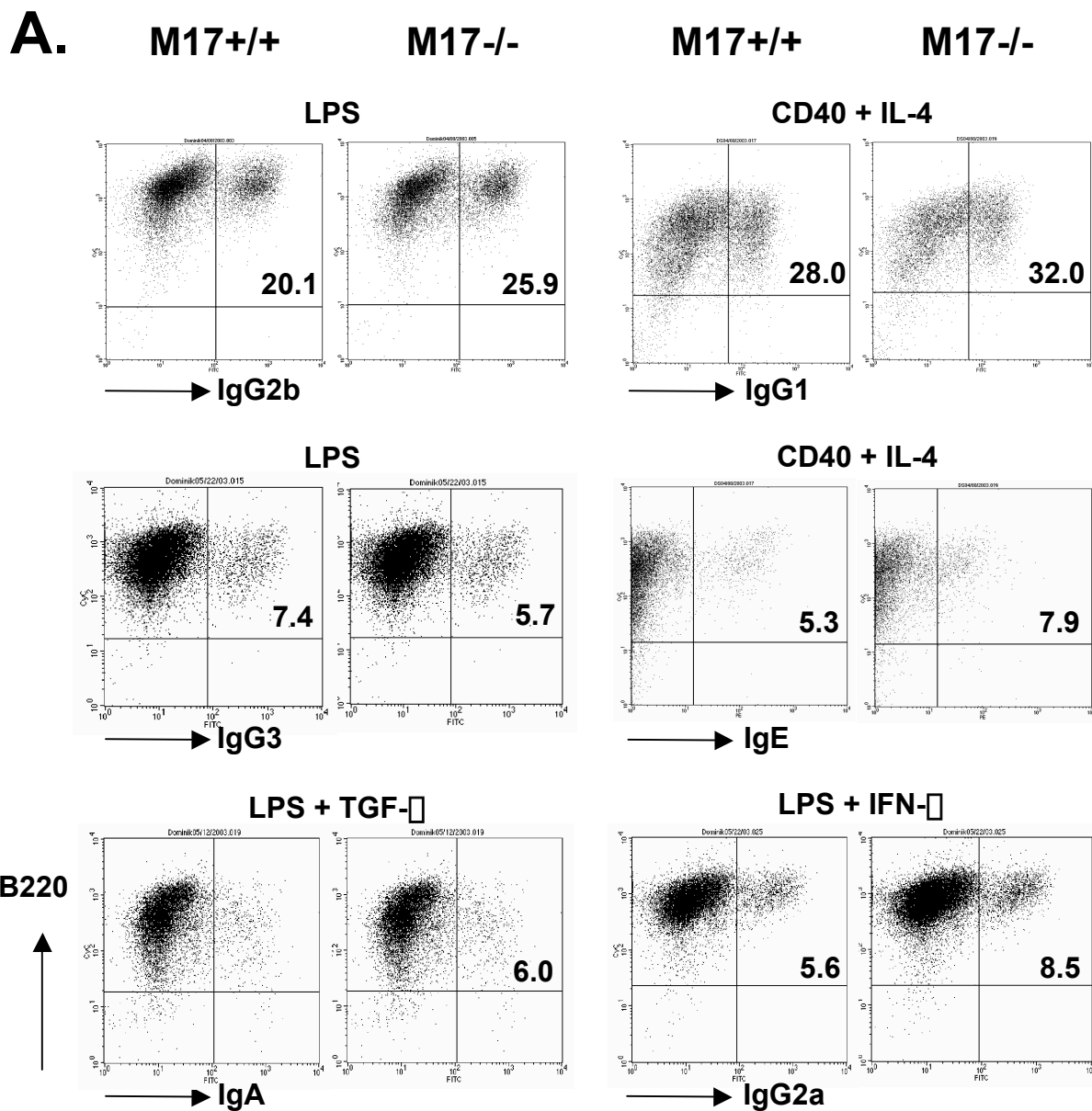
B. CD19+PNA+:
35.7 — 41.2
IgA — IgA
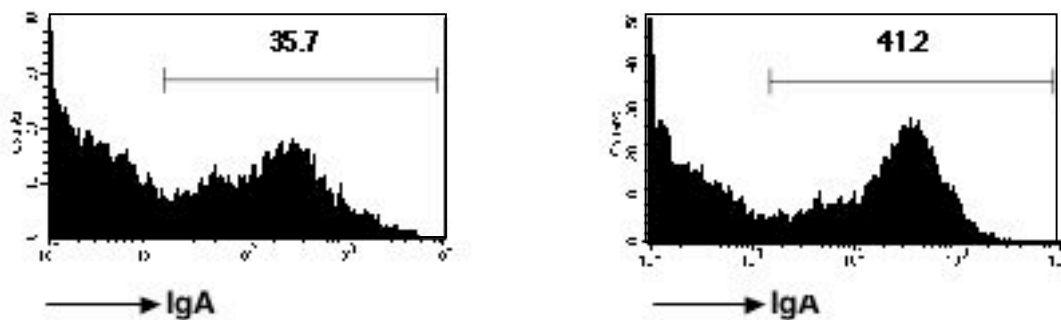
C2.7   GC B Cells of M17-Deficient Mice Mutate Their Ig Genes Efficiently

To elucidate whether M17 is involved in SHM of Ig genes, I studied the intrinsic features of the hypermutation process by analyzing the accumulation of mutations in the intron downstream of the rearranged V gene in the IgH locus (Jolly et al., 1997). I immunized pairs of wild-type and M17-deficient mice with 100 μg NP-CG and isolated GC B cells and naïve B cells 14 days post immunization from spleen to measure the level and pattern of somatic mutations. All mice used for this analysis responded to NP-CG as demonstrated by the presence of elevated levels of NP-CG-specific IgG1 antibodies in the blood (data not shown). The PCR reaction was performed on genomic DNA from 20,000 cell equivalents using a primer pair that anneals in the framework region 3 of most V_HJ558 genes and in the intron downstream of the J_H4 gene, thus comprising a large proportion of rearranged V genes. PCR products were subcloned, sequenced, and subsequently controlled for the absence of clonally related sequences.

Sequences derived from naïve B cells were predominantly unmutated (Table 7). In contrast, the majority of sequences derived from GC B cells of either wild-type or M17-deficient mice contained somatic mutations. Sequences harboring one or more mutations were used to analyze the mutational patterns.

Table 7. Analysis of somatic hypermutation of the JH-CH intron of splenic GC B cells from M17$^{-/-}$ and M17$^{+/+}$

genotype	clones	mutated clones	range (mut./clone)	mutations/bp	% mutations
M17-/-	56	31	1-12	117/15500	0.75
M17 +/+	35	25	1-14	102/12248	0.83
% mutations in naïve B cells: *M17-/-*	0.03%				

Both wild-type and M17-deficient mice were able to mutate their Ig genes with an equivalent average mutation frequency (0.75% versus 0.83%, see Table 7) and the number of mutations per sequence was in similar range (1-12 versus 1-14 mutations per sequence in $M17^{-/-}$ and $M17^{+/+}$, respectively). The analysis of the mutational patterns did not reveal major differences between $M17^{-/-}$ mice and wild-type controls. Adenine remained a highly mutated base in $M17^{-/-}$ mice and there was no difference in the number of deletions or insertions (Figure 22). Moreover, the ratio of transitions versus transversions did not change significantly.

Cell numbers of Peyer's patches are reduced in M17-deficient mice. I therefore asked whether SHM could be affected in this cellular compartment. CD19$^+$Fas$^+$PNA$^+$GC B cells from the Peyer's patches of 2 unimmunized $M17^{-/-}$ mice or wild-type mice were isolated by FACS-purification and analyzed for SHM similarly to the analysis of splenic GC B cells. While the mutation frequency was higher in GC B cells derived from Peyer's patches than in splenic GC B cells, I did not observe an altered mutation frequency in M17-deficient mice when compared

M17 +/+ (n = 102)

from \ to	A	G	C	T	Sum	Tr./Tv.
A	–	25	8	12	45	
G	14	–	9	1	24	1.5
C	1	5	–	5	11	
T	3	2	16	–	21	

M17 -/- (n = 117)

from \ to	A	G	C	T	Sum	Tr./Tv.
A	–	14	10	6	30	
G	13	–	3	3	19	1.3
C	1	2	–	12	15	
T	9	9	19	–	37	

Figure 22. SHM patterns in $M17^{-/-}$ mice. Patterns of nucleotide exchanges in a 500 bp-long region in the intron downstream of the rearranged $V_H D_H J_H 4$ joints of GC B cells derived from pairs of $M17^{+/+}$ and $M17^{-/-}$ mice, respectively. GC B cells were isolated 14 days post immunization with NP-CG. Following cell lysis, a 600 bp fragment was PCR-amplified from 40.000 cell equivalents using a primer pair that anneals in the framework 3 region of most J558 V genes and in the intron downstream of $J_H 4$ gene segment. All values are shown in %. n, the number of mutations; Ts., transitions; Tv., transversions; Ts./Tv., the transions over transversions ratio.

to wild-type controls (1.70% for $M17^{-/-}$ mice versus 1.62% for $M17^{+/+}$ mice). The range of the number of mutations per sequence remained the same and there was no major difference in the mutational pattern (data not shown). Likewise, the ratio of transitions to transversions did not change. Hence, M17 is not required for the efficient introduction of somatic mutations in the Ig genes.

C2.8 Immune Response of M17-Deficient Mice to NP-CG

Finally, I sought to test the primary and secondary antibody response of M17-deficient mice against the T cell-dependent antigen NP-CG. To this end, I immunized groups of 7 wild-type or M17-deficient mice with either 50 μg or 10μg NP-CG in alum per mouse and measured the serum titers of NP-specific IgG1 and Igλ antibodies every 7 days for 4 weeks. The M17-deficient cohort immunized with 50 μg NP-CG yielded a robust and consistent antibody response with a geometric mean of 117 μg/μl of NP-specific IgG1 at the peak of the immune response (Figure 23A). The response was comparable to wild-type controls. M17-deficient mice immunized with 10 μg NP-CG in alum gave rise to a similar immune response against NP-CG, albeit at lower levels. The immune response peaked at 56 μg/ml of NP-specific IgG1 14 days post immunization and was indistinguishable from the response in wild-type mice (Figure 23B). The measurement of the NP-specific Igλ antibodies gave similar results (not shown).

Next, I evaluated the ability of $M17^{-/-}$ mice to mount an efficient secondary immune response against NP-CG. The same mice used for the analysis of the primary immune response were immunized with 10 μg NP-CG without alum 63 days after the primary immunization. The secondary immune response was followed for three weeks. $M17^{-/-}$ mice that had been immunized with 50 μg NP-CG for the primary immune response were also able to mount a secondary response. However, the secondary response was moderately weaker in $M17^{-/-}$ mice than in the wild-type controls (Figure 23C). While $M17^{+/+}$ reached a geometric mean of 804 μg/ml at the peak of the secondary immune response, $M17^{-/-}$ mice peaked at 247μg/ml (Figure 23C). Mice that had been immunized with 10 μg/ml in the primary immune response gave a similar result (Figure 23D). Thus, $M17^{-/-}$ mice have a secondary immune response.
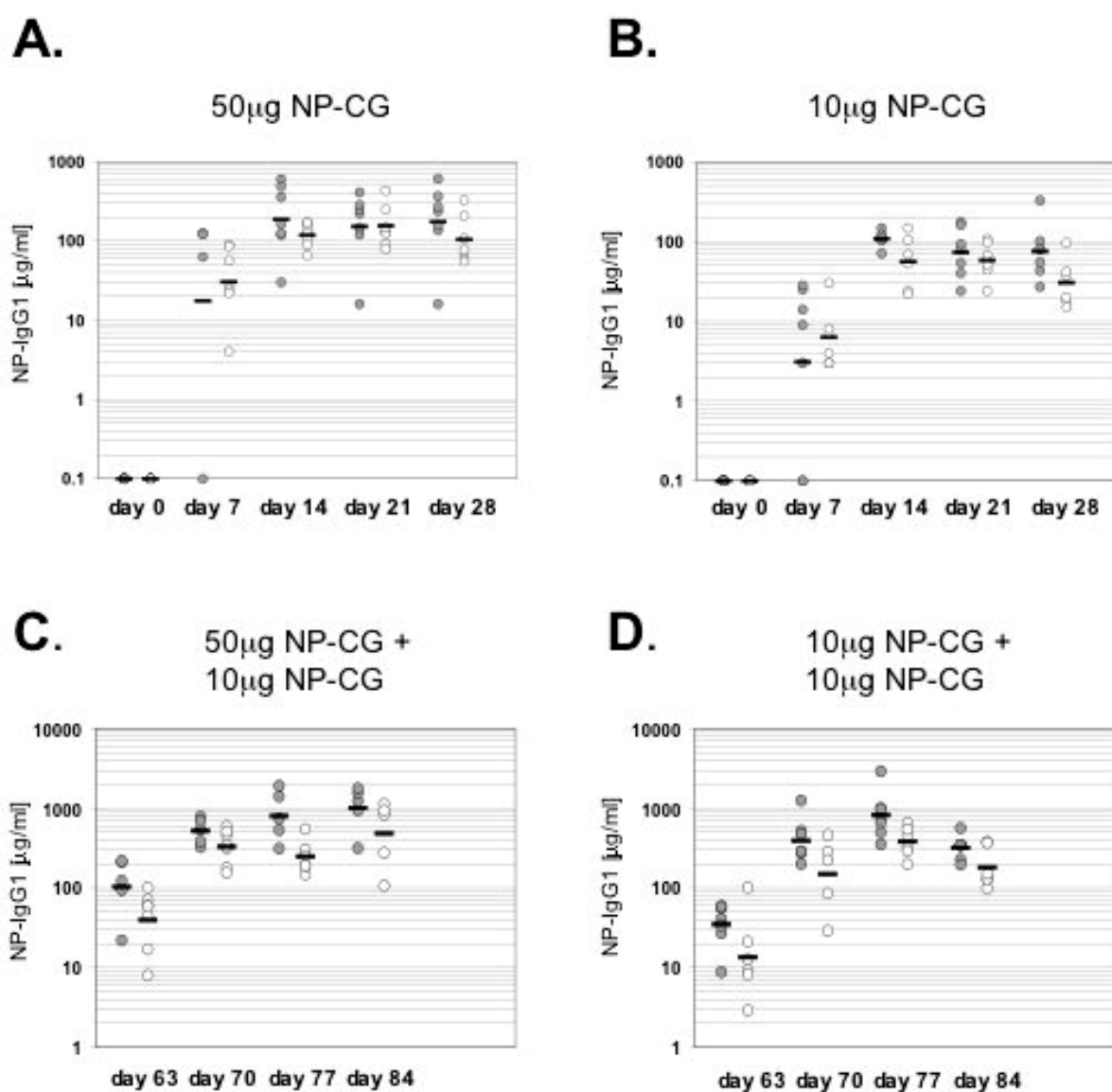
Figure 23. Primary (A, B) and secondary (C, D) immune response of *M17$^{-/-}$* mice and wild-type controls to NP-CG. (A) Primary immunization with 50 µg NP-CG in alum. **(B)** Primary immunization with 10 µg NP-CG in alum. **(C)** Secondary immunization with 10 µg NP-CG without alum of mice previously immunized with 50 µg NP-CG. **(D)** Secondary immunization with 10 µg NP-CG without alum of mice previously immunized with 10 µg. Each circle represents one mouse. Bars indicate the geometric means. Closed circle, *M17$^{+/+}$* mice; open circle, *M17$^{-/-}$* mice.

D.   DISCUSSION

D1.   The Role of Polκ and Other DNA Polymerases in SHM

Error-prone DNA polymerases are required for the bypass of DNA lesions at stalled replication forks. They can bypass their cognate lesions accurately and are mutagenic when copying non-cognate lesions or undamaged templates. Several reported deficiencies of mammalian DNA polymerases were either embryonic lethal (Polβ, Polζ)(Bemark et al., 2000; Esposito et al., 2000a; Gu et al., 1994a; Wittschieben et al., 2000) or resulted in a increased susceptibility to skin cancer (Polη)(Masutani et al., 1999). In contrast, my studies show that Polκ-deficient mice are viable and do not exhibit obvious abnormalities.

The observation of increased sensitivity to killing of Polκ-deficient MEFs following exposure to UV radiation supports the notion that like other specialized DNA polymerases with abnormally low fidelity, Polκ is required for the replicative bypass of one or more types of base damage produced by UV radiation. The independent observation that Polκ is able to bypass the minor photoproduct thymine glycol, but not the major photolesions thymine dimers and [6-4] photoproducts *in vitro* (Fischhaber et al., 2002), confirms the idea that Polκ is required for translesion synthesis across certain types of base damage *in vivo.* Polκ has also been found to serve as an efficient extender from mismatched primer termini generated by other DNA polymerases (Haracska et al., 2002; Washington et al., 2002). In this latter role, Polκ has been implicated in the bypass of thymine dimers (Washington et al., 2002), thus explaining the increased UV sensitivity of Polκ-deficient fibroblasts. Another function of Polκ may be the bypass of aromatic DNA adducts. Expression of Polκ is augmented by aromatic compounds (Ogi et al., 2001) and polyaromatic hydrocarbons such as benzopyrenes serve as good substrates for Polκ (Huang et al., 2003; Suzuki et al., 2002; Zhang et al., 2002). Consequently, increased expression of Polκ has been found in the adrenal cortex, where steroid synthesis occurs, (Velasco-Miguel et al.,

2003) and in specimens of several lung cancers (J et al., 2001).

Thymine glycols represents DNA lesions that often result from the presence of reactive oxygen species (Hegi et al., 1989). Reactive oxygen species have been associated with DNA damage of spermatozoa (Gil-Guzman et al., 2001; Ollero et al., 2001). Polκ copies faithfully across thymine glycols (Fischhaber et al., 2002). The high levels of expression of *Polκ* mRNA in testis in both meiotic and post-meiotic cells (Velasco-Miguel et al., 2003) were suggestive of a possible specialized role(s) for this enzyme during spermatogenesis. However, the architecture of the testis in the Polκ mutant mice appears to be normal and the mice are fertile over several generations. Many error-prone DNA polymerases are strongly expressed in testis (Aoufouchi et al., 2000; Garcia-Diaz et al., 2000; McDonald et al., 1999). Base-excision repair is involved in the repair of spontaneous DNA damage such as thymine glycols and other lesions and is a very efficient DNA repair pathway in germ cells (Olsen et al., 2001). Polλ and Polι, which are also highly expressed in the seminiferous tubules of the mouse testis, have been implicated to operate in base excision repair (Bebenek et al., 2001; Garcia-Diaz et al., 2000; McDonald et al., 1999). It was therefore conceivable that Polκ, Polλ, and Polι together contribute to the genome integrity in testis. However, compound mutants that are deficient of Polκ, Polλ, and Polι are viable, reproduce normally and do not show any visible abnormalities, arguing against cumulative functions of these DNA polymerases during spermatogenesis (unpublished own data). At the present time, I cannot rule out that the absence of Polκ or other DNA polymerases results in the accumulation of mutations in the germline, which might affect fertility or viability of the mice in later generations. In this context, it is interesting to note that one colony of *Polκ*$^{-/-}$ mice developed diabetes insipidus and the onset of the disease decreased over several generations (Errol Friedberg, Southwestern Medical Center, Dallas, USA, personal communication). The reason for this phenotype is not know. However, one can speculate that normally Polκ copies faithfully across base damages that arise during spermatogenesis, such as thymine glycols, and the absence of Polκ leads to mutations, which in this case affected a gene responsible for the this particular phenotype.

Somatic hypermutation introduces mainly point mutations but deletion and insertion also occur (Goossens et al., 1998; Kocks and Rajewsky, 1988; McKean et al., 1984). The discovery of AID has furthered the understanding of the initiation of SHM. Deamination of cytidines by AID leads to the formation of uracil residues. Subsequent DNA replication across this lesion results in the incorporation of adenine opposite uracil and thus to the introduction of C to T transitions (Petersen-Mahrt et al., 2002). UNG-deficient mice fail to efficiently remove uracil residues due to their impaired uracil-deglycosylase function and consequently harbor elevated levels of transition mutations in their Ig genes (Rada et al., 2002). However, although somatic mutations tend to cluster in the context of the RGYW hotspot motifs, they are scattered throughout the Ig genes and occur at all four bases. Importantly, they represent not only transitions but also almost 50% transversions. Which factors can account for this pattern? A role of error-prone DNA polymerases in SHM has long been considered (Bertocci et al., 1998; Brenner and Milstein, 1966; Diaz et al., 1999) and the class of recently discovered error-prone DNA polymerases has attracted considerable attention in this regard. Uracil-deglycosylation creates abasic sites, which are either non-instructive sites during DNA replication or the origin of DNA strand breaks, whose repair involves error-prone short-patch DNA synthesis (Di Noia and Neuberger, 2002; Petersen-Mahrt et al., 2002). Alternatively, the mismatch-repair enzymes MSH2 and MSH6 recognize the U-G mismatches and subsequent error-prone short-patch DNA synthesis introduces mutations (Jacobs et al., 1998; Phung et al., 1998). Error-prone DNA polymerases exhibit varying degrees of processivity or fidelity and different abilities to synthesize from mismatched or misaligned DNA termini. For example, Polι is very mutagenic when copying undamaged template but has poor processivity, whereas Polζ extents mismatched termini efficiently. It is therefore conceivable that the resulting mutation pattern of SHM is due to the combined action of AID and several error-prone DNA polymerases.

The mutagenic nature of Polκ and its expression in B cells were suggestive of a role of this enzyme in SHM mechanism of Ig genes. Here I show that Polκ-deficiency does not affect B cell development and the formation of GC B cells. The

mutant mice are still able to produce normal antibody serum titers and to mount a robust T cell-dependent immune response. To test the ability of $Pol\kappa^{-/-}$ mice to introduce somatic mutations in their Ig genes, I examined the mutation frequency and pattern in the non-biased intron downstream of rearranged V genes containing the J_H4 gene segment. The mutation frequency in sequences derived from $Pol\kappa^{-/-}$ mice (1.0 and 1.1 %) is similar to the ones in sequences derived from wild-type controls (0.9 and 1.3%). Likewise, the mutation pattern of SHM stayed essentially the same between the two groups of mice, even when excluding Gs in the second position of RGYW hotspots. Adenine was still the most frequently mutated base and the ratio of transitions to transversion did not change (1.0 and 1.2 versus 1.0 and 1.1). $Pol\kappa$ can introduce frameshift mutations *in vitro*. However, my analysis does not reveal differences with respect to the number of frameshift or tandem mutations. The present work therefore demonstrates that $Pol\kappa$ is not an essential component of the hypermutation machinery. This finding was recently also confirmed in a $Pol\kappa$-deficient mouse strain that was generated independently from the one analyzed here (Shimizu, 2003).

Several other error-prone DNA polymerases are also dispensable for SHM *in vivo*. Mice deficient of $Pol\beta$, $Pol\delta$, $Pol\lambda$, $Pol\iota$, or $Pol\mu$ mutate their Ig genes efficiently and these polymerases do not show a significant change in their mutational pattern (Bertocci et al., 2002; Esposito et al., 2000a; Longacre et al., 2003; McDonald et al., 2003). Nonetheless, evidence for the involvement of error-prone DNA polymerases in the SHM mechanism has been accumulated in recent years. For example, the error-spectrum of $Pol\eta$ *in vitro* correlates with mutations at SHM hotspots (Pavlov et al., 2002; Rogozin et al., 2001). While the frequency of SHM in $Pol\eta$-deficient XP-V patients reaches normal levels, the mutation pattern is biased towards G-C mutations. Thus, $Pol\eta$ it is probably responsible for many of the mutations at A-T nucleotides (Zeng et al., 2001). $Pol\zeta$ is thought to introduce mutations when extending from mismatches incorporated by other DNA polymerases (Diaz et al., 2001; Zan et al., 2001). One of the latter DNA polymerases may be $Pol\iota$, which was found to interact with $Pol\zeta$. Deficiency of $Pol\iota$ in a hypermutating cell line results in the reduction of G-C mutations (Faili et al., 2002). However, the significance of this finding is unclear, because $Pol\iota$-deficient

mice mutate their Ig genes at normal levels without obvious changes in the mutational patterns (McDonald et al., 2003). This apparent paradox could be explained by the expression of a particular DNA polymerase in cell lines, but the synergistic and redundant action of several DNA polymerases during SHM *in vivo*.

To investigate whether several DNA polymerase have overlapping function during SHM, I started to generated compound mutant mice deficient of Polĸ, Polλ, and Polι. Somatic hypermutation in compound mutant mice deficient of these three DNA polymerases appear to mutate their Ig genes normally. Both the mutation frequency and the mutation patterns resemble those in wild-type controls. The ratio of transition versus transversions remains basically the same and the number of deletions or insertions does not change. In the light of this finding, it seems unlikely that the combined contribution of of Polĸ, Polλ, and Polι to SHM is significant. However, their function in SHM can still be substituted by other error-prone DNA polymerases. One of the candidates for such a function is Polμ. The lymphoid-specific TdT-like Polμ acts in a template-dependent but sequence independent manner and has been implicated in the processing of DNA ends during Ig light chain rearrgangement (Bertocci et al., 2003). However, its expression is not restricted to developing lymphocytes. Polμ is also found in GC B cells and this expression pattern was suggestive of specialized function during SHM. Yet, it is not an essential component for the SHM process as mice deficient of Polμ mutate their Ig genes normally (Bertocci et al., 2002). I am currently in the process of intercrossing Polĸ$^{-/-}$Polλ$^{-/-}$Polι$^{-/-}$ with mice deficient of Polμ to explore the question of the redundant function of DNA polymerases in SHM further.

D2   Function of M17 in the Immune System

Diffuse large B cell lymphomas (DLBCL) are a heterogeneous group of tumors with diverse clinical features and distinct gene expression profiles (Lossos and Levy, 2003). Patients with DLBCL can be subgrouped according to the expression of *HGAL* in these tumors. *HGAL* can serve as a prognostic marker for the clinical outcome in patients with DLBCL (Lossos et al., 2003). High expression of *HGAL* in DLBCL results in a better clinical prognosis with longer survival rates. However, the biological function of HGAL is unknown. In this study, I have investigated mice deficient of M17, the murine homologue of HGAL, to elucidate its role in B cell function.

The *M17* and *HGAL* genes share a similar exon-intron structure and the respective proteins are homologous to each other but not to other known proteins. Both proteins contain several potential phosphorylation sites and include a non-canonical ITAM motif. These features suggest that HGAL and M17 are true homologues (Lossos et al., 2003; Pan et al., 2003). However, M17 and HGAL differ substantially at the N-terminus as HGAL possesses an elongated N-terminus due to exon 2 in the *HGAL* mRNA, which is absent from the published *M17* mRNA. During the course of this analysis, I detected a novel isoform of the *M17* mRNA that contains a previously unidentified exon. The novel exon is located between exon 1 and 2 of the M17 mRNA and of similar length as exon 2 of the HGAL mRNA. It can thus account for the discrepancy in the length of the N-terminus between HGAL and M17.

M17 and HGAL share overlapping but not identical expression patterns. *M17* is expressed at low levels in developing B cells and is predominantly expressed in GC B cells (Christoph, 1993; Christoph et al., 1994). This very specific expression pattern was suggestive for a function of M17 within the GC reaction. Here, M17 may play a role in cell signaling due to the presence of a non-canonical ITAM motif. The expression of HGAL mRNA is upregulated in naïve B cell upon stimulation with the cytokine IL-4. My observation that the expression of *M17* mRNA can also be induced by IL-4 in LPS or CD40-activated B cells suggests that expression of *HGAL* and *M17* are regulated by a similar mechanism. IL-4-mediated signaling plays an important role in GC function and is particularly

essential for CSR from Cμ to the Cγ1 and Cϵ isotypes (Kühn et al., 1991) . Thus, the IL-4-induced expression of M17 is consistent with the notion that M17 plays a role within the GCs, where it may function during certain aspects of IL-4 mediated events.

M17 is expressed in developing B cells (Christoph, 1993). In this study, I show that both the pro-B and pre-B cell fractions are present at wild-type levels in *M17*$^{-/-}$ mice. B cell development appears to be unaffected in the absence of M17. M17 therefore seems to be dispensable for B cell development. However, the precise role of M17 in this cellular compartment requires further investigation. M17 was originally isolated via a cDNA subtraction between GC B cells and LPS-stimulated B cells. Thus, it was not surprising that naïve B cells do not require M17. Splenocytes are present at normal numbers in *M17*$^{-/-}$ mice and the proportions of the major B and T cell subsets are not altered.

Immunization of *M17*$^{-/-}$ mice with a T cell-dependent (TD) antigen leads to the formation of GC B cells and the size of this specialized compartment is similar to wild-type controls. GC B cells in *M17*$^{-/-}$ are morphologically organized like wild-type GCs. GCs of *M17*$^{-/-}$ mice are separated into the dark zone and the FDC-rich light zone and are equal to wild-type GCs with respect to number and size. Thus, M17 is not required for GC formation. M17-deficent B cells proliferate equally well as wild-type controls when stimulated with anti-IgM or anti-CD40 mAbs in the presence of IL-4. It appears unlikely that GC B cell proliferation is affected by the lack of M17. IL-4 is a critical cytokine for CSR to IgG1 and IgE (Kühn et al., 1991). The upregulation of *M17* mRNA after stimulation with an αCD40 mAb and IL-4 suggested the involvement of M17 in CSR to IgG1 and IgE. However, the presence of wild-type levels of antibody serum titers in M17-deficient mice and the *in vitro* ability of B cells from these mice to undergo CSR to all isotypes including the αCD40 and IL-4-induced isotypes IgG1 and IgE show that M17 is not essential for CSR. In addition*, M17*$^{-/-}$ mice undergo efficient SHM in response to a TD antigen. The mutation frequency and patterns are comparable to wild-type mice. Primary TD immune responses reach NP-specific IgG1 levels in the serum similar to those found in wild-type mice and this characteristic is independent of the

amount of immunizing antigen. Thus, M17 is surprisingly dispensable for the core events of the GC reaction during a primary immune response.

Besides the high expression of HGAL in GC B cells, expression of *HGAL* mRNA is also found at low levels in memory B cells (Lossos et al., 2003). *In vitro* studies indicated a role for IL-4 in the promotion of memory B cell formation (Choe et al., 1997) and the alteration of homing properties of B cell during this process (Roy et al., 2002). For this reason, HGAL has been suggested to participate in the differentiation of memory B cells. Some M17$^+$ cells localize to the marginal zone (Christoph, 1993), where memory B cells reside in the spleen. However, *M17$^{-/-}$* mice produce normal NP-specific IgG1 serum titers upon secondary antigen challenge. Although the current data do not lend strong support to the hypothesis of an involvement of M17 in memory B cell formation, it is still possible that M17 is involved in such a process. Further studies involving bone-marrow chimeras of *M17$^{-/-}$* and wild-type cells will help to investigate this question.

The analysis of Peyer's patches M17$^{-/-}$ mice revealed that the absence of M17 affects the Peyer's patches. M17-defcient mice have a reduced number of Peyer's patches per mouse and the individual Peyer's patches are often smaller in size. These two effects combined result in a 2-3 fold reduction of total cells in the Peyer's patches. The ratio of T versus B cells, however, remains normal in Peyer's patches when compared to wild-type mice. In particular, the size of GC B cells populations is not altered in the Peyer's patches of M17$^{-/-}$ mice and the architecture of the GCs is undisturbed. On a functional level, GC B cells in the Peyer's patches of *M17$^{-/-}$* mice are capable of class switching to IgA, the predominant isotype in the gut. Likewise, the reduced number of cells in the Peyer's patches does not affect SHM as both the mutation frequency and mutation patterns are equal to wild-type controls.

It is surprising that the absence of M17 affects the cell number of the Peyer's patches. The lymphotoxin (LT)-driven development of Peyer's patches occurs in three stages (Adachi et al., 1997). It commences in the embryo at day 15 post gestation with the formation of clusters of cells expressing the adhesion molecules VCAM and ICAM and is followed by the entry of hemapoetic cells a few days later. Entry of mature lymphocytes completes the development of mature

Peyer's patches just prior to birth but is not required for the compartmentalization of Peyer's patches (Hashi et al., 2001). The expression pattern of M17 during embryogenesis has not been investigated. Since the cellularity of the Peyer's patches does not change in M17-deficient mice, it seems possible that the reduction in cell numbers is not due to a B cell-specific effect. Alternatively, M17 may modulate homing properties of B cells, which become apparent during the formation and development of Peyer's patches. In this context, it is interesting to note that IL-4 can augment autocrine lymphotoxin production in B cells (Worm et al., 1998). Mice with B cell-specific ablation of LTβ show a disturbed splenic microarchitecture and a reduced size of Peyer's patches with intact B and T cell compartments (Tumanov et al., 2002). The former phenotype is not seen in M17$^{-/-}$ mice. However, in the light of the latter finding, one can speculate that M17-mediated signals might modulate the formation of Peyer's patches.

At the present time, it is unclear whether high expression of HGAL in DLBCL merely identifies a particular subset of lymphomas with a beneficial prognosis or is indeed a reflection of the biological function of HGAL. High expression of BCL6, which is expressed in GCs and serves as another prognostic marker for patients with DLBCL, is also indicative of better overall survival (Lossos et al., 2001). Moreover, elevated co-expression of both genes appears to have cumulative effects with respect to survival (Lossos et al., 2003). Interestingly, expression of both genes can be induced by IL-4. Expression of HGAL and BCL6 therefore identifies GC-derived tumors that are exposed to higher IL-4 levels. IL-4 can inhibit *in vitro* proliferation in lymphoma cells (Defrance et al., 1992; Taylor et al., 1990). Such growth-moderating effects could be mediated by HGAL and M17 and would predict stronger proliferation of *M17$^{-/-}$* B cells and possibly enlarged GCs. These effects have not been observed in *M17$^{-/-}$* mice and hence argue against such a hypothesis. On the other hand, high expression of HGAL and BCL6 may simply identify tumors that originate from B cells at a particular differentiation stage. DLBCL can be separated into distinct subtypes. The more malignant type is derived from activated B cells, while the more benign subtype is of GC B cell origin (Alizadeh et al., 2000). *HGAL* marks subsets of DLBCL with a better prognosis and

may even identify DLBCL derived from particular GC subsets, for example centroblasts or centrocytes. Given the moderate phenotype of $M17^{-/-}$ mice in GC formation and function, I would favor the latter explanation.

In conclusion, M17 does not affect B or T cell development in a major way. M17 is dispensable for GC formation, B cell proliferation, Ig class switching, SHM and the formation of an immune response against a TD antigen. The biology of M17 suggests that *HGAL* serves as a prognostic marker for the improved survival of DLBCL patients in a more indirect way. However, $M17^{-/-}$ mice have less and smaller Peyer's patches, indicating a potential role in the organogenesis of Peyer's patches.

E   SUMMARY

In T cell-dependent immune responses, activated B cells undergo a phase of rapid expansion and form distinct histological structures, the germinal centers (GC). GCs are the sites of secondary antibody diversification. Somatic hypermutation (SHM) introduces mutations into the rearranged V genes, whereas class switch recombination (CSR) alters the IgH constant region to modulate effector function.

The current model of SHM postulates cytidine deamination by AID, followed by error-prone repair that involves short-patch DNA synthesis by error-prone DNA polymerases. The *Polκ* (*DinB1*) gene encodes a specialized mammalian DNA polymerase called DNA polymerase κ. The mouse *Polκ* gene is expressed in most tissues of the body including B cells. The ability of *Polκ* to generate mutations when extending primers on undamaged DNA templates identifies this enzyme as a candidate for the introduction of nucleotide exchanges during SHM. Here, I show that Polκ-deficient mice are viable, fertile and able to mount a normal immune response to the antigen (4-hydroxy-3-nitrophenyl) acetyl-chicken globulin (NP-GC). Polκ-deficient mice mutate their Ig genes normally. *Polκ$^{-/-}$Polλ$^{-/-}$Polι$^{-/-}$* mice also show no defects in SHM, indicating that these error-prone DNA polymerases do not substitute for each other's function during SHM. However, Polκ-deficient embryonic fibroblasts are sensitive to cell death following exposure to ultraviolet radiation, suggesting a role for Polκ in translesion DNA synthesis.

The human gene *HGAL* serves as marker in the prognosis of patients with GC-derived diffuse large B cell lymphomas (DLBCL). The mouse gene *M17* is the homologue of *HGAL*. M17 is predominantly expressed in the GCs, indicating a role in GC function. In the present study, I analyzed *M17$^{-/-}$* mice to investigate the role of M17 in the GC reaction. *M17$^{-/-}$* mice form normal GCs, undergo efficient CSR and SHM and mount a T cell-dependent immune response. Thus, M17 is dispensable for the GC reaction and the current data support a rather indirect role for *HGAL* as a prognostic marker in the biology of DLBCL.

F ZUSAMMENFASSUNG

Aktivierte B Zellen proliferieren während T Zell-abhängigen Immunantworten und bilden definierte histologische Strukturen, die Keimzentren. Dort findet die sekundäre Diversifikation der Antikörper statt: Somatische Hypermutation (SHM) fügt Mutationen in den zusammengefügten V Genen ein und Klassenwechsel-Rekombination ändert die konstante Region der schweren Immunglobulinkette.

Das aktuelle Model der SHM postuliert zunächst eine Cytidin-Deaminierung durch AID und anschliessende fehlerhafte DNA Reperatur, die zum Teil durch fehlerbehaftete DNA Polymerasen verursacht wird. Die fehlerbehaftete DNA Polymerase κ (Polκ) wird in den meisten Geweben exprimiert, darunter auch in B Zellen. Die Fähigkeit von Polκ, Mutationen während der DNA Synthese einfügen zu können, legt eine Beteiligung dieser DNA Polymerase an der SHM nahe. In dieser Arbeit habe ich daher $Pol\kappa^{-/-}$ Mäuse generiert, um diese Frage zu klären. $Pol\kappa^{-/-}$ Mäuse sind lebensfähig und zeugungsfähig. Die mutanten Mäuse haben eine normale T Zell-abhängige Immunantwort und mutieren ihre Immunglobulin Gene in gleichen Massen wie $Pol\kappa^{+/+}$ Mäuse. Analyse von $Pol\kappa^{-/-}Pol\lambda^{-/-}Pol\iota^{-/-}$ Mäusen ergibt ein vergleichbares Ergebnis, was eine austauschbare Funktion der drei DNA Polymerasen in SHM unwahrscheinlich erscheinen lässt. Hingegen ist Polκ wichtig für die DNA Reperatur, da Fibroblasten aus $Pol\kappa^{+/+}$ Mausembryos eine erhöhte Sterblichkeit nach Bestrahlung mit ultraviolettem Licht zeigen.

Das humane Gen *HGAL* dient als Marker für die klinische Prognose von Tumoren des Keimzentrums. Das Maushomolog von *HGAL* heisst *M17* und ist vorwiegend in den Keimzentren exprimiert. Ich habe $M17^{-/-}$ Mäuse analysiert, um die Rolle von M17 in der Keimzentrums-Reaktion zu verstehen. $M17^{-/-}$ Mäuse bilden normale Keimzentren, führen effiziente SHM und Klassenwechsel-Rekombination durch, und reagieren in der Immunantwort ähnlich wie wild-typ Kontrollen. Der gegenwärtige Kenntnisstand unterstützt eher eine indirekte Rolle für *HGAL* als Marker in der Biologie von Tumoren des Keimzentrums.

G   REFERENCES

Adachi, S., Yoshida, H., Kataoka, H., and Nishikawa, S. (1997). Three distinctive steps in Peyer's patch formation of murine embryo. Int Immunol *9*, 507-514.

Alizadeh, A. A., Eisen, M. B., Davis, R. E., Ma, C., Lossos, I. S., Rosenwald, A., Boldrick, J. C., Sabet, H., Tran, T., Yu, X.*, et al.* (2000). Distinct types of diffuse large B-cell lymphoma identified by gene expression profiling. Nature *403*, 503-511.

Allman, D. M., Ferguson, S. E., Lentz, V. M., and Cancro, M. P. (1993). Peripheral B cell maturation. II. Heat-stable antigen(hi) splenic B cells are an immature developmental intermediate in the production of long-lived marrow-derived B cells. J Immunol *151*, 4431-4444.

Alt, F. W., and Baltimore, D. (1982). Joining of immunoglobulin heavy chain gene segments: implications from a chromosome with evidence of three D-JH fusions. Proc Natl Acad Sci U S A *79*, 4118-4122.

Alt, F. W., Yancopoulos, G. D., Blackwell, T. K., Wood, C., Thomas, E., Boss, M., Coffman, R., Rosenberg, N., Tonegawa, S., and Baltimore, D. (1984). Ordered rearrangement of immunoglobulin heavy chain variable region segments. Embo J *3*, 1209-1219.

Aoufouchi, S., Flatter, E., Dahan, A., Faili, A., Bertocci, B., Storck, S., Delbos, F., Cocea, L., Gupta, N., Weill, J. C., and Reynaud, C. A. (2000). Two novel human and mouse DNA polymerases of the polX family. Nucleic Acids Res *28*, 3684-3693.

Baniyash, M., and Eshhar, Z. (1984). Inhibition of IgE binding to mast cells and basophils by monoclonal antibodies to murine IgE. Eur J Immunol *14*, 799-807.

Barnes, D. E., Stamp, G., Rosewell, I., Denzel, A., and Lindahl, T. (1998). Targeted disruption of the gene encoding DNA ligase IV leads to lethality in embryonic mice. Curr Biol *8*, 1395-1398.

Barreto, V., Reina-San-Martin, B., Ramiro, A. R., McBride, K. M., and Nussenzweig, M. C. (2003). C-terminal deletion of AID uncouples class switch recombination from somatic hypermutation and gene conversion. Mol Cell *12*, 501-508.

Bassing, C. H., Swat, W., and Alt, F. W. (2002). The mechanism and regulation of chromosomal V(D)J recombination. Cell *109 Suppl*, S45-55.

Bebenek, K., Tissier, A., Frank, E. G., McDonald, J. P., Prasad, R., Wilson, S. H., Woodgate, R., and Kunkel, T. A. (2001). 5'-Deoxyribose phosphate lyase activity of human DNA polymerase iota in vitro. Science *291*, 2156-2159.

Bemark, M., Khamlichi, A. A., Davies, S. L., and Neuberger, M. S. (2000). Disruption of mouse polymerase zeta (Rev3) leads to embryonic lethality and impairs blastocyst development in vitro. Curr Biol *10*, 1213-1216.

Benner, R., Hijmans, W., and Haaijman, J. J. (1981). The bone marrow: the major source of serum immunoglobulins, but still a neglected site of antibody formation. Clin Exp Immunol *46*, 1-8.

Bertocci, B., De Smet, A., Berek, C., Weill, J. C., and Reynaud, C. A. (2003). Immunoglobulin kappa light chain gene rearrangement is impaired in mice deficient for DNA polymerase mu. Immunity *19*, 203-211.

Bertocci, B., De Smet, A., Flatter, E., Dahan, A., Bories, J. C., Landreau, C., Weill, J. C., and Reynaud, C. A. (2002). Cutting edge: DNA polymerases mu and lambda are dispensable for Ig gene hypermutation. J Immunol *168*, 3702-3706.

Bertocci, B., Quint, L., Delbos, F., Garcia, C., Reynaud, C. A., and Weill, J. C. (1998). Probing immunoglobulin gene hypermutation with microsatellites suggests a nonreplicative short patch DNA synthesis process. Immunity *9*, 257-265.

Betz, A. G., Rada, C., Pannell, R., Milstein, C., and Neuberger, M. S. (1993). Passenger transgenes reveal intrinsic specificity of the antibody hypermutation mechanism: clustering, polarity, and specific hot spots. Proc Natl Acad Sci U S A *90*, 2385-2388.

Bhattacharya, A., Dorf, M. E., and Springer, T. A. (1981). A shared alloantigenic determinant on Ia antigens encoded by the I-A and I-E subregions: evidence for I region gene duplication. J Immunol *127*, 2488-2495.

Birnboim, H. C. (1983). A rapid alkaline extraction method for the isolation of plasmid DNA. Methods Enzymol *100*, 243-255.

Blunt, T., Finnie, N. J., Taccioli, G. E., Smith, G. C., Demengeot, J., Gottlieb, T. M., Mizuta, R., Varghese, A. J., Alt, F. W., Jeggo, P. A., and et al. (1995). Defective DNA-dependent protein kinase activity is linked to V(D)J recombination and DNA repair defects associated with the murine scid mutation. Cell *80*, 813-823.

Bottaro, A., Lansford, R., Xu, L., Zhang, J., Rothman, P., and Alt, F. W. (1994). S region transcription per se promotes basal IgE class switch recombination but additional factors regulate the efficiency of the process. Embo J *13*, 665-674.

Bottomly, K., Luqman, M., Greenbaum, L., Carding, S., West, J., Pasqualini, T., and Murphy, D. B. (1989). A monoclonal antibody to murine CD45R distinguishes CD4 T cell populations that produce different cytokines. Eur J Immunol *19*, 617-623.

Bransteitter, R., Pham, P., Scharff, M. D., and Goodman, M. F. (2003). Activation-induced cytidine deaminase deaminates deoxycytidine on single-stranded DNA but requires the action of RNase. Proc Natl Acad Sci U S A *100*, 4102-4107.

Brenner, S., and Milstein, C. (1966). Origin of antibody variation. Nature *211*, 242-243.

Bross, L., Fukita, Y., McBlane, F., Demolliere, C., Rajewsky, K., and Jacobs, H. (2000). DNA double-strand breaks in immunoglobulin genes undergoing somatic hypermutation. Immunity *13*, 589-597.

Bross, L., Muramatsu, M., Kinoshita, K., Honjo, T., and Jacobs, H. (2002). DNA double-strand breaks: prior to but not sufficient in targeting hypermutation. J Exp Med *195*, 1187-1192.

Cariappa, A., and Pillai, S. (2002). Antigen-dependent B-cell development. Curr Opin Immunol *14*, 241-249.

Casellas, R., Nussenzweig, A., Wuerffel, R., Pelanda, R., Reichlin, A., Suh, H., Qin, X. F., Besmer, E., Kenter, A., Rajewsky, K., and Nussenzweig, M. C. (1998). Ku80 is required for immunoglobulin isotype switching. Embo J *17*, 2404-2411.

Chaudhuri, J., Tian, M., Khuong, C., Chua, K., Pinaud, E., and Alt, F. W. (2003). Transcription-targeted DNA deamination by the AID antibody diversification enzyme. Nature *422*, 726-730.

Cheo, D. L., Ruven, H. J., Meira, L. B., Hammer, R. E., Burns, D. K., Tappe, N. J., van Zeeland, A. A., Mullenders, L. H., and Friedberg, E. C. (1997). Characterization of defective nucleotide excision repair in XPC mutant mice. Mutat Res *374*, 1-9.

Choe, J., Kim, H. S., Armitage, R. J., and Choi, Y. S. (1997). The functional role of B cell antigen receptor stimulation and IL-4 in the generation of human memory B cells from germinal center B cells. J Immunol *159*, 3757-3766.

Chomczynski, P., and Qasba, P. K. (1984). Alkaline transfer of DNA to plastic membrane. Biochem Biophys Res Commun *122*, 340-344.

Christoph, T. (1993) Isolierung und Charakterisierung keimzentrumsspezifischer Gene der Maus, Doktorarbeit, Universitaet zu Koeln, Koeln.

Christoph, T., Rickert, R., and Rajewsky, K. (1994). M17: a novel gene expressed in germinal centers. Int Immunol *6*, 1203-1211.

Coffman, R. L. (1982). Surface antigen expression and immunoglobulin gene rearrangement during mouse pre-B cell development. Immunol Rev *69*, 5-23.

Critchlow, S. E., Bowater, R. P., and Jackson, S. P. (1997). Mammalian DNA double-strand break repair protein XRCC4 interacts with DNA ligase IV. Curr Biol *7*, 588-598.

Cumano, A., and Rajewsky, K. (1986). Clonal recruitment and somatic mutation in the generation of immunological memory to the hapten NP. Embo J *5*, 2459-2468.

Cyster, J. G. (2003). Homing of antibody secreting cells. Immunol Rev *194*, 48-60.

Defrance, T., Fluckiger, A. C., Rossi, J. F., Magaud, J. P., Sotto, J. J., and Banchereau, J. (1992). Antiproliferative effects of interleukin-4 on freshly isolated non-Hodgkin malignant B-lymphoma cells. Blood *79*, 990-996.

Di Noia, J., and Neuberger, M. S. (2002). Altering the pathway of immunoglobulin hypermutation by inhibiting uracil-DNA glycosylase. Nature *419*, 43-48.

Dialynas, D. P., Quan, Z. S., Wall, K. A., Pierres, A., Quintans, J., Loken, M. R., Pierres, M., and Fitch, F. W. (1983). Characterization of the murine T cell surface molecule, designated L3T4, identified by monoclonal antibody GK1.5: similarity of L3T4 to the human Leu-3/T4 molecule. J Immunol *131*, 2445-2451.

Diaz, M., Velez, J., Singh, M., Cerny, J., and Flajnik, M. F. (1999). Mutational pattern of the nurse shark antigen receptor gene (NAR) is similar to that of mammalian Ig genes and to spontaneous mutations in evolution: the translesion synthesis model of somatic hypermutation. Int Immunol *11*, 825-833.

Diaz, M., Verkoczy, L. K., Flajnik, M. F., and Klinman, N. R. (2001). Decreased frequency of somatic hypermutation and impaired affinity maturation but intact germinal center formation in mice expressing antisense RNA to DNA polymerase zeta. J Immunol *167*, 327-335.

Dickerson, S. K., Market, E., Besmer, E., and Papavasiliou, F. N. (2003). AID mediates hypermutation by deaminating single stranded DNA. J Exp Med *197*, 1291-1296.

Doi, T., Kinoshita, K., Ikegawa, M., Muramatsu, M., and Honjo, T. (2003). De novo protein synthesis is required for the activation-induced cytidine deaminase function in class-switch recombination. Proc Natl Acad Sci U S A *100*, 2634-2638.

Dominguez, O., Ruiz, J. F., Lain de Lera, T., Garcia-Diaz, M., Gonzalez, M. A., Kirchhoff, T., Martinez, A. C., Bernad, A., and Blanco, L. (2000). DNA polymerase mu (Pol mu), homologous to TdT, could act as a DNA mutator in eukaryotic cells. Embo J *19*, 1731-1742.

Ehrenstein, M. R., and Neuberger, M. S. (1999). Deficiency in Msh2 affects the efficiency and local sequence specificity of immunoglobulin class-switch recombination: parallels with somatic hypermutation. Embo J *18*, 3484-3490.

Ehrenstein, M. R., Rada, C., Jones, A. M., Milstein, C., and Neuberger, M. S. (2001). Switch junction sequences in PMS2-deficient mice reveal a microhomology-mediated mechanism of Ig class switch recombination. Proc Natl Acad Sci U S A *98*, 14553-14558.

Esposito, G., Godindagger, I., Klein, U., Yaspo, M. L., Cumano, A., and Rajewsky, K. (2000a). Disruption of the Rev3l-encoded catalytic subunit of polymerase zeta in mice results in early embryonic lethality. Curr Biol *10*, 1221-1224.

Esposito, G., Texido, G., Betz, U. A., Gu, H., Muller, W., Klein, U., and Rajewsky, K. (2000b). Mice reconstituted with DNA polymerase beta-deficient fetal liver cells are able to mount a T cell-dependent immune response and mutate their Ig genes normally. Proc Natl Acad Sci U S A *97*, 1166-1171.

Faili, A., Aoufouchi, S., Flatter, E., Gueranger, Q., Reynaud, C. A., and Weill, J. C. (2002). Induction of somatic hypermutation in immunoglobulin genes is dependent on DNA polymerase iota. Nature *419*, 944-947.

Fischhaber, P. L., Gerlach, V. L., Feaver, W. J., Hatahet, Z., Wallace, S. S., and Friedberg, E. C. (2002). Human DNA polymerase kappa bypasses and extends beyond thymine glycols during translesion synthesis in vitro, preferentially incorporating correct nucleotides. J Biol Chem *277*, 37604-37611.

Frank, K. M., Sekiguchi, J. M., Seidl, K. J., Swat, W., Rathbun, G. A., Cheng, H. L., Davidson, L., Kangaloo, L., and Alt, F. W. (1998). Late embryonic lethality and impaired V(D)J recombination in mice lacking DNA ligase IV. Nature *396*, 173-177.

Friedberg, E. C., Wagner, R., and Radman, M. (2002). Specialized DNA polymerases, cellular survival, and the genesis of mutations. Science *296*, 1627-1630.

Fukita, Y., Jacobs, H., and Rajewsky, K. (1998). Somatic hypermutation in the heavy chain locus correlates with transcription. Immunity *9*, 105-114.

Garcia-Diaz, M., Dominguez, O., Lopez-Fernandez, L. A., de Lera, L. T., Saniger, M. L., Ruiz, J. F., Parraga, M., Garcia-Ortiz, M. J., Kirchhoff, T., del Mazo, J*., et al.* (2000). DNA polymerase lambda (Pol lambda), a novel eukaryotic DNA polymerase with a potential role in meiosis. J Mol Biol *301*, 851-867.

Gay, D., Saunders, T., Camper, S., and Weigert, M. (1993). Receptor editing: an approach by autoreactive B cells to escape tolerance. J Exp Med *177*, 999-1008.

Gerlach, V. L., Aravind, L., Gotway, G., Schultz, R. A., Koonin, E. V., and Friedberg, E. C. (1999). Human and mouse homologs of Escherichia coli DinB (DNA polymerase IV), members of the UmuC/DinB superfamily. Proc Natl Acad Sci U S A *96*, 11922-11927.

Gerlach, V. L., Feaver, W. J., Fischhaber, P. L., and Friedberg, E. C. (2001). Purification and characterization of pol kappa, a DNA polymerase encoded by the human DINB1 gene. J Biol Chem *276*, 92-98.

Gil-Guzman, E., Ollero, M., Lopez, M. C., Sharma, R. K., Alvarez, J. G., Thomas, A. J., Jr., and Agarwal, A. (2001). Differential production of reactive oxygen species by subsets of human spermatozoa at different stages of maturation. Hum Reprod *16*, 1922-1930.

Gilfillan, S., Dierich, A., Lemeur, M., Benoist, C., and Mathis, D. (1993). Mice lacking TdT: mature animals with an immature lymphocyte repertoire. Science *261*, 1175-1178.

Goodman, M. F. (2002). Error-prone repair DNA polymerases in prokaryotes and eukaryotes. Annu Rev Biochem *71*, 17-50.

Goossens, T., Klein, U., and Kuppers, R. (1998). Frequent occurrence of deletions and duplications during somatic hypermutation: implications for oncogene translocations and heavy chain disease. Proc Natl Acad Sci U S A *95*, 2463-2468.

Grawunder, U., Leu, T. M., Schatz, D. G., Werner, A., Rolink, A. G., Melchers, F., and Winkler, T. H. (1995). Down-regulation of RAG1 and RAG2 gene expression in preB cells after functional immunoglobulin heavy chain rearrangement. Immunity *3*, 601-608.

Grawunder, U., Wilm, M., Wu, X., Kulesza, P., Wilson, T. E., Mann, M., and Lieber, M. R. (1997). Activity of DNA ligase IV stimulated by complex formation with XRCC4 protein in mammalian cells. Nature *388*, 492-495.

Gruetzman, R. (1981) Vergleichende Idiotypische Analyse von Rezeptoren mit Spezifitaet fuer Histokompatibilitaetsantigene, PhD, Cologne, Cologne.

Gu, H., Marth, J. D., Orban, P. C., Mossmann, H., and Rajewsky, K. (1994a). Deletion of a DNA polymerase β gene segment in T cells using cell type-specific gene targeting. Science *265*, 103-106.

Gu, H., Marth, J. D., Orban, P. C., Mossmann, H., and Rajewsky, K. (1994b). Deletion of a DNA polymerase beta gene segment in T cells using cell type-specific gene targeting. Science *265*, 103-106.

Gu, H., Tarlinton, D., Muller, W., Rajewsky, K., and Forster, I. (1991). Most peripheral B cells in mice are ligand selected. J Exp Med *173*, 1357-1371.

Gulley, M. L., Ogata, L. C., Thorson, J. A., Dailey, M. O., and Kemp, J. D. (1988). Identification of a murine pan-T cell antigen which is also expressed during the terminal phases of B cell differentiation. J Immunol *140*, 3751-3757.

Haracska, L., Prakash, L., and Prakash, S. (2002). Role of human DNA polymerase kappa as an extender in translesion synthesis. Proc Natl Acad Sci U S A *99*, 16000-16005.

Hardy, R. R., Carmack, C. E., Shinton, S. A., Kemp, J. D., and Hayakawa, K. (1991). Resolution and characterization of pro-B and pre-pro-B cell stages in normal mouse bone marrow. J Exp Med *173*, 1213-1225.

Hardy, R. R., and Hayakawa, K. (2001). B cell development pathways. Annu Rev Immunol *19*, 595-621.

Harriman, G. R., Bradley, A., Das, S., Rogers-Fani, P., and Davis, A. C. (1996). IgA class switch in I alpha exon-deficient mice. Role of germline transcription in class switch recombination. J Clin Invest *97*, 477-485.

Hashi, H., Yoshida, H., Honda, K., Fraser, S., Kubo, H., Awane, M., Takabayashi, A., Nakano, H., Yamaoka, Y., and Nishikawa, S. (2001). Compartmentalization of Peyer's patch anlagen before lymphocyte entry. J Immunol *166*, 3702-3709.

Hayakawa, K., Hardy, R. R., Parks, D. R., and Herzenberg, L. A. (1983). The "Ly-1 B" cell subpopulation in normal immunodefective, and autoimmune mice. J Exp Med *157*, 202-218.

Hegi, M. E., Sagelsdorff, P., and Lutz, W. K. (1989). Detection by 32P-postlabeling of thymidine glycol in gamma-irradiated DNA. Carcinogenesis *10*, 43-47.

Herzenberg, L. A., and Black, S. J. (1980). Regulatory circuits and antibody responses. Eur J Immunol *10*, 1-11.

Herzenberg, L. A., Stall, A. M., Lalor, P. A., Sidman, C., Moore, W. A., and Parks, D. R. (1986). The Ly-1 B cell lineage. Immunol Rev *93*, 81-102.

Ho, F., Lortan, J. E., MacLennan, I. C., and Khan, M. (1986). Distinct short-lived and long-lived antibody-producing cell populations. Eur J Immunol *16*, 1297-1301.

Hogan, B., Constantini, F., and Lacy, I. (1987). Manuipulating the mouse embryo, Cold Spring Harbor Laboratory Press).

Honjo, T., and Alt, F. W. (1995). Immunoglobulin genes, 2nd edn (London ; San Diego, Academic Press).

Huang, X., Kolbanovskiy, A., Wu, X., Zhang, Y., Wang, Z., Zhuang, P., Amin, S., and Geacintov, N. E. (2003). Effects of base sequence context on translesion synthesis past a

bulky (+)-trans-anti-B[a]P-N2-dG lesion catalyzed by the Y-family polymerase pol kappa. Biochemistry *42*, 2456-2466.

Iwasato, T., Shimizu, A., Honjo, T., and Yamagishi, H. (1990). Circular DNA is excised by immunoglobulin class switch recombination. Cell *62*, 143-149.

J, O. W., Kawamura, K., Tada, Y., Ohmori, H., Kimura, H., Sakiyama, S., and Tagawa, M. (2001). DNA polymerase kappa, implicated in spontaneous and DNA damage-induced mutagenesis, is overexpressed in lung cancer. Cancer Res *61*, 5366-5369.

Jacobs, H., Fukita, Y., van der Horst, G. T., de Boer, J., Weeda, G., Essers, J., de Wind, N., Engelward, B. P., Samson, L., Verbeek, S.*, et al.* (1998). Hypermutation of immunoglobulin genes in memory B cells of DNA repair- deficient mice. J Exp Med *187*, 1735-1743.

Jansen, J. G., and de Wind, N. (2003). Biological functions of translesion synthesis proteins in vertebrates. DNA Repair (Amst) *2*, 1075-1085.

Johnson, R. E., Prakash, S., and Prakash, L. (2000a). The human DINB1 gene encodes the DNA polymerase Poltheta. Proc Natl Acad Sci U S A *97*, 3838-3843.

Johnson, R. E., Washington, M. T., Haracska, L., Prakash, S., and Prakash, L. (2000b). Eukaryotic polymerases iota and zeta act sequentially to bypass DNA lesions. Nature *406*, 1015-1019.

Jolly, C., and Neuberger, M. (2001). Somatic hypermutation of immunoglobulin kappa transgenes: Association of mutability with demethylation. Immunol Cell Biol *79*, 18-22.

Jolly, C. J., Klix, N., and Neuberger, M. S. (1997). Rapid methods for the analysis of immunoglobulin gene hypermutation: application to transgenic and gene targeted mice. Nucleic Acids Res *25*, 1913-1919.

Jolly, C. J., Wagner, S. D., Rada, C., Klix, N., Milstein, C., and Neuberger, M. S. (1996). The targeting of somatic hypermutation. Semin Immunol *8*, 159-168.

Jung, S., Rajewsky, K., and Radbruch, A. (1993). Shutdown of class switch recombination by deletion of a switch region control element. Science *259*, 984-987.

Karasuyama, H., Kudo, A., and Melchers, F. (1990). The proteins encoded by the VpreB and lambda 5 pre-B cell-specific genes can associate with each other and with mu heavy chain. J Exp Med *172*, 969-972.

Kinoshita, T., Takeda, J., Hong, K., Kozono, H., Sakai, H., and Inoue, K. (1988). Monoclonal antibodies to mouse complement receptor type 1 (CR1). Their use in a distribution study showing that mouse erythrocytes and platelets are CR1-negative. J Immunol *140*, 3066-3072.

Kirchgessner, C. U., Patil, C. K., Evans, J. W., Cuomo, C. A., Fried, L. M., Carter, T., Oettinger, M. A., and Brown, J. M. (1995). DNA-dependent kinase (p350) as a candidate gene for the murine SCID defect. Science *267*, 1178-1183.

Kitamura, D., Kudo, A., Schaal, S., Muller, W., Melchers, F., and Rajewsky, K. (1992). A critical role of lambda 5 protein in B cell development. Cell *69*, 823-831.

Klein, G. (1999). Immunoglobulin gene associated chromosomal translocations in B-cell derived tumors. Curr Top Microbiol Immunol *246*, 161-167.

Kocks, C., and Rajewsky, K. (1988). Stepwise intraclonal maturation of antibody affinity through somatic hypermutation. Proc Natl Acad Sci U S A *85*, 8206-8210.

Kocks, C., and Rajewsky, K. (1989). Stable expression and somatic hypermutation of antibody V regions in B-cell developmental pathways. Annu Rev Immunol 7, 537-559.

Komori, T., Okada, A., Stewart, V., and Alt, F. W. (1993). Lack of N regions in antigen receptor variable region genes of TdT- deficient lymphocytes. Science *261*, 1171-1175.

Krop, I., Shaffer, A. L., Fearon, D. T., and Schlissel, M. S. (1996). The signaling activity of murine CD19 is regulated during cell development. J Immunol *157*, 48-56.

Kühn, R., Rajewsky, K., and Müller, W. (1991). Generation and analysis of interleukin-4 deficient mice. Science *254*, 707-710.

Kuppers, R., Klein, U., Hansmann, M. L., and Rajewsky, K. (1999). Cellular origin of human B-cell lymphomas. N Engl J Med *341*, 1520-1529.

Lawrence, C. W., and Hinkle, D. C. (1996). DNA polymerase zeta and the control of DNA damage induced mutagenesis in eukaryotes. Cancer Surv *28*, 21-31.

Ledbetter, J. A., and Herzenberg, L. A. (1979). Xenogeneic monoclonal antibodies to mouse lymphoid differentiation antigens. Immunol Rev *47*, 63-90.

Leo, O., Foo, M., Sachs, D. H., Samelson, L. E., and Bluestone, J. A. (1987). Identification of a monoclonal antibody specific for a murine T3 polypeptide. Proc Natl Acad Sci U S A *84*, 1374-1378.

Li, Y. S., Hayakawa, K., and Hardy, R. R. (1993). The regulated expression of B lineage associated genes during B cell differentiation in bone marrow and fetal liver. J Exp Med *178*, 951-960.

Löffert, D., Ehlich, A., Müller, W., and Rajewsky, K. (1996). Surrogate light chain expression is required to establish immunoglobulin heavy chain allelic exclusion during early B cell development. Immunity *4*, 133-144.

Longacre, A., Sun, T., Goldsby, R. E., Preston, B. D., and Storb, U. (2003). Ig gene somatic hypermutation in mice defective for DNA polymerase delta proofreading. Int Immunol *15*, 477-481.

Lossos, I. S., Alizadeh, A. A., Rajapaksa, R., Tibshirani, R., and Levy, R. (2003). HGAL is a novel interleukin-4-inducible gene that strongly predicts survival in diffuse large B-cell lymphoma. Blood *101*, 433-440.

Lossos, I. S., Jones, C. D., Warnke, R., Natkunam, Y., Kaizer, H., Zehnder, J. L., Tibshirani, R., and Levy, R. (2001). Expression of a single gene, BCL-6, strongly predicts survival in patients with diffuse large B-cell lymphoma. Blood *98*, 945-951.

Lossos, I. S., and Levy, R. (2003). Diffuse large B-cell lymphoma: insights gained from gene expression profiling. Int J Hematol *77*, 321-329.

Lyons, A. B., and Parish, C. R. (1994). Determination of lymphocyte division by flow cytometry. J Immunol Methods *171*, 131-137.

MacLennan, I. C. (1994). Germinal centers. Annu Rev Immunol *12*, 117-139.

Mandel, T. E., Phipps, R. P., Abbot, A., and Tew, J. G. (1980). The follicular dendritic cell: long term antigen retention during immunity. Immunol Rev *53*, 29-59.

Manis, J. P., Gu, Y., Lansford, R., Sonoda, E., Ferrini, R., Davidson, L., Rajewsky, K., and Alt, F. W. (1998). Ku70 is required for late B cell development and immunoglobulin heavy chain class switching. J Exp Med *187*, 2081-2089.

Manis, J. P., Tian, M., and Alt, F. W. (2002). Mechanism and control of class-switch recombination. Trends Immunol *23*, 31-39.

Manz, R. A., Thiel, A., and Radbruch, A. (1997). Lifetime of plasma cells in the bone marrow. Nature *388*, 133-134.

Martin, F., and Kearney, J. F. (2002). Marginal-zone B cells. Nat Rev Immunol *2*, 323-335.

Maruyama, M., Lam, K. P., and Rajewsky, K. (2000). Memory B-cell persistence is independent of persisting immunizing antigen. Nature *407*, 636-642.

Masutani, C., Kusumoto, R., Yamada, A., Dohmae, N., Yokoi, M., Yuasa, M., Araki, M., Iwai, S., Takio, K., and Hanaoka, F. (1999). The XPV (xeroderma pigmentosum variant) gene encodes human DNA polymerase eta. Nature *399*, 700-704.

Matsuoka, M., Yoshida, K., Maeda, T., Usuda, S., and Sakano, H. (1990). Switch circular DNA formed in cytokine-treated mouse splenocytes: evidence for intramolecular DNA deletion in immunoglobulin class switching. Cell *62*, 135-142.

McBlane, J. F., van Gent, D. C., Ramsden, D. A., Romeo, C., Cuomo, C. A., Gellert, M., and Oettinger, M. A. (1995). Cleavage at a V(D)J recombination signal requires only RAG1 and RAG2 proteins and occurs in two steps. Cell *83*, 387-395.

McDonald, J. P., Frank, E. G., Plosky, B. S., Rogozin, I. B., Masutani, C., Hanaoka, F., Woodgate, R., and Gearhart, P. J. (2003). 129-derived strains of mice are deficient in DNA polymerase iota and have normal immunoglobulin hypermutation. J Exp Med *198*, 635-643.

McDonald, J. P., Rapic-Otrin, V., Epstein, J. A., Broughton, B. C., Wang, X., Lehmann, A. R., Wolgemuth, D. J., and Woodgate, R. (1999). Novel human and mouse homologs of Saccharomyces cerevisiae DNA polymerase eta. Genomics *60*, 20-30.

McKean, D., Huppi, K., Bell, M., Staudt, L., Gerhard, W., and Weigert, M. (1984). Generation of antibody diversity in the immune response of BALB/c mice to influenza virus hemagglutinin. Proc Natl Acad Sci U S A *81*, 3180-3184.

McMillan, R., Longmire, R. L., Yelenosky, R., Lang, J. E., Heath, V., and Craddock, C. G. (1972). Immunoglobulin synthesis by human lymphoid tissues: normal bone marrow as a major site of IgG production. J Immunol *109*, 1386-1394.

McWhir, J., Selfridge, J., Harrison, D. J., Squires, S., and Melton, D. W. (1993). Mice with DNA repair gene (ERCC-1) deficiency have elevated levels of p53, liver nuclear abnormalities and die before weaning. Nat Genet *5*, 217-224.

Meira, L. B., Devaraj, S., Kisby, G. E., Burns, D. K., Daniel, R. L., Hammer, R. E., Grundy, S., Jialal, I., and Friedberg, E. C. (2001). Heterozygosity for the mouse Apex gene results in phenotypes associated with oxidative stress. Cancer Res *61*, 5552-5557.

Miltenyi, S., Muller, W., Weichel, W., and Radbruch, A. (1990). High gradient magnetic cell separation with MACS. Cytometry *11*, 231-238.

Mostoslavsky, R., Alt, F. W., and Bassing, C. H. (2003). Chromatin dynamics and locus accessibility in the immune system. Nat Immunol *4*, 603-606.

Mullis, K. B., and Faloona, F. A. (1987). Specific synthesis of DNA in vitro via a polymerase-catalyzed chain reaction. Methods Enzymol *155*, 335-350.

Muramatsu, M., Kinoshita, K., Fagarasan, S., Yamada, S., Shinkai, Y., and Honjo, T. (2000). Class switch recombination and hypermutation require activation-induced cytidine deaminase (AID), a potential RNA editing enzyme. Cell *102*, 553-563.

Nagaoka, H., Muramatsu, M., Yamamura, N., Kinoshita, K., and Honjo, T. (2002). Activation-induced deaminase (AID)-directed hypermutation in the immunoglobulin Smu region: implication of AID involvement in a common step of class switch recombination and somatic hypermutation. J Exp Med *195*, 529-534.

Nemazee, D. A., and Burki, K. (1989). Clonal deletion of B lymphocytes in a transgenic mouse bearing anti-MHC class I antibody genes. Nature *337*, 562-566.

Neuberger, M. S., Ehrenstein, M. R., Klix, N., Jolly, C. J., Yelamos, J., Rada, C., and Milstein, C. (1998). Monitoring and interpreting the intrinsic features of somatic hypermutation. Immunol Rev *162*, 107-116.

Neuberger, M. S., Harris, R. S., Di Noia, J., and Petersen-Mahrt, S. K. (2003). Immunity through DNA deamination. Trends Biochem Sci *28*, 305-312.

Nishikawa, S., Sasaki, Y., Kina, T., Amagai, T., and Katsura, Y. (1986). A monoclonal antibody against Igh6-4 determinant. Immunogenetics *23*, 137-139.

Nussenzweig, A., Chen, C., da Costa Soares, V., Sanchez, M., Sokol, K., Nussenzweig, M. C., and Li, G. C. (1996). Requirement for Ku80 in growth and immunoglobulin V(D)J recombination. Nature *382*, 551-555.

Oettinger, M. A., Schatz, D. G., Gorka, C., and Baltimore, D. (1990). RAG-1 and RAG-2, adjacent genes that synergistically activate V(D)J recombination. Science *248*, 1517-1523.

Ogi, T., Kato, T., Jr., Kato, T., and Ohmori, H. (1999). Mutation enhancement by DINB1, a mammalian homologue of the Escherichia coli mutagenesis protein dinB. Genes Cells *4*, 607-618.

Ogi, T., Mimura, J., Hikida, M., Fujimoto, H., Fujii-Kuriyama, Y., and Ohmori, H. (2001). Expression of human and mouse genes encoding polkappa: testis-specific developmental regulation and AhR-dependent inducible transcription. Genes Cells *6*, 943-953.

Ohashi, E., Bebenek, K., Matsuda, T., Feaver, W. J., Gerlach, V. L., Friedberg, E. C., Ohmori, H., and Kunkel, T. A. (2000). Fidelity and processivity of DNA synthesis by DNA polymerase kappa, the product of the human DINB1 gene. J Biol Chem *275*, 39678-39684.

Ohmori, H., Friedberg, E. C., Fuchs, R. P., Goodman, M. F., Hanaoka, F., Hinkle, D., Kunkel, T. A., Lawrence, C. W., Livneh, Z., Nohmi, T.*, et al.* (2001). The Y-family of DNA polymerases. Mol Cell *8*, 7-8.

Okazaki, I. M., Kinoshita, K., Muramatsu, M., Yoshikawa, K., and Honjo, T. (2002). The AID enzyme induces class switch recombination in fibroblasts. Nature *416*, 340-345.

Ollero, M., Gil-Guzman, E., Lopez, M. C., Sharma, R. K., Agarwal, A., Larson, K., Evenson, D., Thomas, A. J., Jr., and Alvarez, J. G. (2001). Characterization of subsets of human spermatozoa at different stages of maturation: implications in the diagnosis and treatment of male infertility. Hum Reprod *16*, 1912-1921.

Olsen, A. K., Bjortuft, H., Wiger, R., Holme, J., Seeberg, E., Bjoras, M., and Brunborg, G. (2001). Highly efficient base excision repair (BER) in human and rat male germ cells. Nucleic Acids Res *29*, 1781-1790.

Owen, J. J., Wright, D. E., Habu, S., Raff, M. C., and Cooper, M. D. (1977). Studies on the generation of B lymphocytes in fetal liver and bone marrow. J Immunol *118*, 2067-2072.

Pan, Z., Shen, Y., Du, C., Zhou, G., Rosenwald, A., Staudt, L. M., Greiner, T. C., McKeithan, T. W., and Chan, W. C. (2003). Two newly characterized germinal center B-cell-associated genes, GCET1 and GCET2, have differential expression in normal and neoplastic B cells. Am J Pathol *163*, 135-144.

Papavasiliou, F. N., and Schatz, D. G. (2000). Cell-cycle-regulated DNA double-stranded breaks in somatic hypermutation of immunoglobulin genes. Nature *408*, 216-221.

Papavasiliou, F. N., and Schatz, D. G. (2002). The activation-induced deaminase functions in a postcleavage step of the somatic hypermutation process. J Exp Med *195*, 1193-1198.

Pasparakis, M., and Kollias, G. (1995). Production of cytokine transgenic and knockout mice. In Cytokines: A Practical Approach, F. R. Balkwill, ed. (Oxford, Oxford University Press), pp. 297-324.

Pasqualucci, L., Neumeister, P., Goossens, T., Nanjangud, G., Chaganti, R. S., Kuppers, R., and Dalla-Favera, R. (2001). Hypermutation of multiple proto-oncogenes in B-cell diffuse large-cell lymphomas. Nature *412*, 341-346.

Pavlov, Y. I., Rogozin, I. B., Galkin, A. P., Aksenova, A. Y., Hanaoka, F., Rada, C., and Kunkel, T. A. (2002). Correlation of somatic hypermutation specificity and A-T base pair substitution errors by DNA polymerase eta during copying of a mouse immunoglobulin kappa light chain transgene. Proc Natl Acad Sci U S A *99*, 9954-9959.

Petersen-Mahrt, S. K., Harris, R. S., and Neuberger, M. S. (2002). AID mutates E. coli suggesting a DNA deamination mechanism for antibody diversification. Nature *418*, 99-103.

Pham, P., Bransteitter, R., Petruska, J., and Goodman, M. F. (2003). Processive AID-catalysed cytosine deamination on single-stranded DNA simulates somatic hypermutation. Nature *424*, 103-107.

Phung, Q. H., Winter, D. B., Cranston, A., Tarone, R. E., Bohr, V. A., Fishel, R., and Gearhart, P. J. (1998). Increased hypermutation at G and C nucleotides in

immunoglobulin variable genes from mice deficient in the MSH2 mismatch repair protein. J Exp Med *187*, 1745-1751.

Poltoratsky, V., Woo, C. J., Tippin, B., Martin, A., Goodman, M. F., and Scharff, M. D. (2001). Expression of error-prone polymerases in BL2 cells activated for Ig somatic hypermutation. Proc Natl Acad Sci U S A *98*, 7976-7981.

Rada, C., Ehrenstein, M. R., Neuberger, M. S., and Milstein, C. (1998). Hot spot focusing of somatic hypermutation in MSH2-deficient mice suggests two stages of mutational targeting. Immunity *9*, 135-141.

Rada, C., and Milstein, C. (2001). The intrinsic hypermutability of antibody heavy and light chain genes decays exponentially. Embo J *20*, 4570-4576.

Rada, C., Williams, G. T., Nilsen, H., Barnes, D. E., Lindahl, T., and Neuberger, M. S. (2002). Immunoglobulin isotype switching is inhibited and somatic hypermutation perturbed in UNG-deficient mice. Curr Biol *12*, 1748-1755.

Rajewsky, K. (1996). Clonal selection and learning in the antibody system. Nature *381*, 751-758.

Ramiro, A. R., Stavropoulos, P., Jankovic, M., and Nussenzweig, M. C. (2003). Transcription enhances AID-mediated cytidine deamination by exposing single-stranded DNA on the nontemplate strand. Nat Immunol *4*, 452-456.

Rao, M., Lee, W. T., and Conrad, D. H. (1987). Characterization of a monoclonal antibody directed against the murine B lymphocyte receptor for IgE. J Immunol *138*, 1845-1851.

Reaban, M. E., and Griffin, J. A. (1990). Induction of RNA-stabilized DNA conformers by transcription of an immunoglobulin switch region. Nature *348*, 342-344.

Reaban, M. E., Lebowitz, J., and Griffin, J. A. (1994). Transcription induces the formation of a stable RNA.DNA hybrid in the immunoglobulin alpha switch region. J Biol Chem *269*, 21850-21857.

Reina-San-Martin, B., Difilippantonio, S., Hanitsch, L., Masilamani, R. F., Nussenzweig, A., and Nussenzweig, M. C. (2003). H2AX is required for recombination between immunoglobulin switch regions but not for intra-switch region recombination or somatic hypermutation. J Exp Med *197*, 1767-1778.

Retter, M. W., and Nemazee, D. (1998). Receptor editing occurs frequently during normal B cell development. J Exp Med *188*, 1231-1238.

Revy, P., Muto, T., Levy, Y., Geissmann, F., Plebani, A., Sanal, O., Catalan, N., Forveille, M., Dufourcq-Labelouse, R., Gennery, A*., et al.* (2000). Activation-induced cytidine deaminase (AID) deficiency causes the autosomal recessive form of the Hyper-IgM syndrome (HIGM2). Cell *102*, 565-575.

Reynaud, C. A., Aoufouchi, S., Faili, A., and Weill, J. C. (2003). What role for AID: mutator, or assembler of the immunoglobulin mutasome? Nat Immunol *4*, 631-638.

Reynaud, C. A., Frey, S., Aoufouchi, S., Faili, A., Bertocci, B., Dahan, A., Flatter, E., Delbos, F., Storck, S., Zober, C., and Weill, J. C. (2001). Transcription, beta-like DNA polymerases and hypermutation. Philos Trans R Soc Lond B Biol Sci *356*, 91-97.

Roes, J., Muller, W., and Rajewsky, K. (1995). Mouse anti-mouse IgD monoclonal antibodies generated in IgD-deficient mice. J Immunol Methods *183*, 231-237.

Roes, J., and Rajewsky, K. (1993). Immunoglobulin D (IgD)-deficient mice reveal an auxiliary receptor function for IgD in antigen-mediated recruitment of B cells. J Exp Med *177*, 45-55.

Rogozin, I. B., and Kolchanov, N. A. (1992). Somatic hypermutagenesis in immunoglobulin genes. II. Influence of neighbouring base sequences on mutagenesis. Biochim Biophys Acta *1171*, 11-18.

Rogozin, I. B., Pavlov, Y. I., Bebenek, K., Matsuda, T., and Kunkel, T. A. (2001). Somatic mutation hotspots correlate with DNA polymerase eta error spectrum. Nat Immunol *2*, 530-536.

Rolink, A., Grawunder, U., Winkler, T. H., Karasuyama, H., and Melchers, F. (1994). IL-2 receptor alpha chain (CD25, TAC) expression defines a crucial stage in pre-B cell development. Int Immunol *6*, 1257-1264.

Rolink, A., and Melchers, F. (1996). B-cell development in the mouse. Immunol Lett *54*, 157-161.

Rolink, A., Melchers, F., and Andersson, J. (1996). The SCID but not the RAG-2 gene product is required for S mu-S epsilon heavy chain class switching. Immunity *5*, 319-330.

Rosenwald, A., Wright, G., Chan, W. C., Connors, J. M., Campo, E., Fisher, R. I., Gascoyne, R. D., Muller-Hermelink, H. K., Smeland, E. B., Giltnane, J. M*., et al.* (2002). The use of molecular profiling to predict survival after chemotherapy for diffuse large-B-cell lymphoma. N Engl J Med *346*, 1937-1947.

Roy, M. P., Kim, C. H., and Butcher, E. C. (2002). Cytokine control of memory B cell homing machinery. J Immunol *169*, 1676-1682.

Saiki, R. K., Scharf, S., Faloona, F., Mullis, K. B., Horn, G. T., Erlich, H. A., and Arnheim, N. (1985). Enzymatic amplification of beta-globin genomic sequences and restriction site analysis for diagnosis of sickle cell anemia. Science *230*, 1350-1354.

Sale, J. E., and Neuberger, M. S. (1998). TdT-accessible breaks are scattered over the immunoglobulin V domain in a constitutively hypermutating B cell line. Immunity *9*, 859-869.

Sambrook, J., E.F., F., and Maniatis, T. (1989). Molecular Cloning, Cold Spring Harbor Laboratory Press).

Sambrook, J., and Russell, D. W. (2001). Molecular cloning : a laboratory manual, 3rd edn (Cold Spring Harbor, N.Y., Cold Spring Harbor Laboratory Press).

Schatz, D. G., Oettinger, M. A., and Baltimore, D. (1989). The V(D)J recombination activating gene, RAG-1. Cell *59*, 1035-1048.

Schlissel, M. S. (2003). Regulating antigen-receptor gene assembly. Nat Rev Immunol *3*, 890-899.

Schriever, F., and Nadler, L. M. (1992). The central role of follicular dendritic cells in lymphoid tissues. Adv Immunol *51*, 243-284.

Schwenk, F., Baron, U., and Rajewsky, K. (1995). A cre-transgenic mouse strain for the ubiquitous deletion of loxP- flanked gene segments including deletion in germ cells. Nucleic Acids Res *23*, 5080-5081.

Shaffer, A. L., Lin, K. I., Kuo, T. C., Yu, X., Hurt, E. M., Rosenwald, A., Giltnane, J. M., Yang, L., Zhao, H., Calame, K., and Staudt, L. M. (2002). Blimp-1 orchestrates plasma cell differentiation by extinguishing the mature B cell gene expression program. Immunity *17*, 51-62.

Shimizu, T., Shinkai, Y., Ogi, T., Ohmori, H., Azuma, T. (2003). The absence of DNA polymerase kappa does not affect somatic hypermutation of the mouse immunoglobulin heavy chain gene. Immunology Letters *86*, 265-270.

Silver, L. M. (1995). Mouse genetics: concepts and practice, Oxford University Press).

Stavnezer, J. (1996). Immunoglobulin class switching. Curr Opin Immunol *8*, 199-205.

Storb, U., Peters, A., Klotz, E., Kim, N., Shen, H. M., Hackett, J., Rogerson, B., and Martin, T. E. (1998a). Cis-acting sequences that affect somatic hypermutation of Ig genes. Immunol Rev *162*, 153-160.

Storb, U., Peters, A., Klotz, E., Kim, N., Shen, H. M., Kage, K., Rogerson, B., and Martin, T. E. (1998b). Somatic hypermutation of immunoglobulin genes is linked to transcription. Curr Top Microbiol Immunol *229*, 11-19.

Su, I., and Tarakhovsky, A. (2000). B-1 cells: orthodox or conformist? Curr Opin Immunol *12*, 191-194.

Sugo, N., Aratani, Y., Nagashima, Y., Kubota, Y., and Koyama, H. (2000). Neonatal lethality with abnormal neurogenesis in mice deficient in DNA polymerase beta. Embo J *19*, 1397-1404.

Suzuki, N., Ohashi, E., Kolbanovskiy, A., Geacintov, N. E., Grollman, A. P., Ohmori, H., and Shibutani, S. (2002). Translesion synthesis by human DNA polymerase kappa on a DNA template containing a single stereoisomer of dG-(+)- or dG-(-)-anti-N(2)-BPDE (7,8-dihydroxy-anti-9,10-epoxy-7,8,9,10-tetrahydrobenzo[a]pyrene). Biochemistry *41*, 6100-6106.

Tarlinton, D. (1998). Germinal centers: form and function. Curr Opin Immunol *10*, 245-251.

Taylor, C. W., Grogan, T. M., and Salmon, S. E. (1990). Effects of interleukin-4 on the in vitro growth of human lymphoid and plasma cell neoplasms. Blood *75*, 1114-1118.

Tiegs, S. L., Russell, D. M., and Nemazee, D. (1993). Receptor editing in self-reactive bone marrow B cells. J Exp Med *177*, 1009-1020.

Tissier, A., McDonald, J. P., Frank, E. G., and Woodgate, R. (2000). poliota, a remarkably error-prone human DNA polymerase. Genes Dev *14*, 1642-1650.

Torres, R. M., and Kuehn, R. (1997). Laboratory Protocols for Conditional Gene Targeting (Oxford, Oxford University Press).

Torres, R. M., and Kühn, R. (1997). Laboratory protocols for conditional gene targeting (Oxford ; New York, Oxford Uninversity Press).

Tsubata, T., and Reth, M. (1990). The products of pre-B cell-specific genes (lambda 5 and VpreB) and the immunoglobulin mu chain form a complex that is transported onto the cell surface. J Exp Med *172*, 973-976.

Tumanov, A., Kuprash, D., Lagarkova, M., Grivennikov, S., Abe, K., Shakhov, A., Drutskaya, L., Stewart, C., Chervonsky, A., and Nedospasov, S. (2002). Distinct role of surface lymphotoxin expressed by B cells in the organization of secondary lymphoid tissues. Immunity *17*, 239-250.

van Gent, D. C., McBlane, J. F., Ramsden, D. A., Sadofsky, M. J., Hesse, J. E., and Gellert, M. (1995). Initiation of V(D)J recombination in a cell-free system. Cell *81*, 925-934.

Velasco-Miguel, S., Richardson, J. A., Gerlach, V. L., Lai, W. C., Gao, T., Russell, L. D., Hladik, C. L., White, C. L., and Friedberg, E. C. (2003). Constitutive and regulated expression of the mouse Dinb (Polkappa) gene encoding DNA polymerase kappa. DNA Repair (Amst) *2*, 91-106.

Washington, M. T., Johnson, R. E., Prakash, L., and Prakash, S. (2002). Human DINB1-encoded DNA polymerase kappa is a promiscuous extender of mispaired primer termini. Proc Natl Acad Sci U S A *99*, 1910-1914.

Weiss, U., and Rajewsky, K. (1990). The repertoire of somatic antibody mutants accumulating in the memory compartment after primary immunization is restricted through affinity maturation and mirrors that expressed in the secondary response. J Exp Med *172*, 1681-1689.

Wittschieben, J., Shivji, M. K., Lalani, E., Jacobs, M. A., Marini, F., Gearhart, P. J., Rosewell, I., Stamp, G., and Wood, R. D. (2000). Disruption of the developmentally regulated Rev3l gene causes embryonic lethality. Curr Biol *10*, 1217-1220.

Woo, C. J., Martin, A., and Scharff, M. D. (2003). Induction of somatic hypermutation is associated with modifications in immunoglobulin variable region chromatin. Immunity *19*, 479-489.

Worm, M., Ebermayer, K., and Henz, B. (1998). Lymphotoxin-alpha is an important autocrine factor for CD40 + interleukin-4-mediated B-cell activation in normal and atopic donors. Immunology *94*, 395-402.

Yokoyama, W. M., Koning, F., Kehn, P. J., Pereira, G. M., Stingl, G., Coligan, J. E., and Shevach, E. M. (1988). Characterization of a cell surface-expressed disulfide-linked dimer involved in murine T cell activation. J Immunol *141*, 369-376.

Yoshikawa, K., Okazaki, I. M., Eto, T., Kinoshita, K., Muramatsu, M., Nagaoka, H., and Honjo, T. (2002). AID enzyme-induced hypermutation in an actively transcribed gene in fibroblasts. Science *296*, 2033-2036.

Yu, K., Chedin, F., Hsieh, C. L., Wilson, T. E., and Lieber, M. R. (2003). R-loops at immunoglobulin class switch regions in the chromosomes of stimulated B cells. Nat Immunol *4*, 442-451.

Yu, K., and Lieber, M. R. (2003). Nucleic acid structures and enzymes in the immunoglobulin class switch recombination mechanism. DNA Repair (Amst) *2*, 1163-1174.

Zan, H., Komori, A., Li, Z., Cerutti, A., Schaffer, A., Flajnik, M. F., Diaz, M., and Casali, P. (2001). The Translesion DNA Polymerase zeta Plays a Major Role in Ig and bcl-6 Somatic Hypermutation. Immunity *14*, 643-653.

Zeng, X., Winter, D. B., Kasmer, C., Kraemer, K. H., Lehmann, A. R., and Gearhart, P. J. (2001). DNA polymerase eta is an A-T mutator in somatic hypermutation of immunoglobulin variable genes. Nat Immunol *2*, 537-541.

Zhang, J., Bottaro, A., Li, S., Stewart, V., and Alt, F. W. (1993). A selective defect in IgG2b switching as a result of targeted mutation of the I gamma 2b promoter and exon. Embo J *12*, 3529-3537.

Zhang, Y., Wu, X., Guo, D., Rechkoblit, O., and Wang, Z. (2002). Activities of human DNA polymerase kappa in response to the major benzo[a]pyrene DNA adduct: error-free lesion bypass and extension synthesis from opposite the lesion. DNA Repair (Amst) *1*, 559-569.

Zhang, Y., Yuan, F., Wu, X., Wang, M., Rechkoblit, O., Taylor, J. S., Geacintov, N. E., and Wang, Z. (2000a). Error-free and error-prone lesion bypass by human DNA polymerase kappa in vitro. Nucleic Acids Res *28*, 4138-4146.

Zhang, Y., Yuan, F., Xin, H., Wu, X., Rajpal, D. K., Yang, D., and Wang, Z. (2000b). Human DNA polymerase kappa synthesizes DNA with extraordinarily low fidelity. Nucleic Acids Res *28*, 4147-4156.

Zhu, C., Bogue, M. A., Lim, D. S., Hasty, P., and Roth, D. B. (1996). Ku86-deficient mice exhibit severe combined immunodeficiency and defective processing of V(D)J recombination intermediates. Cell *86*, 379-389.

H   ABBREVIATIONS

AID   activation-induced deaminase

APC   Allophycocyanine

BCR   B cell receptor

bp   base-pairs

BSA   bovine serum albumin

C   constant region

CSR   class switch recombination

D   diversity gene segment

DLBCL   diffuse large B cell lymphoma

DMEM   Dulbecco's modified Eagle medium

DMSO   Dimethylsuloxide

EDTA   ethylene-diamine tetraacidic acid

EGFP   enhanced green fluorescence protein

ES cell   embryonic stem cell

FACS   fluorescence assisted cell sorting

FCS   fetal calf serum

FDC   follicular dendritic cell

FITC   Fluoresceine-isocyanate

GC   germinal center

Ig   immunoglobulin

IgH   immunoglobulin of the heavy chain locus

IgL   immunoglobulin of the light chain loci

IL-4   Interleukin-4

i.p.   intra-peritoneally

J   joining gene segment

kDa   kilo Dalton

LA   long arm of homology

LIF   leukemia inhibitory factor

LPS   lipopolysaccaride

mAb   monoclonal antibody

MACS   magnetic cell sorting

MEF	mouse embryonic feeder cells
MLN	mesenteric lymph node
NHEJ	non-homologous end joining
PBS	phosphate-buffered saline
PCR	polymerase chain reaction
PE	Pycoerythrine
Pol	DNA polymerase
PNA	peanut agglutinin
PP	Peyer's patches
R	purine (adenine or guanine)
RPMI	Rosewell-Park-Memorial-Institute cell culture medium
RSS	recognition signal sequence
SA	short arm of homology
SDS	sodium dodecyl sulfate
SP	spleen
SHM	somatic hypermutation
TD	T cell-dependent
Tris	tris(hydroxymethyl)amineethane
W	adenine or thymidine
WT	wild-type
V	variable gene segment or variable region
Y	pyrimidine (cytidine or thymidine)

I   CURRICULUM VITAE

Dominik Schenten

Date of Birth: June 30, 1971

Place of Birth   Trier, Germany

<u>Education</u>

1978-1982   Deutsche Evangelische Oberschule, Cairo, Egypt

1982-1988   Treviris-Gymnasium Trier, Germany

1988-1991   Auguste-Victoria Gymnasium, Trier, Germany

1991   Abitur

1992-1998   Biochemistry, Free University Berlin, Germany

  1995-1996   Instituto Quimico de Sarría, Barcelona, Spain

  1996-1998   Dana-Farber Cancer Institute,
                        Harvard Medical School, Boston, MA, USA
                        Diploma-Thesis "Characterization of Molecularly
                        Cloned Simian Immunodeficiency Viruses"

1998   Diploma in Biochemistry

<u>Dissertation</u>

1999-2004   University of Cologne, Germany

  1999-2001   Institute for Genetics, Cologne, Germany

  2001-2004   Center for Blood Research,
                        Harvard Medical School, Boston, MA, USA

Boston, MA, USA; December 12, 2003

J   ERKLÄRUNG

Ich versichere, dass ich die von mir vorgelegte Dissertation selbstständig angefertigt, die verwendeten Quellen und Hilfsmittel vollständig angegeben und die Stellen der Arbeit – einschliesslich Tabellen und Abbildungen-, die anderen Werken im Wortlaut oder dem Sinn nach entnommen sind, in jedem Einzelfall als Entlehnung kenntlich gemacht habe; dass diese Dissertation noch an keiner Fakultät oder Universität zur Prüfung vorgelegt hat; dass sie abgesehen von der unten angegebenen Teilpublikation noch nicht veröffentlicht worden ist, sowie dass ich eine solche Veröffentlichung vor dem Abschluss des Promotionsverfahrens nicht vornehmen werde. Die Bestimmungen der Promotionsordnung sind mir bekannt. Die von mir vorgelegte Dissertation ist von Prof. Dr. Klaus Rajewsky betreut worden.

Teilpublikation:

Schenten, D., Gerlach, V. L., Guo, C., Velasco-Miguel, S., Hladik, C. L., White, C. L., Friedberg, E. C., Rajewsky, K., and Esposito, G. (2002). DNA polymerase kappa deficiency does not affect somatic hypermutation in mice. Eur J Immunol 32, 3152-60.

Boston, MA, USA, den 12.12.2003

Dominik Schenten

H   ACKNOWLEDGEMENTS